ETH
Eidgenössische Technische Hochschule Zürich
Swiss Federal Institute of Technology Zurich

Percolation Theory Applied to Financial Markets: A Cluster Description of Herding Behavior Leading to Bubbles and Crashes

Master's Thesis

Maximilian G. A. Seyrich

February 20, 2015

Advisor: Professor Didier Sornette

Chair of Entrepreneurial Risk
Department of Physics
Department MTEC
ETH Zurich

Abstract

In this thesis, we clarify the herding effect due to cluster dynamics of traders. We provide a framework which is able to derive the crash hazard rate of the Johannsen-Ledoit-Sornette model (JLS) as a power law diverging function of the percolation scaling parameter. Using this framework, we are able to create reasonable bubbles and crashes in price time series. We present a variety of different kinds of bubbles and crashes and provide insights into the dynamics of financial markets. Our simulations show that most of the time, a crash is preceded by a bubble. Yet, a bubble must not end with a crash. The time of a crash is a random variable, being simulated by a Poisson process. The crash hazard rate plays the role of the intensity function. The headstone of this thesis is a new description of the crash hazard rate. Recently discovered super-linear relations between groups sizes and group activities, as well as percolation theory, are applied to the Cont-Bouchaud cluster dynamics model.

Contents

Chapter 1

Motivation

Many financial crashes, including the crash of October 1929 as well as the recent financial crash which started in 2007, were preceded by at least one bubble [1]. However, a bubble being defined as the deviation of the observed price from the fundamental values, its detection of a bubble turns out to be very difficult: the determination of the actual fundamental value is almost impossible.

The Johanson-Ledoit-Sornette Model (JLS) provides a different access to bubbles [2][3][4][5]. It defines a bubble as a transient "faster-than-exponential" growth, resulting from local self-reinforcing imitations between traders. In the risk-driven JLS model, crashes and bubbles are explained by local imitation of traders propagating spontaneously into global cooperation. This global cooperation among traders may cause a crash.

Why do agents imitate? Sornette applies the Ising model from statistical physics in order to quantitatively analyze the imitation of traders [6][7]: Initially idiosyncratic beliefs among traders predominate due to lacking information which might allow to adequately price the asset. This noise corresponds to the fluctuations described in the Ising model. Later on, traders poll their colleagues and friends in order to price the asset. This behavior may lead to a coupling among traders similarly to the coupling of spins. This perspective allows to reduce markets to systems that are determined by a fight between order (due to couplings) and disorder (due to idiosyncratic noise).

The system can undergo a phase transition from a disordered state where the idiosyncratic noise dominates, to the ordered state where the imitations dominate. Passing the critical point of the phase transition, global cooperation occurs in analogy to the occurrence of magnetization in the Ising model once the Curie point has been reached. Such a transition can lead to a large shift in the number of buyers and sellers. Kyle provides a model that relates

the difference in the number of sellers and buyers linearly to the price [8]. Therefore, the phase transition can cause a fall in prices which is called a crash. On the other hand, a raise of the price, a positive crash, would be possible as the system is symmetrical. However, we will constrain ourselves to crashes in the usual sense without limiting the generality of our theory.

The transition to global cooperation of traders is in good analogy to the dynamics of critical phenomena in physics. The hallmark of criticality is a power law in the scaling parameter. The exponent of this power law is universal, meaning that it does not depend on the specific details of a physical system, but rather on the dimension, the range as well as the interaction. According to the JLS model, the price is driven by the risk of a crash. The crash possesses a stochastic description by a crash hazard rate which is assumed to scale with such a power law.

Many dynamical models have already implemented this concept. This thesis tackles the crash hazard rate by a cluster approach, in order to clarify the mechanism behind bubbles and crashes. A mathematical work by Cont and Bouchaud provides a framework to model herding processes with the help of cluster dynamics [9]. They suggest that imitating agents group together and can be described as a single super-trader which is a cluster of traders with one unique opinion. These clusters can correspond to mutual funds or to herding among security analysts in the context of a stock market.

In this thesis, we provide a framework that extends the cluster description of Cont and Bouchaud by means of percolation theory [10]. We investigate the cluster formation as we approach the critical regions of phase transitions and show that a crash and a preceding bubble are related to the networks of the traders. This relation allows us to perform price simulations and create bubbles and crashes only by varying the underlying trader network. We present a variety of different kinds of bubbles and crashes, and provide interesting insights into the dynamics of financial markets.

We start with an introduction of the theoretical background in chapter "Models & Methods". Chapter "Results" presents our framework and price simulations with bubbles and crashes therein. The last chapter, "Conclusion", summarizes our main findings and provides an outlook for possible improvements of our framework. The "Appendix" gives further explanations and figures.

Chapter 2

Models & Methods

This section presents the models and methods we will need in order to describe bubbles and crashes as well as perform simulations to describe them. We start with a brief summary of the JLS model and an introduction of the crash hazard rate. This is followed by a short overview of percolation theory and of the Ising model. Finally, Glauber dynamics, the Ornstein-Uhlenbeck process and the non-homogeneous Poisson process are explained.

2.1 The Johanson-Ledoit-Sornette (JLS) Model

The Johanson-Ledoit-Sornette (JLS) model provides an alternative access to bubbles as it defines them as a transient "faster-than-exponential" growth, resulting from local self-reinforcing imitations between traders. The model claims that characteristic log-periodic signatures can be detected in bubbles before a crash occurs. This allows to predict changes of phases and price bubbles by studying the time series of a financial asset. In the following, we state the key ingredients of the JLS model and show the derivation of the price equation.

The model makes the following assumptions:

- The market can be divided into traders with rational expectations and noise traders. The latter are influenced by other traders and thus may exhibit herding behavior.
- Local self-reinforcement of noise traders and the resulting herding effects are responsible for the bubble as well as the crash. A crash may occur if the herding effects exceed a critical point and many traders sell at the same time. For a motivation of these herding effects, see [6]. Due to the ubiquity of noise, the JLS model proposes a stochastic description of a crash by using a crash hazard rate.

- A crash is not a deterministic outcome of the bubble, i.e., the time of the crash is a random variable. Therefore, it is rational for traders to stay invested in the asset although it exhibits a bubble behavior as long as the return excesses the expected risk.
- The asset is purely speculative and pays no dividends in a market where we ignore the interest rate, risk aversion, information asymmetry and the market-clearing condition.

Under these assumptions, one can derive an equation for the dynamics of the price evolution. Applying the last assumption, rational expectation is equivalent to the familiar martingale hypothesis. For the price $p_{\text{rice}}(t)$ of the asset at time t and the expectation $E_t[\bullet]$ conditional on information revealed up to time t, we get

$$\forall t' > t : E_t[p_{\text{rice}}(t')] = p_{\text{rice}}(t). \tag{2.1}$$

We model a crash as a jump-process dj which takes the value $dj = 1$ when a crash occurs and $dj = 0$ for all other times. The time of the crash t^* is a *random variable* which is described by the *deterministic* crash hazard rate $h(t)$. It gives the conditional probability that there is a crash between t and $t + dt$ given that the crash has not occurred yet. The probability for having a crash in the time interval t and $t + dt$ is thus given by $h(t)dt$. See appendix A for a more precise statistical derivation of the crash hazard rate.

Assume that the price drops by a fixed percentage κ at the crash. We denote μ as the return of the asset. Furthermore, we add a Wiener process with infinitesimal increment $dw(t)$. It describes the volatility of the price. We scale it with a constant η times price. Altogether, we obtain the price dynamics

$$dp_{\text{rice}}(t) = \mu(t)p_{\text{rice}}(t)dt - \kappa p_{\text{rice}}(t)dj(t) + \eta \cdot p_{\text{rice}}(t)dw(t) \qquad \text{for } t < t^* \tag{2.2}$$

which are valid for all time before the crash. The crash hazard rate enters this equation when we calculate the expected price change dp. Combining the last two equations and using the linearity of the expectation we get

$$E_t[dp_{\text{rice}}(t')] = \mu(t')p_{\text{rice}}(t')dt - \kappa p_{\text{rice}}(t')h(t')dt + 0 = 0, \qquad \forall t' > t :, \tag{2.3}$$

where we used $E_t[dj] = 1 \cdot h(t)dt + 0 \cdot (1 - h(t)dt) = h(t)dt$ and $E_t[dw] = 0$. Rearranging the last equation links the return to the crash hazard rate:

$$\mu(t') = \kappa h(t') \qquad \forall t' > t. \tag{2.4}$$

Plugging this relation into equation (2.2), we finally get an expression for the price before a crash, driven only by the crash hazard rate and a random walk:

$$\frac{dp_{\text{rice}}(t)}{p_{\text{rice}}} = \kappa h(t)dt - \kappa dj(t) + \eta dw(t) \qquad \text{for } t < t^*. \tag{2.5}$$

Using discrete time steps, we can reformulate this equation as a recursive formula for the price at any time t before the crash. We substitute the Wiener process by a symmetrical random walk, which we will also call dw in the following. The symmetrical random walk is the pendant of the Wiener process as it converges to a Wiener process in the limit of an infinite number of time-steps [11].

$$p_{\text{rice}}(t) = p_{\text{rice}}(t-1)\left[\kappa h(t) - \kappa dj(t) + \eta \Delta w(t)\right] \qquad \text{for } t < t^*. \tag{2.6}$$

We will use this equation in our price simulations. The higher the probability of a crash, the faster the price must go up in order to satisfy the martingale condition. Intuitively, an asset that might crash must be compensated by higher returns in order to stay attractive for investors.

In the risk-driven JLS model, crashes and bubbles are explained by local imitation of traders propagating spontaneously into global cooperation, as we outlined in the introduction. This global cooperation, also called herding, was explained as the phase where order dominates. A large shift in the marketbook, leading to a crash according to the Kyle model [8], is possible in this herding phase. If the price is risk-driven, the crash hazard rate describes the price as seen above. In statistical terms, the crash hazard rate is the conditional probability that the crash occurs in the time interval $[t, t+dt]$, given that it has not happened yet. Note that it is a rate with unit 1 over time; in particular, it is not a probability (see appendix for further explanations). The transition to the herding phase is in good analogy to the dynamics of critical phenomena in physics. The hallmark of criticality is a power law with universal exponent. The crash hazard rate is assumed to be a power law in time multiplied by a log-periodic factor. For simplicity, we neglect the latter and concentrate on the power law behavior:

$$h(t) \propto (t_c - t)^{\alpha} \tag{2.7}$$

Our goal is to present a framework which is able to derive this power law divergence of the crash hazard rate. Cont and Bouchaud presented a model of a herding process using cluster dynamics [9]. They suggest that imitating agents group together and can be described as a cluster of traders with one unique opinion. They state that these clusters can correspond to mutual funds or to herding among security analysts in the context of a stock market. Cluster dynamics are described by percolation theory, which we summarize now.

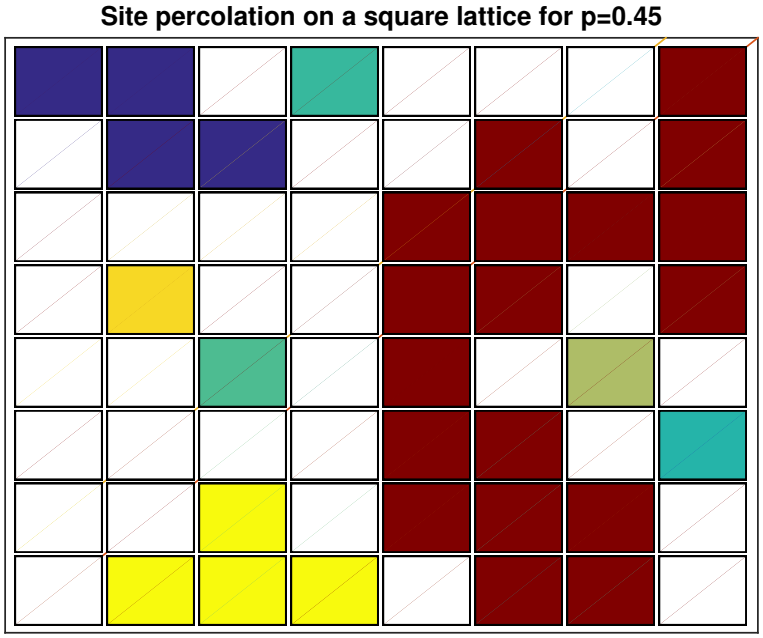

Figure 2.1: Site percolation on the two dimensional square lattice for $p = 0.45$. We have one percolating cluster of size $s = 18$ (red), two clusters of size $s = 4$ and five clusters of size $s = 1$. The red cluster goes from the upper boundary to the opposite boundary. The cluster percolates and the system exhibits *percolation*.

2.2 Percolation theory

2.2.1 Introduction

Percolation theory is a quite old, but widely used, model in statistical physics [10]. It is simple to define;yet it is able to describe phase transitions in material science, neural science or socio-science. We will describe our financial system of the stylized market introduced above by using percolation theory.

What is percolation? Imagine a chessboard which consists of $8 \times 8 = 64$ fields. Suppose that a tree is on a field with probability p and the field is empty with probability $1 - p$. Figure 2.1 shows a realization of this configuration. The set of occupied nearest neighbor fields forms a clusters. Nearest neighbors of a field are the fields to the north, to the south, to the west and to the east. In the figure, clusters are in the same color. Suppose now that we set fire on all the fields at the top. Will the fire arrive at the bottom for a given probability p if a burning tree passes the fire to its nearest neighbors? We need a chain of occupied sites from top to bottom, i.e., we need a so-called percolating cluster. The figure exhibits such a percolating clus-

ter. Generally, percolation theory tries to derive theoretical answers to this question as well as to provide the distribution and properties of the clusters in the limit of an infinite number of fields. Fields are called sites and the nearest neighbor can have a more general form by introducing a bond: Two sites are neighbored if there is a bond between them. Bonds between any two sites are possible. Any such arbitrary graph can then be investigated by percolation theory.

2.2.2 Percolation Point and Cluster Number

The percolation threshold p_c is the value of probability p for which an infinite cluster occurs for the first time. It is a unique deterministic value in the limit of an infinite system. Percolation points for a wide bandwidth of graphs are known exactly or have been calculated numerically. Stauffer and Aharony [10] state that the percolation threshold for an infinite chessboard as underlying graph structure, in percolation terminology called site percolation model on the square lattice, is given by $p_c \simeq 0.592746$. The cluster number $n_p(s)$ is the distribution of clusters of finite size s per site depending only on the probability p. It is also a deterministic variable in the limit of an infinite system. Due to the fractal structure of clusters, the cluster number is not dependent on the square lattice size up to volatility. Stauffer and Ahorny state that the cluster number at the percolation threshold is a power law in the size s, whereas it exhibits an additional exponential factor for all other values of p. The following relations for the cluster number are valid not only for the square lattice, but for all different kinds of graphs:

$$n_p(s) \propto \begin{cases} s^{-\tau} \exp(-\frac{s}{s^*}) & \text{for } p < p_c, \\ s^{-\tau} & \text{for } p = p_c, \\ s^{-\tau} \exp(-\frac{s^{1-1/d}}{s^*}) & \text{for } p > p_c. \end{cases} \tag{2.8}$$

Here, we have introduced the Fisher exponent τ from the Fisher droplet model. It can be derived analytically on the square lattice: $\tau = \frac{187}{91} \approx 2.05$. We will use also the variable μ, which is linked to the Fisher exponent by $\tau = 1 + \mu$. The dimension of the system is d. The variable s^* denotes the size of the largest cluster and scales with another critical exponent σ via

$$s^*(p) \propto |p - p_c|^{\frac{1}{\sigma}}. \tag{2.9}$$

The exponent is equal to $\sigma = \frac{36}{91} \approx 0.3956$ on the two dimensional square lattice. The exponential factor acts as a cut-off. Cluster sizes bigger than the cut-off size s^* have no significant contributions to a sum over the cluster number. For cluster sizes $s < s^*$, the effective cluster number can be approximated by a power law with the Fisher exponent τ. Sums over the

cluster number multiplied by the cluster size s are called moments. The first moment of the cluster size distribution equals

$$\sum_{s}^{\infty} s \cdot n(s) = \begin{cases} p & \text{for } p < p_c., \\ p - \text{const} \cdot |p - p_c|^{\frac{5}{36}} & \text{for } p > p_c. \end{cases} \tag{2.10}$$

If the percolating cluster occurs, it lowers the sum, as the biggest cluster s^* is no longer part of the summation. This lowering explains the subtracting term in the case $p > p_c$. It is the strength or weight of the percolating cluster P which is a power law in $p - p_c$ with according exponent $\beta = \frac{36}{5}$ for the two dimensional square lattice. The second moment, also called mean cluster size, diverges near p_c as a power law, i.e.,

$$\sum_{s}^{\infty} s^2 \cdot n(s) \propto |p - p_c|^{-\gamma}. \tag{2.11}$$

The exponent is equal to $\gamma = \frac{43}{18} \approx 2.3889$ on the two dimensional square lattice. We summarize the introduced exponents in table 2.1.

Table 2.1: Critical exponents for the site percolation on a square lattice with percolation threshold at $p_c = 0.592746$.

Exponent	Analytical value	Approximated value
τ	187/91	2.0549
σ	36/91	0.3956
γ	43/18	2.3889

2.2.3 Finite Size Effects

Financial markets consist of a finite number of traders. The relations derived in the $L \to \infty$ limit have to be slightly modified if we are on a finite lattice. Let us motivate this again on the chessboard. It is very unlikely that we have a percolating cluster of trees the first time exactly for $p_c = 0.592746$. If we try many values of p below the threshold, we will sooner or later get a percolating cluster. Due to the finite size of the system, the cluster distribution and the percolation transition become randomly influenced variables. Other finite size effects are a shifting of the percolation threshold to lower values and a rounding of the mean cluster size instead of a diverging power law [12]. Finite size effects are visualized in figure 3.2.

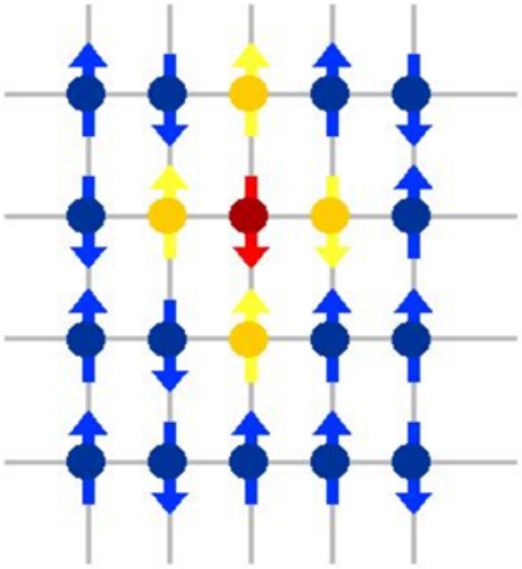

Figure 2.2: Plot of a two dimensional lattice spin model. The red spin is influenced by the four nearest neighbors in yellow.[1]

2.3 Ising Model

2.3.1 Introduction

The Ising model is a theoretical framework in statistical mechanics explaining ferromagnetism [7][13]. Spins act as magnetic dipoles which means that they can be in one of the two states $\sigma_i = \pm 1$. Sitting on a lattice spins interact with their nearest neighbors. Figure 2.2 illustrates such a lattice [1]. This interaction is described by the coupling strength $J > 0$ for ferromagnets. The Hamiltonian of the Ising model is given by

$$H = -J \sum_{\langle i,j \rangle} s_i s_j - h \sum_i s_i \tag{2.12}$$

where h is an external magnetic field and The system is connected to a heat bath with energy $k_B T$ leading to the Boltzmann distribution $P(s_{\pm 1}) \propto \exp(H_{\pm 1}/k_B T)$. The solution of the energy minimization of this Hamiltonian was provided by Ernest Ising for the one dimensional model in his doctoral thesis in 1925. There is no finite critical temperature, a phase transition occurs only at $T = 0$. Lars Onsager proved in 1944 that there is indeed a phase transition for a finite critical temperature $T_c = \frac{2J}{k_B \log(1+\sqrt{2})} \simeq 2.27 \frac{J}{k_B}$ in two dimensions [14]. The system undergoes a transition from the disordered

[1] http://www.lancaster.ac.uk/pg/jamest/Group/physics2.html Date: 19th January 2015

phase where fluctuations dominate the correlation between the spins, into an ordered phase where the correlations between the spins dominate the fluctuations. The critical point T_c is also called Curie point.

2.3.2 Glauber Dynamics in the Ising Model

Glauber dynamics extends the Ising model by providing a simulation of non-equilibrium dynamics [15]. It is a discrete Markov chain that has the equilibrium state of the Ising model as its stationary distribution. Starting from any initial condition, we can let the Ising system evolve to its equilibrium state. It is a so-called single-flip algorithm. Given a configuration of spins at time t, Glauber dynamics investigates each single spin by introducing a random variable with two events: a spin can flip its state or stay in the same state. The Boltzmann distribution with temperature T, a function of the energy change of the two events, gives access to the probability of this random variable.

$$P_i(flip) = \frac{1}{1 + \exp(\Delta E_{i,j}(K)/cdotK)} \tag{2.13}$$

Not flipping is the conjugated event and thus has the probability $1 - P_{i,j}(flip)$. The change of energy $\Delta E(K)_{i,j}$ for flipping or staying is dependent on the nearest neighbors j and the inverse temperature $K = \frac{J}{k_B T}$. It does not depend on the actual value of the spin states but on the number of states that have the same state. Figure 2.3 illustrates the different probabilities of flipping on the square lattice for different values of K. After all spins have been investigated once, we obtain the new configuration of the system at time-step $t + 1$. In the end, the system will converge to its stationary state after t_m time-steps called the mixing time. However, the mixing time t_m of the Glauber dynamics can be quite high. Indeed, it is a function of the number of spins n. Mixing times t_m for the Glauber dynamics are

$$t_m \propto \begin{cases} n \log(n) & \text{for } K \ll K_c, \\ n^{\frac{3}{2}} & \text{for } K \simeq K_c, \\ \exp(\sqrt{n}) & \text{for } K > K_c. \end{cases} \tag{2.14}$$

Especially in the ordered phase, the convergence is very slow, as the mixing time grows exponential with the number of spins. That is why we start our simulations not in an arbitrary spin configuration, but with a configuration where 75% of the states are in one state. This lowers the mixing time as we are much closer to the stationary state for $K > K_c$, where the Glauber dynamics converge very slowly. In the region $K < K_c$, we take an arbitrary starting configuration.

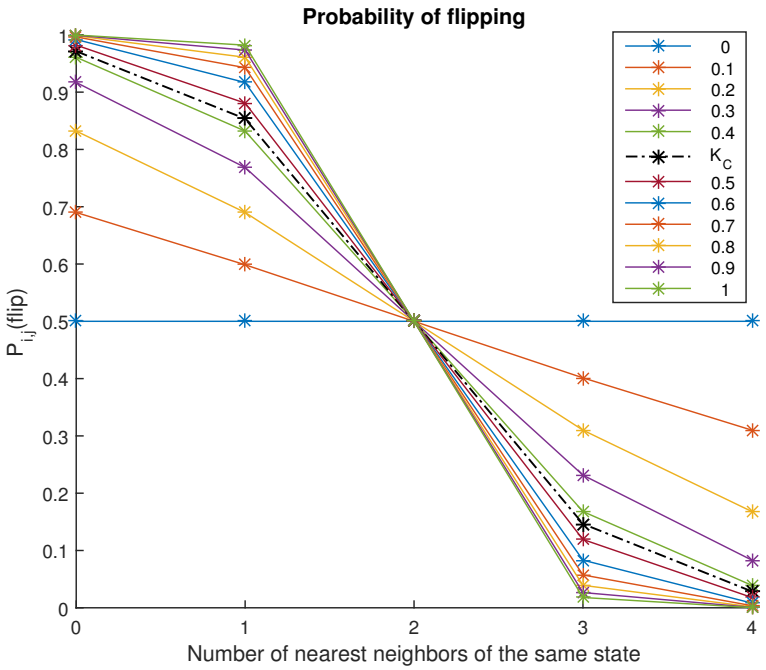

Figure 2.3: Plot of the probability of flipping as a function of spins of same sign in the neighborhood for different values of inverse temperature K. The constant line is for the smallest interaction $K = 0$.

2.4 Ising and JLS Model

The Ising model has a wide application range since it is easy to define, and its behavior is rich. The principal story of the Ising model, the fight between order and disorder, has been applied in very different research areas like the activity of neurons in the brain [16], the description of spin glasses in physics [17] and, as already stated in the introduction, to crashes in financial economics occurring due to the herding behavior of traders [6][18]. In the latter case, traders are assumed to be organized into networks (friends, families, colleagues etc.). They are influenced by their nearest neighbors just as the spins in the Ising model. The thermal fluctuations are substituted by idiosyncratic belief. If we apply the Ising model, the system of traders can undergo a phase transition similarly to the phase transition of the ensemble of magnetic dipoles. Herding behavior on financial markets, described in analogy to the Ising coupling, can lead to global imitation at such a critical point triggering a crash.

2.5 Ising Model and Percolation Theory

The Ising model can be described by percolation theory. The concepts are similar and there are indeed lots of analogies, but there are also some important differences. The connectedness of sites is not an interacting dynamical but a graphical property. In the Ising model, we have to determine the Hamiltonian of our system, minimize it with the help of calculus from statistical physics before we can calculate the correlation and therefore the interaction between two spins. In graph theory, we can describe connections between agents. To get correlation between the agents, one still needs to define a way of interactions (e.g. the Cont-Bouchaud-model: everybody in a cluster takes the same state defines an interaction[9]). We also have to be aware of an important difference between a phase transition and a percolation transition. The former is dynamical, due to couplings, whereas the latter is a geometrical effect. Think of a random landscape with islands and oceans. Now, if the water level is lowered, Islands will get larger and larger and suddenly, there will be a continent. The underlying structure has not changed, a percolation threshold appears as the answer to the question "when will there be a largest connected component"? In a dynamical physical transition however, there are couplings that force the system into another state.

Nonetheless, the site percolation model seems to be a generic candidate to describe the Ising model, as sites have also two possible states: it can be occupied or not occupied. We associate each spin in state $s_i = 1$ with an occupied site and each spin in state $s_i = -1$ with an unoccupied site. Nearest neighbors of an occupied site are not dynamically coupled to this site, but they are said to be connected to it if they are also occupied. The set of connected sites forms a cluster which we call Ising cluster in the following. Coniglio and Klein showed in [19] that the percolating threshold coincides with the critical Curie point in two dimensions. Moreover, they showed that the linear dimension, identified as the connectedness length, diverges as the Ising correlation length close to the critical point.

However, in three dimensions, a percolating cluster occurs already for a temperature $T_p = 4.52$, whereas the ordered phase starts at the Curie Point $T_c = 4.44$. The second moment of the percolation model, the mean cluster size S, diverges as a power law $(T - T_c)^{-\gamma_p}$ when we approach the percolation point. The exponent is known to be $\gamma_p = 1.91$. The second moment of the Ising model, the susceptibility, also diverges as a power law, but with exponent $\gamma = 1.75$ when we come close to the Ising critical point. Ising clusters are too big to describe Ising droplets from the Fisher droplet model [20]. This becomes clearer when we think of the $T \to \infty$ limit: Couplings between spins vanish due to the fluctuations, but clusters can still be there. Coniglio and Klein solved this problem by introducing additional bonds

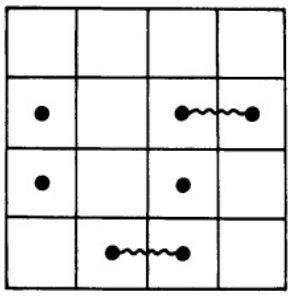

Figure 2.4: Occupied sites are denoted by points and the bonds by lines. This configuration shows two Ising clusters of size $s = 2$ and $s = 5$ whereas it exhibits five Ising Droplets, three isolated ones and two of size $s = 2$.

between sites in a cluster. The probability of such a bond is chosen to be $p_B = 1 - e^{-2\frac{J}{k_B T}}$. New clusters are formed under the condition that they have to be clusters in the former sense and additionally be connected by a bond. Both clusters are illustrated in 2.4. In this model, the mean cluster size diverges with the same exponent as the susceptibility and the percolation point coincides with the Curie point in this approach also in three dimensions.

2.6 Time Evolution: Non-Homogeneous Poisson Process and Ornstein Uhlenbeck Process

If we want to simulate a real crash, we need a time evolution of the crash hazard rate $h(t)$ due to varying networks, as well as a realization of the crash time t^*. To achieve the former, we can set p linear in time as a first simple time evolution. Another possibility is the Ornstein-Uhlenbeck process. To achieve the latter, we simulate the random variable by a non-homogeneous Poisson Process realization. We summarize the Poisson-process and the Ornstein-Uhlenbeck process in the following.

2.6.1 Non-Homogeneous Poisson Process

Poisson processes are a convenient tool if the intensity function is very small and these rare events have high impact. Poisson processes are used to simulate radioactive decay in physics [21], phone calls [22] in socio-science or plate tectonics spontaneous stress release in geology [23]. Our application of the Poisson process will be in close analogy to the stress-release simulation in seismology. Bubbles in our case correspond to the stress between tectonic plates and the crash acts like a release. The crash hazard rate $h(t)$ plays the roll of the intensity function which we will introduce in the following.

Point Process

For our purposes we consider a point process on the real line in continuous time. A point process j on the real line is nothing else than a counting measure. It can be seen as counting the occurrences of some events which happen at certain times $\{t_i\}$ [24]. A temporal point process dj can take only one of two possible values at each time-step t, i.e.,

$$dj(t) \in \{0, 1\} \qquad \forall t \tag{2.15}$$

The value $dj(t) = 1$ indicates that an event occurs at that time t and the value $dj(t) = 0$ indicates that the event does not occur at time t.

The event is the crash in our case. A crash occurs if the point process takes the value $dj(t) = 1$, and for all other times the process takes the value $dj = 0$. Recall that a crash is described via the crash hazard rate $h(t)$ which is the probability of having a crash in the infinitesimal time interval between $[t, t + dt]$ and thus $dj(t) = 1$. The probability for having no crash, in numbers $dj(t) = 0$, is the complementary probability $1 - h(t)$.

Renewal Process

As we are only interested in the behavior before the crash, we use a renewable process [24]. The formal definition might be a bit abstract, but we will soon relate it to our model:
Consider $\{X_i\}$ a collection of real-valued iid random variables with distribution function F. Then the renewal process is

$$N(t) = \sum_{k=1}^{\infty} 1_{\{S_k \leq t\}}, \text{ where } S_k = \sum_{i=1}^{k} X_i.$$

In our model the random variables $\{X_i\}$ are the time between two subsequent crashes. Its distribution function F is therefore also called the interarrival distribution function. Thus, the sum of the $\{X_i\}$, $S_k = \sum_{i=1}^{k} X_i$ is the time till the k-th crash. Our indicator function $1_{\{S_k \leq t\}}$ then clearly is equal to zero if k crashes did not happen before or at time t, and is equal to one if k crashes did happen before or at time t. Hence, $N(t)$ is our renewal process which counts the number of crashes till and including time t.

Homogeneous Poisson Process

The simplest class of a point process is the Poisson process [24][25]. It is a renewal process characterized by the fact that the interarrival distribution function F is the exponential distribution with parameter λ_0 (which one can show to be also the expected events per unit time). The Poisson process has

a conditional intensity function that gives the expected events per unit time as $\lambda(t|H_t)$. If the process is in addition independent of time t, it is called a *homogeneous Poisson process*. It has a constant conditional intensity function that gives the expected events λ_0 per unit time as

$$\lambda(t|H_t) = \lambda_0. \tag{2.16}$$

The number of events $k = N(t+dt) - N(t)$ in the time interval $[t, t+dt]$ follows a Poisson distribution with associated parameter $\lambda_0 \cdot dt$ explaining the name:

$$P(k) = \frac{e^{-\lambda_0 dt}(\lambda_0 dt)^k}{k!} \qquad k = \{0, 1, 2, \ldots\} \tag{2.17}$$

An algorithm that simulates a homogeneous Poisson process with intensity λ_0 up to an end time T has to determine all the times t_N of event occurrences for $t < T$. This can be done by the following algorithm with intensity λ up to time T [26]:

Algorithm Homogeneous Poisson process

1. $t = 0$, $N = 0$
2. Generate random variable $r = \text{uniform}(0, 1)$.
3. Event time: $t + [-\frac{1}{\lambda_0}\log(r)]$. If $t > T$, then stop.
4. Set $N = N + 1$ and $t_N = t$.
5. Go back to 2.

Non-Homogeneous Poisson Process

A *non-homogeneous Poisson process* [25] is a Poisson process with time-dependent intensity function $\lambda(t)$

$$\lambda(t|H_t) = \lambda(t). \tag{2.18}$$

It is still independent of the history of past events. The expected number of events in the time interval $[a, b]$ has to be calculated using an integral:

$$N_{\text{t,t+dt}} = \int_t^{t+dt} \lambda(s)ds. \tag{2.19}$$

The probability distribution for $k = \{0, 1, 2 \ldots\}$ events in the time-interval $[t, t+dt]$ becomes a Poisson distribution with associated parameter $N_{\text{a,b}}$:

$$P(k) = \frac{e^{-N_{\text{a,b}}}(N_{\text{a,b}})^k}{k!} \tag{2.20}$$

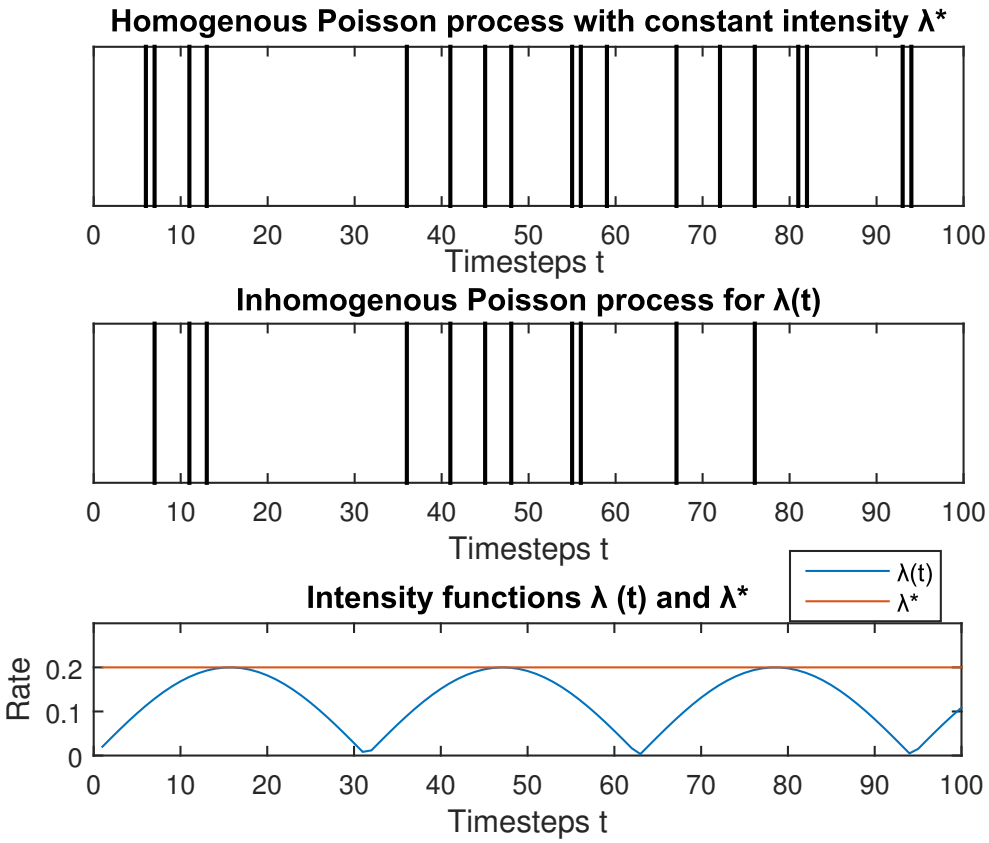

Figure 2.5: Simulations of a homogeneous Poisson process with intensity function $\lambda*$ and of a non-homogeneous Poisson process with intensity function $\lambda(t)$. The event times of the latter one are the "thinned" event times of the former. The third plot exhibits the corresponding intensity functions.

It is more difficult to simulate a non-homogeneous Poisson process than a homogeneous one. Here, we use the thinning method [27]. The intuitive idea is the following: one determines the maximum of the intensity function $\hat{\lambda} = \max(\lambda(t))$, then simulates a homogeneous Poisson process with intensity $\hat{\lambda}$ and finally "thins" the occurred events by an acceptance/rejection algorithm. The homogeneous Poisson process with the maximum intensity $\hat{\lambda} = \max(\lambda(t))$ gives too many events. The acceptance/rejection algorithm reduces the times of the events to t_N which are a good realization of the true values. This can be done by the following algorithm:

Algorithm Non-homogeneous Poisson process (Thinning) [26]

1. $t = 0$, $N = 0$
2. Generate random variable $r_1 = \text{uniform}(0, 1)$

3. Event time: $t + \left[-\frac{1}{\hat{\lambda}} \log(r)\right]$. If $t > T$, then stop.
4. Generate random variable $r_2 = \text{uniform}(0, 1)$
5. If $r_2 \leq \frac{\lambda(t)}{\hat{\lambda}}$, then set $N = N + 1$ and $t_N = t$.
6. Go back to 2.

Figure 2.5 illustrates this. Simulations of a homogeneous Poisson process with intensity function $\lambda*$ and of a non-homogeneous Poisson process with intensity function $\lambda(t)$ are given as well as a plot of the two intensity functions. The non-homogeneous event times are the "thinned" event times of the homogeneous Poisson process.

2.6.2 Ornstein-Uhlenbeck Process

We will describe our control parameter as a random walk trapped in a quadratic potential. We use the Ornstein-Uhlenbeck (OU) process [28] which exhibits exactly these properties. The process is mean reverting which means that it drifts to a long-term mean value over time. Mathematically spoken, it is a stationary, Gaussian and Markovian process. It is the continuous time analogue of the discrete auto-regressive model AR(1).

The Ornstein-Uhlenbeck process is a stochastic process that satisfies the following stochastic differential equation

$$dp_t = \vartheta(\mu - p_t)dt + \sigma dW_t, \tag{2.21}$$

with the parameters:

1. W_t is a standard Brownian motion on $t \in [0, \infty)$;
2. $\vartheta > 0$ is the rate of mean reversion;
3. μ is the long-term mean of the process;
4. $\sigma > 0$ is the volatility or average magnitude of random fluctuations that are modeled as Brownian motions.

If we ignore the random fluctuations due to the Brownian Motion W_t in the process, we see that X_t has an overall drift towards a mean value μ. The process X_t reverts to this mean exponentially, at rate ϑ. The magnitude of this reversion is in direct proportion to the distance between the current value of X_t and μ. Consequently, the overall drift exhibits indeed a quadratic potential. Two realizations of the OU-process are shown in figure 2.6. In the top plot, parameters are chosen such that the excursions are short. The process reverts very fast to its mean value (short memory). In the bottom plot, parameters are chosen such that excursions are long. The process reverts very slowly to the mean value (long memory).

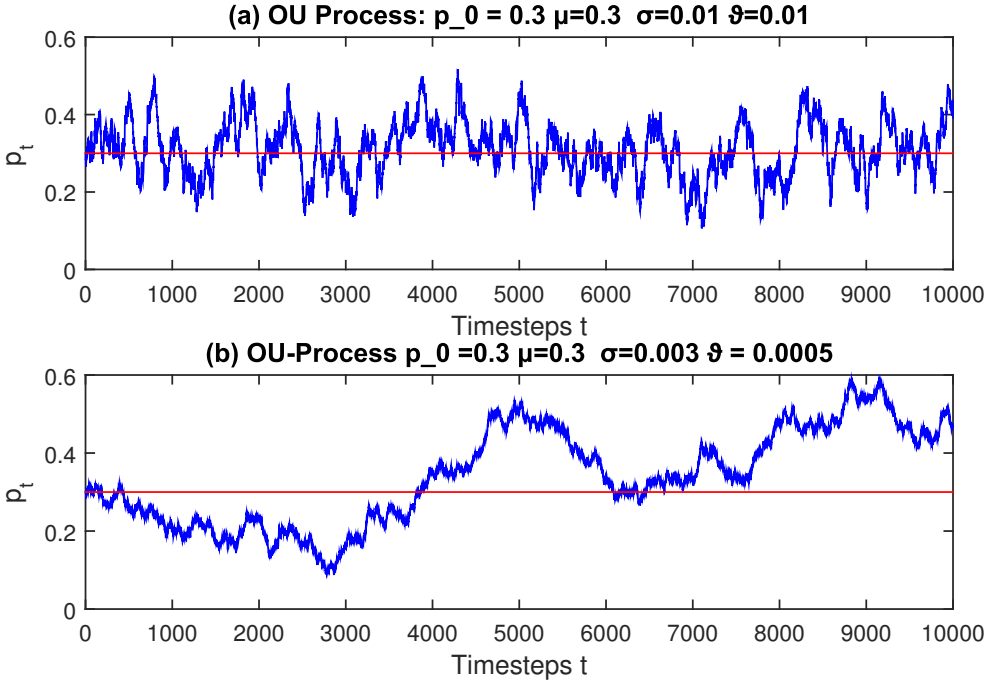

Figure 2.6: Two realizations of the OU-process. (a) Parameters are chosen such that the excursions are short, the process reverts very fast to its mean value (short memory). (b) Parameters are chosen such that excursions are long return very slowly to the mean value (long memory).

Chapter 3

Results I: New Description of The Crash Hazard Rate

In this chapter, we present a framework that allows us to determine the crash hazard rate, and simulate crashes and bubbles described by the crash hazard rate. First, we reformulate the access to the crash hazard rate presented by Cont and Bouchaud in [9] and by Sornette in [6] by using cluster dynamics and super-linear relations between contributions and group sizes. The second part derives a theoretical estimate of a power law divergence near a critical parameter using percolation theory. In the third part, we confirm our theoretical results by brute force simulations on the Potts model [29] for $q \to 1$ on the 2d square lattice. In the last part, we provide a second verification of the presented framework above using the Potts model with $q = 2$, also known as the Ising Model. Price simulations using this framework are presented in the next chapter.

3.1 Crashes as Large Cluster Sell-offs

In the JLS Model, the crash hazard rate gives the conditional probability that there is a crash at the time-step t given that the crash has not occurred yet. The product $h(t)dt$ is the probability that a crash occurs between t and $t + dt$. We introduce a cluster description of this deterministic variable by applying percolation theory.

A crash is a coordinated sell-off of a large number of agents. A large shift in the number of buyers and sellers in the market-book will occur if two conditions are fulfilled:

1. We need a huge network of imitating noise traders that are participating in the market. We make the same assumption as Cont and Bouchaud in their framework: Noise traders influence each other so strongly that everybody in the network does the same. The network be-

comes a herd consisting completely of either buying or selling agents. Mathematically, we state that we need a large network of size $s > s_m$ of synchronous agents. The specific value of s_m is investigated later.

2. One of these large networks must change its choice from buying to selling or the other way around. One trader is enough to carry the whole network since agents in a network are synchronous. For simplicity, we focus on positive bubbles and negative price crashes.

The probability $h(t)dt$ for a crash is the joint probability for all possibilities of having the two independent conditions above both fulfilled. We use graph theory to describe the networks of the traders. They are represented by sites and the networks by bonds. Two traders which influence each other are represented by a bond connecting them. We can generate a graph that represents the network and obtain clusters of connected, in the market participating, traders. Percolation theory provides a mathematical expression for condition (1). The probability of having a network of size s is expressed by the cluster number $n_t(s)$. The clusters can change in time, therefore, the cluster number is also a function of time t. Of course, the choice of such a cluster can vary with time. We call a change from buying to selling or the other way around the network becomes *active*. We denote with $P_{\text{active}}(s)$ the probability that a cluster of size s gets active in a time interval of length dt. This is the second condition stated above. How often does a cluster become active? What influences the choice of the group? Group dynamics are often described by super-linear relations. It has been found out that the social quantities of cities (such as productions or new inventions) scale super-linearly with its population [30]. More recently, a super-linear dependence between contributions in Open-Source programs and the number of contributors has been discovered [31]. The following equation with the variables R as productivity and N as group size holds in both cases.

$$R \propto N^a \tag{3.1}$$

The triggering activity of an investment for a group of size s can be described in analogy to such a production or activity process benefiting from collective interactions and processes similar to or the same as those for production and productivity. Thus, the rate R for a cluster being active can be expressed by a term which is super-linear in s with an exponent a. The probability $P_{\text{active}}(s)$ that there is an active trader in a cluster of size s in a time-interval of length dt becomes

$$P_{\text{active}}(s) \propto s^a dt. \tag{3.2}$$

Note that there is no time dependence in the probability for an active trader since it is a mean value over time.

Multiplying the probabilities for the two conditions and summing up over cluster sizes larger than s_m leads to

$$h(t)dt = \sum_{s=s_m}^{\infty} P_{\text{active}}(s)n(s). \tag{3.3}$$

We insert the super-linear relation and get

$$h(t)dt = dt \sum_{s=s_m}^{\infty} s^a n_t(s). \tag{3.4}$$

This holds for all time and we can access the crash hazard rate:

$$h(t) = \sum_{s=s_m}^{\infty} s^a n_t(s) \qquad \forall t \tag{3.5}$$

We have not specified the value of s_m. We investigate this at the end of the next section.

3.2 Theoretical Derivation: The crash hazard rate diverges with a power law

Theorem 3.1 *The crash hazard rate h undergoes a critical transition near the percolation threshold for $a > \mu$. It diverges as a power law of the scaling parameter p that a site is occupied. The power law exponent is given by $\alpha = -\frac{a-\mu}{\sigma}$.*

$$h(p) \propto \frac{1}{a-\mu} \frac{1}{|p-p_c|^{\frac{a-\mu}{\sigma}}} \qquad \text{for } a > \mu \tag{3.6}$$

Proof Recall from the last section that we can write the crash hazard rate h as a deterministic probabilistic variable depending only on the clusters of the underlying network of traders.

$$h = \sum_{s=s_m}^{\infty} s^a n(s) \tag{3.7}$$

In section 2.2 we saw that there exists a cutoff size s^* above which there are no significant contributions to a sum over the cluster number. The cluster number can be approximated by a power law with exponent $\tau = 1 + \mu$ for $s < s^*$. Recall that the cut-off size equals the size of the largest clusters and diverges as a power law near the percolation threshold with scaling exponent σ:

$$s^* \propto \frac{1}{|p-p_c|^{\frac{1}{\sigma}}}. \tag{3.8}$$

Applying this to the sum above yields

$$h \propto \sum_{s_m}^{\infty} s^a n(s) \propto \sum_{s_m}^{s^*} \frac{s^a}{s^{1+\mu}} = \sum_{s_m}^{s^*} \frac{1}{s^{1+\mu-a}}. \tag{3.9}$$

The sum can be transformed into an integral without significant loss of accuracy via

$$h(p) \simeq \sum_{s_m}^{s^*(p)} \frac{1}{s^{1+\mu-a}} \simeq \int_{s_m}^{s^*(p)} \frac{ds}{s^{1+\mu-a}} \qquad \text{for } a \neq a\mu \tag{3.10}$$

The integral can easily be computed. We obtain:

$$h(p) \simeq \frac{-1}{\mu - a} \frac{1}{s^{\mu-a}}\Big|_{s=s_m}^{s=s^*(p)} = \begin{cases} \frac{1}{\mu-a}\left(\frac{1}{s_m^{\mu-a}} - \frac{1}{(s^*)^{\mu-a}}\right) & \text{for } a < \mu \\ \frac{1}{a-\mu}\left(s^*(p)^{a-\mu} - s_m^{a-\mu}\right) & \text{for } a > \mu \end{cases} \tag{3.11}$$

With $s^*(p) \gg s_m$, we can approximate

$$h(p) \simeq \begin{cases} \frac{1}{\mu-a}\frac{1}{s_m^{\mu-a}} & \text{for } a < \mu \\ \frac{1}{a-\mu} s^*(p)^{a-\mu} & \text{for } a > \mu \end{cases}. \tag{3.12}$$

We focus on the latter, $a > \mu$. As a last step, we insert the power law in p for s^* (equation (2.9)) and arrive at

$$h(p) \propto \frac{1}{a-\mu} \frac{1}{|p - p_c|^{\frac{a-\mu}{\sigma}}} \qquad \text{for } a > \mu. \tag{3.13}$$

□

We still have not specified the value of the minimum cluster size s_m for a crash. According to our derivation above, s_m must be much smaller than the cut-off size s^*. On the other hand, we need a large shift in the market book in order to have a crash. The Kyle model states [8]

$$p \simeq \frac{1}{D}(B(t) - S(t)) \propto \frac{1}{N(t)}(B(t) - S(t)). \tag{3.14}$$

The price of an asset is proportional to the difference between the number of buyers $B(t)$ and the number of sellers $S(t)$ at a given time t. The constant is $1/D$ with D denoting the market depth. The market depth is proportional to the number N of traders that are actively participating in the market. The larger the number of traders, the more extreme the difference in the market book must be in order to obtain the same price change. We conclude that the minimum cluster size depends on the number of traders in the market N. But how many percent of traders are needed to cause a crash? It is not an

easy task to state a concrete value. Therefore,we will assume that clusters must be larger than 1% of the active traders and keep in mind, that this value might actually be larger. We state:

$$s_m = 0.01 \cdot N \tag{3.15}$$

3.3 Explicit Calculation: The crash hazard rate determined by the Site Percolation Model

This section presents the results for the crash hazard rate h calculated explicitly using the site percolation model. It is the limit of the Potts model for $q \to 1$. As underlying graph we always use the two dimensional square lattice with open boundary conditions. We allow traders to be in two states: They are either actively participating in the market if their site is occupied or not actively participating if their corresponding site it unoccupied. Bonds are only between nearest neighbors as we are on the square lattice. Recall that, on the square lattice, nearest neighbors are in the same cluster if they are both occupied. Clusters are formed in dependence of which trader are actively in the market. The number of active participants in the market drives the crash hazard rate. For large lattices, it is related in good approximation directly to the probability p that a site is occupied. The probability p becomes in the following the control parameter of our system. Note that this framework is also used to describe dilute magnets in combination with the Ising model [10]. The spontaneous diverging susceptibility is the analogous phenomena to the diverging crash hazard rate. The first part reproduces the most important results of percolation theory and the properties of its clusters on the square lattice. The second part presents the crash hazard rate as a function of the probability that a site is occupied. We investigate the dependence of the crash hazard rate on the square lattice size L, the superlinear exponent a and the control variable p. We end this section with the determination of the explicitly calculated power law exponent α_{exp} of the crash hazard rate and a comparison to the theoretical estimation α derived above.

3.3.1 Cluster Number and Finite Size Effects

For a lattice of infinite length L at the critical point p_c, the cluster number $n(s)$ is a power law distribution as a function of the cluster size s. We reproduce the so-called Fisher exponent τ for a lattice of size $L = 1000$ in figure 3.1. We obtain $\tau = -1.95$ by a linear regression in the log-log-plot. Note that we use logarithmic binning to reach values up to $n(s) \simeq 10^{-12}$ instead of $n(s) \simeq 10^{-6}$. Our result is in good agreement with the analytic value $\tau_{\text{theo}} = 187/91 \simeq 2.05$ [10]. We can also estimate the Fisher exponent applying the Hill estimator. This yields $\tau = 1.88$ and we see

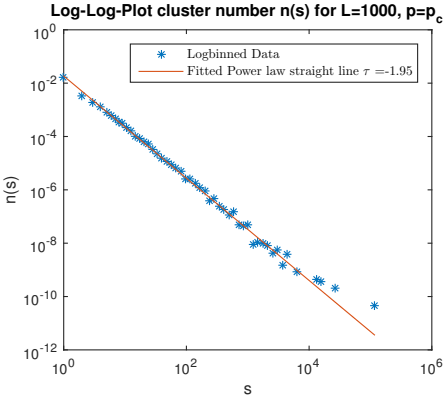

(a) Log-log-plot of the cluster number $n(s)$ versus the cluster size s at the percolation threshold p_c. The linear regression of the logarithmically binned data provides the Fisher exponent $\tau = -1.95$. This is very close to the analytic value $\tau_{\text{theo}} = \frac{187}{91} \simeq 2.05$. Using the Hill estimator instead yields $\tau = 1.88$.

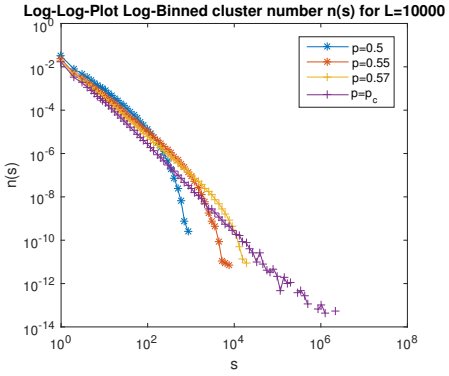

(b) Log-log-Plot of the cluster number $n(s)$ versus cluster size s for different site occupation probabilities p. Exponential decay is visible for $p < p_c$ leading to the cut-off in sums over the cluster number.

Figure 3.1: Cluster number $n(s)$

that the logarithmic binning gives a better estimate than the popular Hill estimator in our case.

In the theoretical derivation of the crash hazard rate, we use the exponential cut-off for contributions in the sum over the cluster number. We visualize the exponential factor $\exp(-s/s^*)$ in the cluster number on the square lattice of size $L = 10000$ in figure 3.1. For probabilities p smaller than the critical percolation probability p_c, the cluster number $n(s)$ indeed exhibits the exponential decay.

Lowering the lattice size to $L = 100$ and $L = 10$, we can investigate the so-called finite size effects on the cluster numbers and provide a value for the shift for the percolation threshold. In figure 3.2, we see that the cluster number becomes little volatile for $L = 100$ and highly volatile for $L = 10$. The further we are away from the $L \to \infty$ limit, the stronger the cluster number deviates from the deterministic curve presented above. The curves for $L = 1000$ and $L = 100$ are identical up to the volatility. This confirms the fractal structure of the clusters, also called self-similarity. What happens to the percolation threshold for these lattice sizes? Again, if we are further from the $L \to \infty$ limit, we will have larger volatility. As figure 3.2 shows, the probability of having an infinite cluster is no longer a sharp step-function. The smaller the lattice size, the more blurred the percolation threshold becomes. But it is not the only finite size effect on the percolation threshold. If we take the point where the infinity cluster probability becomes $P_\infty = \frac{1}{2}$

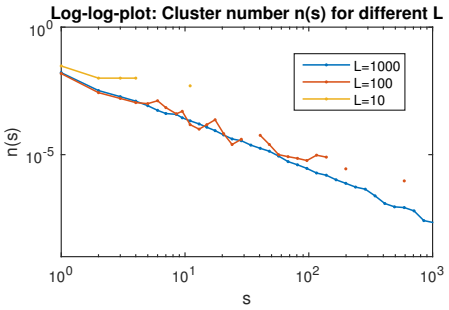

(a) Log-log-Plot of the cluster number $n(s)$ versus the cluster size s for different lattice sizes L at $p = p_c$. Finite size effects lead to a volatile cluster number for $L = 100$ and $L = 10$.

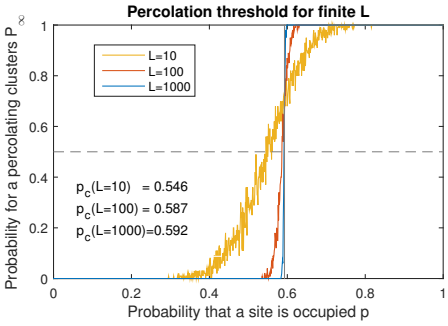

(b) Plot of the probability of having a percolating cluster as a function of the probability p of a site being occupied for different lattice sizes L. The step-function transition at $p_c = 0.592746$ in the $L \to \infty$-limit gets more and more blurred for smaller sizes L and is shifted to the left.

Figure 3.2: Finite size effects

as the percolation threshold, we see a shift to the left depending on the lattice size. The smaller the lattice size, the larger the shift (see table 3.1). We can confirm the well-known results from percolation theory. These finite size effects are important for the analysis of the crash hazard rate which we present in the next section.

L	10	100	1000	$L \to \infty$
p_c	0.546	0.589	0.592	0.593

Table 3.1: Shift of the percolation threshold p_c for finite lattice sizes L.

3.3.2 Crash hazard rate h_{exp} for varying square lattice size L

We present the results for the explicitly calculated crash hazard rate $h_{\text{exp}}(p)$ for lattice sizes L of three different orders. We initialize a new random site percolation lattice for each value of p. We extract the clusters and calculate the crash hazard rate $h(p)$. Note that if we want to compare the results to the theoretical crash hazard rate, we have to scale the theoretical crash hazard rate by a constant $C_<$(see equation (3.6)) in the phase $p < p_c$ and by a constant $C_>$ in the phase $p > p_c$. The two constants are not equal because the amplitude of the two phases are not equal [32]. The constants are set to the mean of the ratio $h_{\text{theo}}(p_i)/h_{\text{hexp}}(p_i)$ for values of p in the according phase.

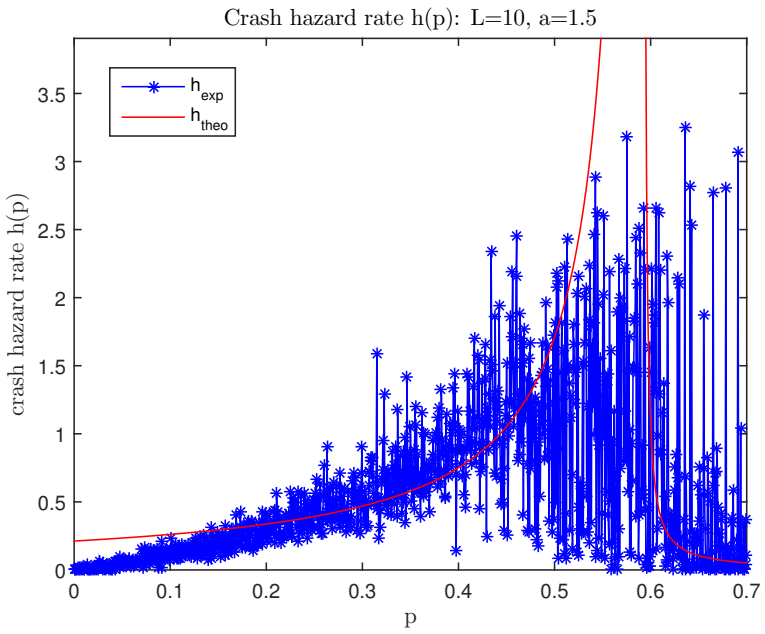

Figure 3.3: Plot of the explicitly calculated crash hazard rate $h_{\text{exp}}(p)$ (blue) and the theoretical one $h_{\text{exp}}(p)$ (red) for a single realization on the $L = 10$ square lattice. The crash hazard rate increases slightly and the volatility increases strongly for growing control parameter p. But the power law behavior is cut off already near $p \simeq 0.5$ far away from the critical point.

The explicitly calculated crash hazard rate $h_{\text{exp}}(p)$ on a 10×10 square lattice is not diverging with a power law as one reaches the percolation threshold of the $L \to \infty$ limit. Though it is near the red line of the theoretical power law for values larger of the control parameter larger than 0.2 and smaller than 0.5. We have power-law behavior starting near $p = 0.2$ which is already cut off near $p \simeq 0.5$. Finite size effects are dominating on small lattices and are the explanation for the the cut-off. For this order of lattice size, there is a small maximum for the size of the biggest cluster s^* which is reached very fast. This leads to a limit for the explicitly calculated crash hazard rate $h_{\text{exp}}(p)$. The cluster number $n(s)$ and the percolation point p_c are still a random variable for this size. We conclude that finite size effects influence the crash hazard rate strongly for lattices of size $L = 10$. Finite size effects lead to a cut-off in the power law behavior and an increasing volatility.

The explicitly calculated crash hazard rate $h_{\text{exp}}(p)$ on a square lattice of size $L = 100$ shows a divergence if one approaches the percolation threshold $p_c(L = 100) = 0.587$. This divergence is in good agreement with the power law divergence of the theoretical crash hazard rate $h_{\text{theo}}(p)$. As figure 3.4 shows, the blue points ($h_{\text{exp}}(p)$) are well described by the red curve ($h_{\text{theo}}(p)$)

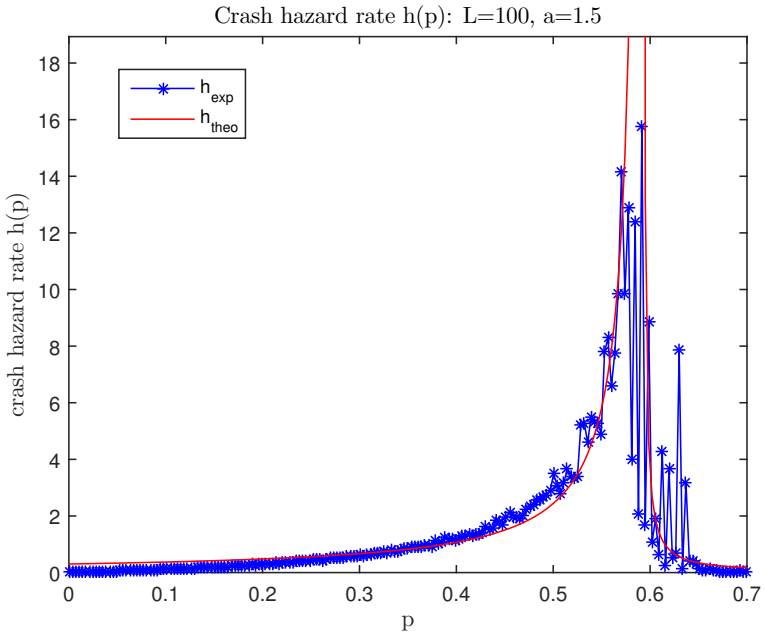

Figure 3.4: Plot of the explicitly calculated crash hazard rate $h_{\text{exp}}(p)$ (blue) and the theoretical one $h_{\text{exp}}(p)$ (red) for a single realization on the $L = 100$ square lattice. The crash hazard rate shows a divergence if one approaches the percolation threshold p_c. This is in a good agreement with the theoretical estimate. The volatility is increased in the critical region.

up to $p = 0.55$. The volatility starts to increase much later than in the previous case. Finite size effects also start later, but are still visible. As seen in the previous section, the percolation transition is still not a sharp step function and the probability of having a percolating cluster becomes blurred. As before, the cluster number $n(s)$ is random influenced. The crash hazard rate h(p) gets massively lowered if we turn an almost percolating biggest cluster into a percolating cluster, since the percolating cluster is no longer considered in the sum over all cluster sizes and the crash hazard rate $h_{\text{exp}}(p)$ decreases strongly. Thus, the crash hazard rate also takes small values near the percolation threshold, leading to a high volatility.

The explicitly calculated crash hazard rate $h_{\text{exp}}(p)$ on a 1000×1000 square lattice shows a clear divergence when one approaches the percolation threshold p_c. Figure 3.5 shows clearly that the red and the blue curve are almost identical. We have a relatively sharp percolation transition: For the control parameter $p = 0.6$ still close to p_c, the crash hazard is drastically decreased with respect to the peak. The increase in the volatility, which we observed in the preceding results, is no longer visible. Finite size effects become negligible for $L = 1000$. The square lattice of 1000×1000 sites exhibits a

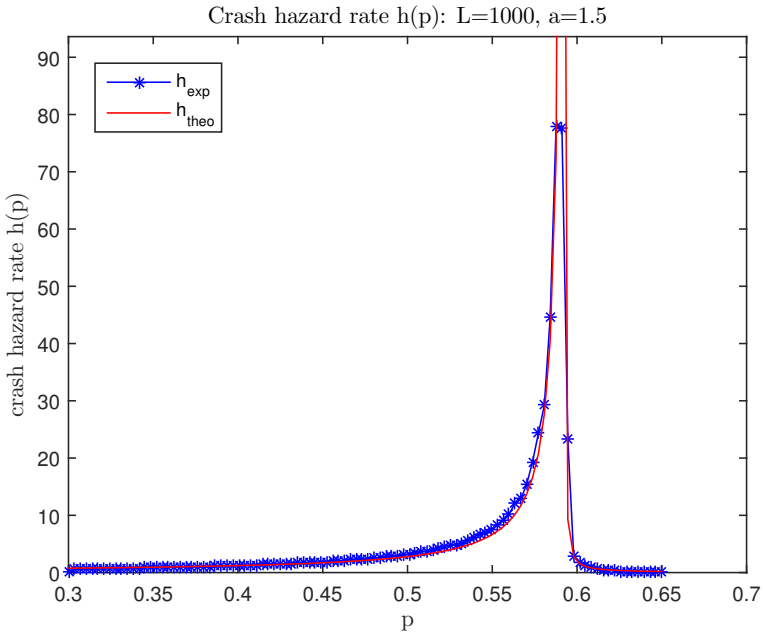

Figure 3.5: Plot of the explicitly calculated crash hazard rate $h_{\text{exp}}(p)$ (blue) and the theoretical one $h_{\text{exp}}(p)$ (red) for a single realization on the $L = 1000$ square lattice. The crash hazard rate shows a divergence in very good agreement with the theoretical estimate. For a large lattice, one can observe a self-averaging property. No volatility is visible and finite size effects are negligible.

self-averaging property and is convenient to filter finite size effects such as raising volatility. Graphs get clearer if they are not blurred by raising volatility. However, as we will see later, finite size effects are again visible if we consider intervals closer to the percolation threshold.

3.3.3 Crash hazard rate h_{exp} for varying super-linear contribution exponent a

What will happen if we vary the super-linear coefficient a which determines the probability that the cluster becomes active?

In order to investigate this issue, we plot the explicitly calculated crash hazard rate $h_{\text{exp}}(p)$ for four different super-linear contribution exponents a with all other parameters kept constant. The realization of the networks is done as in the previous case. We initialize a random site percolation lattice for each value of p and calculate the crash hazard rate $h(p)$. We use the same lattice initialization for all four values of a. The underlying network for each plot is thus the same. The lattice size is chosen to be 100×100 in order to

avoid high volatility. Figure 3.6 shows the crash hazard rate for a broad spectrum of the super-linear exponent a. It takes values in the range $a \in [1, 2]$. Figure 3.7 exhibits the behavior for four values near the potential critical value of $a = \mu \simeq 1.05$.

In Figure 3.6, we see that no divergence is visible for $a = 1 < 1.05 \simeq \mu$. Indeed, the crash hazard rate $h_{\exp}(p)$ is the first moment and gets equal to the control parameter p following the well-known relation from percolation theory:

$$\sum_s s \cdot n(s) = \begin{cases} p & \text{for } p < p_c \\ p - C \cdot |p - p_c|^{\frac{5}{36}} & \text{for } p > p_c \end{cases} \tag{3.16}$$

If the percolating cluster occurs, it lowers the sum as already explained above. This lowering explains the subtrahend in the second case. It is the strength or weight of the percolating cluster P with according exponent $\beta = \frac{36}{5}$ for the two dimensional square lattice.

All the three remaining curves satisfy $a > \mu$ and exhibit the expected divergence with increasing volatility near the percolation threshold p_c. The curves are very similar to each other differing only in the order of magnitude.

Figure 3.7 shows four plots with the super-linear coefficient near to its critical value $a = \mu = 1.05$. The graphs show very different characteristics. The first one, calculated for $a = 0.95$, is concave for $p < p_c$. It does not have the potential to diverge near the percolation threshold. The second graph, calculated for $a = 1$, has already been discussed above. This value seems to be the border between convex and concave crash hazard rates. The two latter graphs are convex curves. They would have the potential to diverge. However, the divergence is very moderate even very close to the percolation threshold p_c. We would have to come very close to the critical value in order to obtain divergence for such small power law exponents. Actually, all these four graphs have in common that the crash hazard rate does not take high values even close to p_c. We do not see an abrupt change in the crash hazard rate as one goes from $a < \mu$ to $a > \mu$ as one could have expected according to the theoretical considerations in section 3.2.

From these observations we infer that: If the super-linear coefficient is in the regime $a > \mu$, it determines only the degree of divergence of a convex function as does the exponent in a power law divergence. In the regime $a < \mu$, the crash hazard rate becomes a concave function and there is obviously no divergence. The transition from one regime to the other is not phase-transition-like, as the divergence emerges rather smoothly with increasing a.

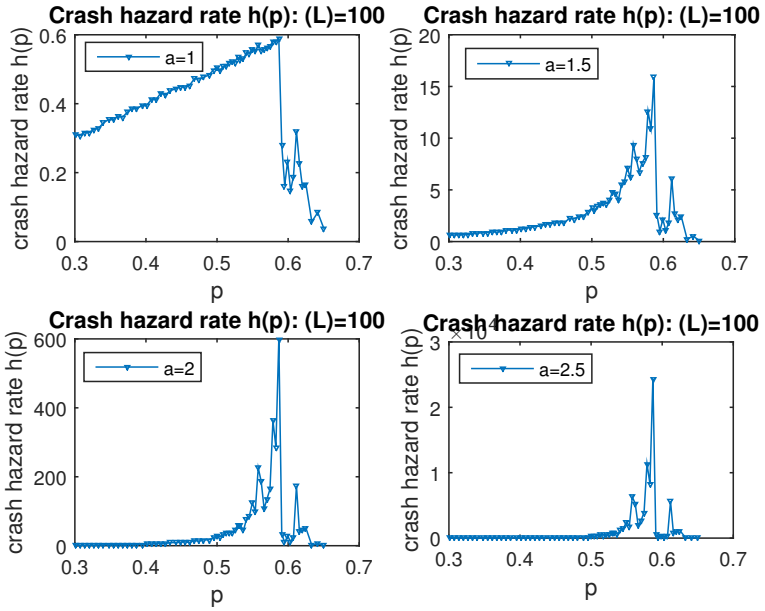

Figure 3.6: Plot of the explicitly calculated crash hazard rate $h_{\text{exp}}(p)$ for different superlinear contribution exponent a. Note that the underlying networks are the same for each plot. For $a = 1 < 1.05 \simeq \mu$, no divergence is visible. Indeed, the crash hazard rate gets equal to the control parameter p. All three remaining curves show divergence with increasing volatility near the percolation threshold p_c.

3.3.4 Comparing the exponent and investigating the robustness of the power law divergence

In this section, we corroborate the assumption of a power law behavior of the crash hazard rate close to the percolation threshold. We present results for the power law exponent α_{exp} of the explicitly calculated crash hazard rate. Furthermore, we check the robustness of the result of the exponent. We use a square lattice of size $L = 100$ respectively $L = 1000$ and vary the superlinear coefficient a to get intervals of validity for the control parameter p. We use linear regression in the shifted log-log-plot to extract the power law exponent α_{exp} of the explicitly calculated crash hazard rate $h_{\text{exp}}(p)$. Note that we use the value that gives the best fit to a power law (least square method) for p_c. The two values $p_c(L = 100) = 0.5915$ and $p_c(L = 1000) = 0.5924$ are in good agreement with the shifted percolation points due to finite size effects calculated in (3.3.1).

The theoretical straight line with gradient $\alpha_{\text{theo}} = -1.13$ seems to be accurate for $0.4 < p < 0.55$ on the square lattice with size $L = 100$ and for $0.4 < p < 0.59$ on the square lattice with size $L = 1000$ (see figure 3.8). However,

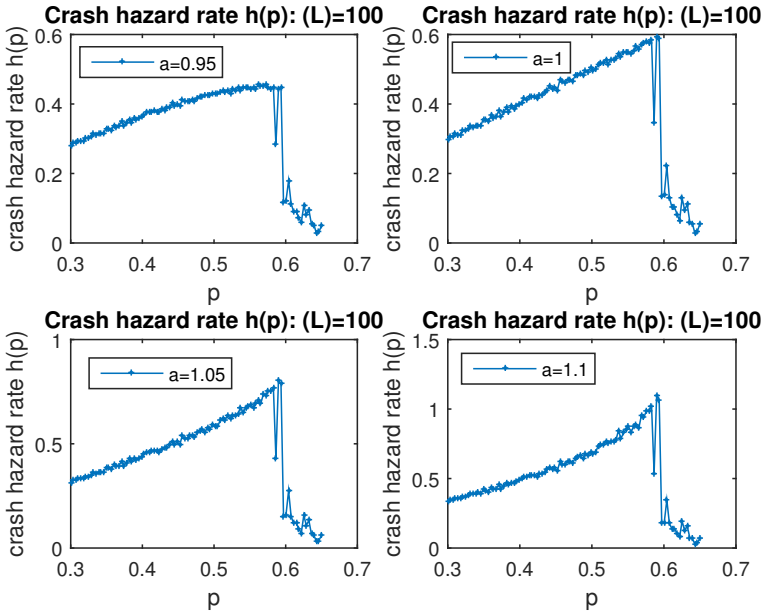

Figure 3.7: Plot of the explicitly calculated crash hazard rate $h_{\text{exp}}(p)$ for super-linear contribution exponents near the critical value $a = 1.05$. The crash hazard rate does not take high values even close to p_c in any graph. Note that the underlying networks are the same for each plot.

systematic deviations from the power law straight line arise for values $p < 0.4$ as well as for values $p > 0.59$. The deviated values are lower than the expected ones. The two curves differ in their behavior near the percolation threshold. Deviation starts near $p = 0.55$ for $L = 100$ and much more later, namely $p = 0.59$, for $L = 1000$. Explanations for these observations are given below.

We compare the results for the exponent of the explicitly calculated crash hazard rate to the theoretical exponent in table (3.2). The values for the former are obtained by linear regression where the deviated values are excluded.

The first row of the table presents the result for the square lattice of size $L = 100$. The control parameter p is confined to the interval $[0.4, 0.55]$ to avoid the outliers. The theoretical exponent α_{theo} seems to be a reasonable estimate, although systematic deviations are visible. The exponent α is lower for small super-linear exponents a than the theoretical one and higher for larger a.

The second row presents the result for the lattice of size $L = 1000$. As seen in figure 3.8, the deviation starts later than for the lattice size $L = 100$ and we

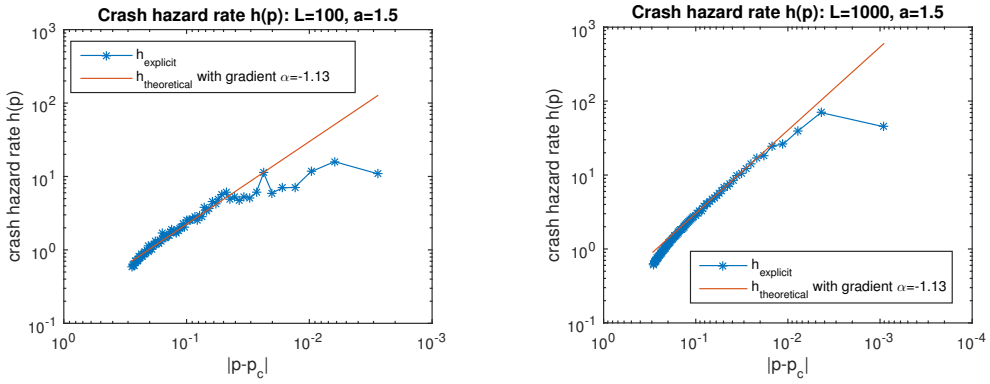

Figure 3.8: Reversed log-log-plot of the explicit calculated crash hazard rate $h_{\text{exp}}(p)$ versus $|p_c - p|$ for the super-linear exponent $a = 1.5$ and square lattice sizes $L = 100$ on the left and $L = 1000$ on the right. The theoretical straight line with exponent $\alpha_{\text{theo}} = -1,13$ seems to be accurate for $0.4 < p < 0.55$ on the left and $0.4 < p < 0.59$ on the right. Note that we use the value that gives the best fit for p_c. The actual values on the horizontal line are the difference $|p - p_c|$.

can confine the control parameter to a larger interval $[0.4, 0.59]$. The majority of the exponents get slightly closer to its theoretical estimate, but differences are still visible.

The third row presents the result for the lattice of size $L = 1000$ with the control parameter confined to an interval closer to the percolation threshold $[0.5, 0.59]$. The theoretical exponent α_{theo} is a very good estimate of these explicitly calculated exponents. We conclude that the larger the lattice size L and the more we confine the control parameter near to the percolation threshold, the better the theoretical estimate is. This can be explained as follows:

Finite size effects are responsible for the lowering of the exponent α for values close to the percolation threshold. Since the system is finite, the crash hazard rate cannot really diverge to infinity. This effect is called rounding in percolation theory. Values far away from the percolation threshold are lowered in the same way independently of the lattice size (compare figure 3.8 and 3.9). The lower bound of the power law regime is actually dependent on the super-linear exponent a. Figure 3.9 indicates that the power law behavior begins earlier the larger the super-linear exponents is. For an exponent of $a = 2$, the power law regime seems to begin at least near $p = 0.4$ while we reach the the power law regime not until $p = 0.52$ for $a = 1.1$. These finite size effects explain why we get the best results in the third column in table (3.2): For larger lattice sizes, the influence of finite size effects on our

Table 3.2: Comparison of the explicitly calculated exponents $\alpha[100]$ and $\alpha[1000]$ versus the theoretical value $\alpha_{\text{theo}} = -\frac{a-\mu}{\sigma}$. The number in the square bracket denotes the square lattice size L. Only values of the control parameter in the given interval are used to extract the exponent.

a	$\alpha[100]$ $p \in [0.4, 0.55]$	$\alpha[1000]$ $p \in [0.4, 0.59]$	$\alpha[1000]$ $p \in [0.5, 0.59]$	α_{theo}
1.05	-0.19	-0.25	-0.18	0
1.2	-0.51	-0.49	-0.46	-0.37
1.33	-0.73	-0.72	-0.70	-0.70
1.5	-1.14	-1.16	-1.15	-1.13
1.67	-1.49	-1.58	-1.54	-1.55
2	-2.09	-2.31	-2.37	-2.39
2.5	-3.02	-3.48	-3.43	-3.65
3	-4.19	-4.78	-4.81	-4.92

results decreases. Additionally, we can push our interval closer to p_c. This improves the results as we can put more weight on values close to the percolation point. If we confine ourselves to the interval $p \in [0.5, 0.6]$, for which the explicitly calculated crash hazard rate does not diverge as a power law, are then mostly excluded.

Estimations of boundaries for the validity of the theoretical estimation of the exponent α depend both on the super linear exponent a and on the square lattice size L. Finite size effects are visible in the region of $p > 0.54$ for a square lattice of size $L = 100$, and in the region of $p > 0.58$ for a square lattice of size $L = 1000$ in our results. We take these values as our estimation for the upper boundaries. For both lattice sizes, the theoretical estimation $\alpha = -\frac{a-\mu}{\sigma}$ seems to be invalid near $p = 0.3$. Indeed, the beginning of the straight line does not depend on the lattice size L but on the super linear exponent a.

3.3.5 Conservative Traders

We have seen high volatility in the crash hazard rate above for lattice sizes $L = 10$ and even $L = 100$. We re-initialized the whole lattice for every value of p. We implicitly assumed that traders can change frequently from participating to not participating. If we want a framework for more conservative traders that do not change their choice so often, we consider to initialize the lattice by adding site by site. Clusters are created and grow the same way as before. The number of participating traders N becomes deterministic being our control parameter which is clearly related to the former control

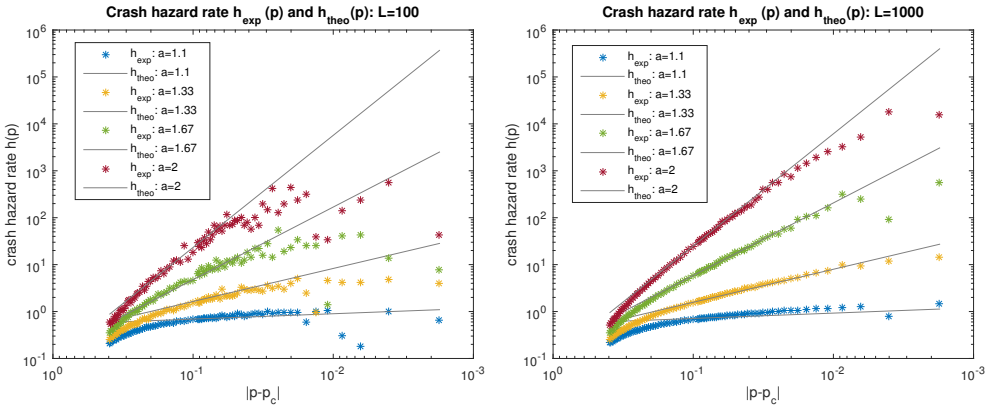

(a) Plot of the explicitly calculated crash hazard rate $h_{\exp}(p)$ for super-linear contribution exponents $a = (1.1, 1.5, 1.67, 2)$ on the square lattice of size $L = 100$.

(b) Plot of the explicitly calculated crash hazard rate $h_{\exp}(p)$ for super-linear contribution exponents $a = (1.1, 1.5, 1.67, 2)$ on the square lattice of size $L = 1000$.

Figure 3.9: Crash hazard rate for different super-linear coefficient a. The lower bound for power law behavior is depending on the super-linear exponent a. Rounding due to finite size effects can be lowered for larger lattice sizes L.

parameter:

$$p = \frac{N}{L^2} \tag{3.17}$$

The main difference to above is that clusters cannot change abruptly when we slightly adjust the control parameter as we just add some sites and do not reinitialize the whole lattice. Figure 3.10 exhibits of the crash hazard rate under this modification for a single realization. The crash hazard rate is a much less volatile curve as large cluster changes are no longer possible. Figure 3.10 illustrate diverging curves for very small lattice sizes of $L = 4$ and $L = 10$. Yet, we get very different peaks for different realizations. Furthermore, we observe that the crash hazard rate is again not symmetrical as the the decay is rounded off on the right side of the threshold. Finally, note that the difference between the two ways of calculating the crash hazard rate becomes more and more less for larger lattice sizes. Therefore, we use only the one presented first for our price simulations.

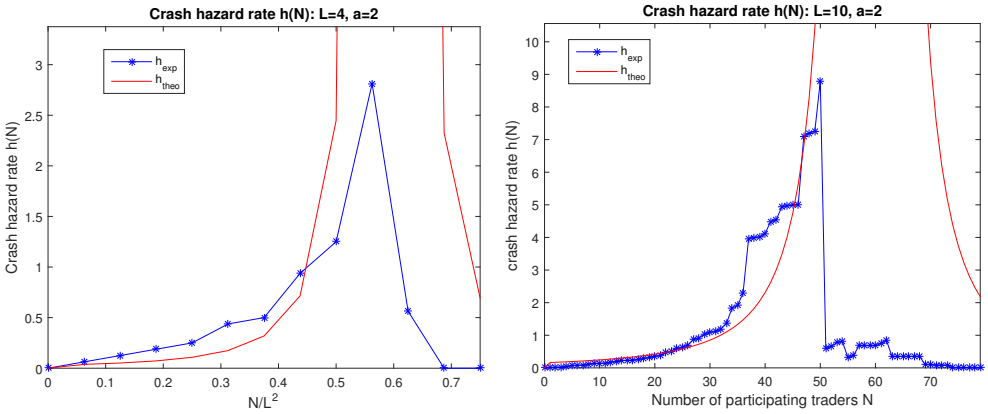

(a) Plot of the explicitly calculated crash hazard rate $h_{\text{exp}}(N)$ (blue) and the theoretical one $h_{\text{exp}}(p)$ (red) for a single realization on the $L = 4$ square lattice. We increase the new control parameter N by adding site by site. The crash hazard rate is diverging near $N/L^2 = 55$ in this realization. We see much less volatility in contrary to the previous results where we re-initialized the whole lattice for each new value of the control parameter.

(b) Plot of the explicitly calculated crash hazard rate $h_{\text{exp}}(N)$ (blue) and the theoretical one $h_{\text{exp}}(p)$ (red) for a single realization on the $L = 10$ square lattice. We increase the new control parameter N by adding site by site. The crash hazard rate is diverging near $N = 50$ in this realization. We see much less volatility in contrary to the previous results where we re-initialized the whole lattice for each new value of the control parameter.

Figure 3.10: Crash hazard rate for fixed number of participants realized by adding site by site.

3.4 A second approach to the crash hazard rate via Ising Clusters

In this section, we present another confirmation of the divergence of the crash hazard rate. We use again site percolation on the square lattice as underlying graph, but this time, we use the Ising model and Glauber dynamics to create clusters. The Ising model is the Potts model if we choose $q = 2$. In our model, sites describe traders that are participating in the market by choosing one of two states: spin-up stands for ”buying” or ”bullish” and spin-down for ”selling” or ”bearish”. Clusters are defined as all sites of equal spin which are connected via a nearest neighbor path. Coniglio and Klein called them Ising clusters, so we will also use this name in the following. The inverse temperature of the Ising model $K = \frac{J}{kT}$, with coupling constant J between nearest neighbors, plays the role of the control parameter. It describes the imitation strength between traders. The first part of this section presents the properties of the Ising clusters. The second part provides the crash hazard rate as a function of the control parameter K for different lattice sizes L. We end this section with the determination of the exponent α_{exp} and a comparison with the theoretical approximated exponent α_{theo}.

3.4.1 Cluster number for site percolation on the Ising model

First, we want to get familiar with the properties of the clusters created by Glauber dynamics. We investigate the critical value in our system and we confirm Coniglio and Klein's theory of the relation between the Ising critical points and the percolation point. This is followed by a section about the Ising cluster number analogously to the treatment of the cluster number of random graph site percolation above.

The critical point in our model is the percolation threshold of K. Figure 3.12 and 3.13 show the probability of having an infinite cluster P_∞ and the magnetization m as a function of the Ising control parameter K. The magnetization as well as the probability of having an infinite cluster exhibit phase transitions at $K = 0.44$ as predicted by Coniglio and Klein. The value is in good agreement with the analytically determined Curie Point $K_c = 0.4407$. Consequently, we can use the Curie point as the critical point of our system. The cluster number for the Ising model behaves very similar to the cluster number for the random graph percolation. We see a straight line in the log-log-plot for $K = K_c$ (see figure 3.11). The cluster number is a power law in the cluster size s. We extract $\tau = -2.17$ as the gradient of the straight line. Furthermore, we observe an exponential decay of the cluster number away from the critical point K_c.

3.4.2 Crash hazard rate

We present the results for the explicitly calculated crash hazard rate $h_{\text{exp}}(K)$ as a function of the imitation strength K for a single realization on different lattice sizes L. We start with $K_1 = 0.1$ and a random configuration of spins and apply $t(L)$ rounds of Glauber dynamics. Recall that the mixing time of the Glauber dynamics is a function of the lattice size L. We extract the cluster configuration and calculate the crash hazard rate $h_{\text{hexp}}(K_1)$. We proceed by applying again t Glauber dynamics but with parameter K_2. The crash hazard rate is calculated and we proceed to K_3. In this way, we calculate recursively the crash hazard rates for all given K. Note that if we want to compare the results to the theoretical crash hazard rate, we have to scale the theoretical crash hazard rate by a constant (see equation 3.6). The constant is set to the mean of the ratio $h_{\text{theo}}(K_i)/h_{\text{hexp}}(K_i)$ for $K < K_c$.

The explicitly calculated crash hazard rate $h_{\text{exp}}(K)$ on a 10×10 square lattice is not diverging as one reaches the percolation threshold K_c. Figure 3.12 exhibits a high volatile curve and a peak at $K = 0.4$ on the left side. This occurs due to finite size effects which can be seen in the right plot. We observe a non vanishing probability for an infinite number P_∞. This is in agreement with Coniglio and Klein's theory that the Ising cluster are too large to describe actual Ising Droplets. Coniglio and Klein's site-bond per-

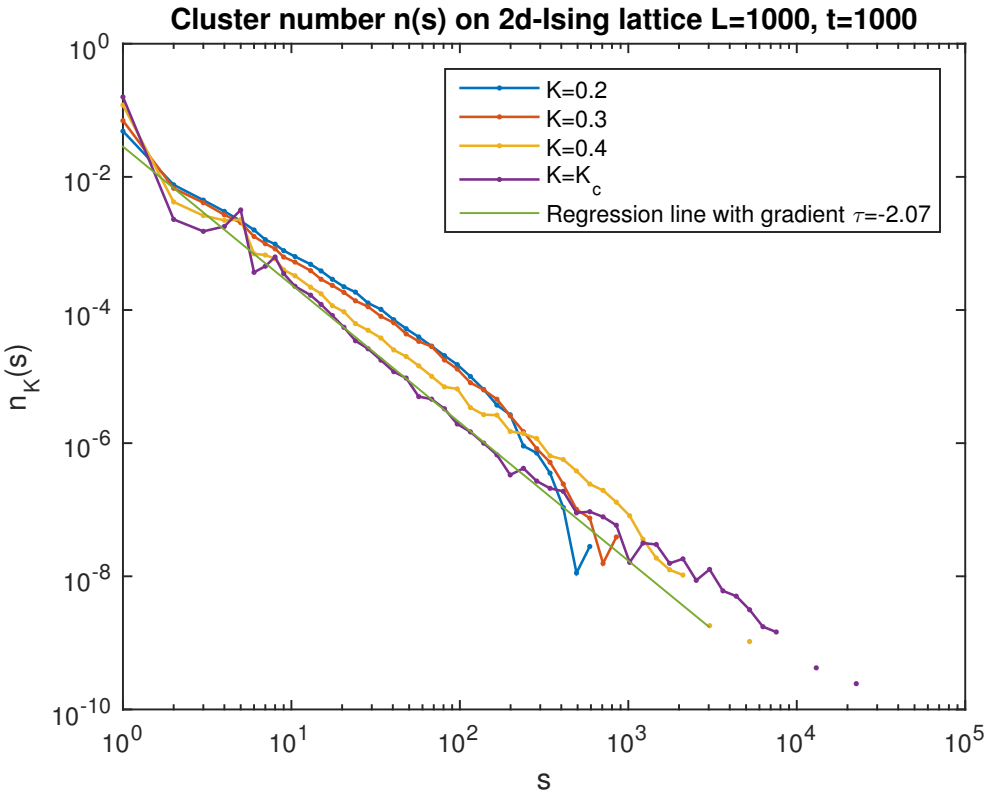

Figure 3.11: Log-log-plot of the cluster number $n(s)$ versus cluster size s for different values of the control parameter K. The linear regression for the cluster number at the critical point gives the fisher exponent $\tau = 2.07$. This is very close to the analytic value in the literature of $\tau_{\text{theo}} = \frac{187}{91} \simeq 2.05$.

colation could improve the outcome of this framework as the magnetization is not intensively blurred.

The explicitly calculated crash hazard rate $h_{\text{exp}}(K)$ on a 100×100 square lattice shows a divergence if one approaches the percolation threshold K_c. This divergence is in a good agreement with the power law divergence of the theoretical crash hazard rate $h_{\text{theo}}(p)$. The left plot of figure (3.4) shows this using $t = 10^6$ rounds of Glauber dynamics. The blue points $(h_{\text{exp}}(p))$ are well described by the red curve $(h_{\text{theo}}(p))$ up to volatility. The explicit calculated crash hazard rate exhibits high volatility as we come close to the percolation threshold.

The explicitly calculated crash hazard rate $h_{\text{exp}}(p)$ on a 1000×1000 square lattice shows a clear divergence if one approaches the percolation threshold p_c. In figure (3.5) we observe that the red and the blue curve are almost identical. We have a relatively sharp percolation transition: For the control

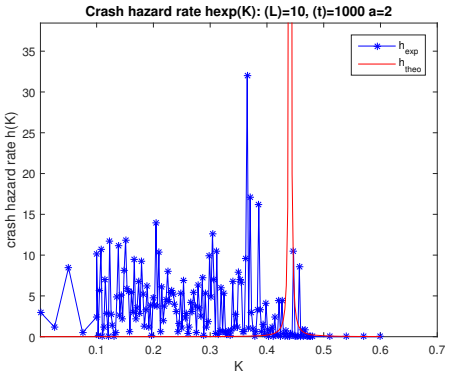

(a) Plot of the explicitly calculated crash hazard rate $h_{\exp}(K)$ and the theoretical one $h_{\exp}(K)$ for a single realization on the square lattice of size $L = 10$. The crash hazard rate increases slightly and the volatility increases strongly for growing control parameter K.

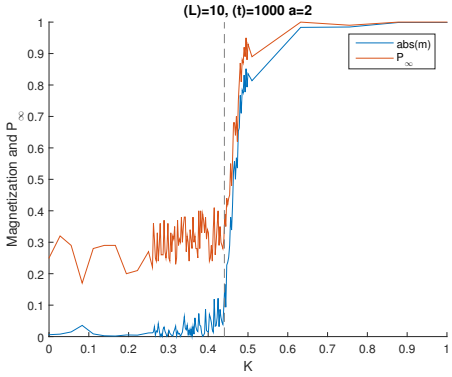

(b) Plot for the probability P_∞ of having an infinite cluster and the absolute value of the magnetization m as a function of the Ising control parameter K averaged over 100 realizations. The percolation threshold is highly blurred as opposed to the critical thermal transition point. These strong finite size effects explain the high volatility for the crash hazard rate on the square lattice of size $L = 10$.

Figure 3.12: Square lattice of size $L = 10$

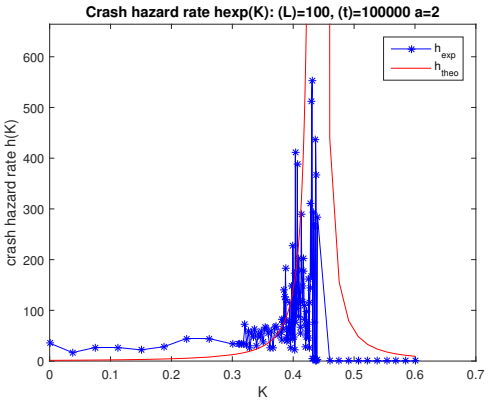

(a) Plot of the explicitly calculated crash hazard rate $h_{\exp}(K)$ and the theoretical one $h_{\exp}(K)$ for a single realization using $t = 10^6$ rounds of Glauber dynamics on the square lattice of size $L = 100$. Up to volatility, the blue explicit crash hazard rate is well described by the theoretical estimate in red. The volatility increases strongly as we get close to the percolation threshold K.

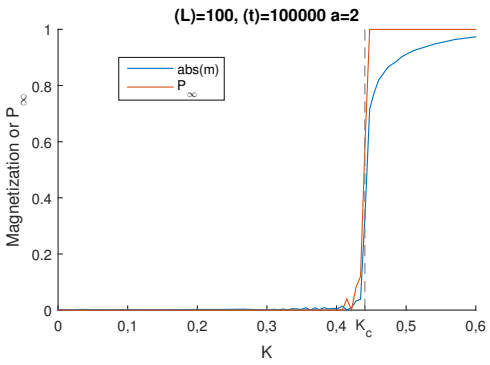

(b) Plot for the probability P_∞ of having an infinite cluster and the absolute value of the magnetization m as a function of the Ising control parameter K averaged over 25 realizations. The percolation threshold is much less blurred as in the previous case and the probability for a percolating cluster vanishes for $K \to 0$.

Figure 3.13: Square lattice of size $L = 100$.

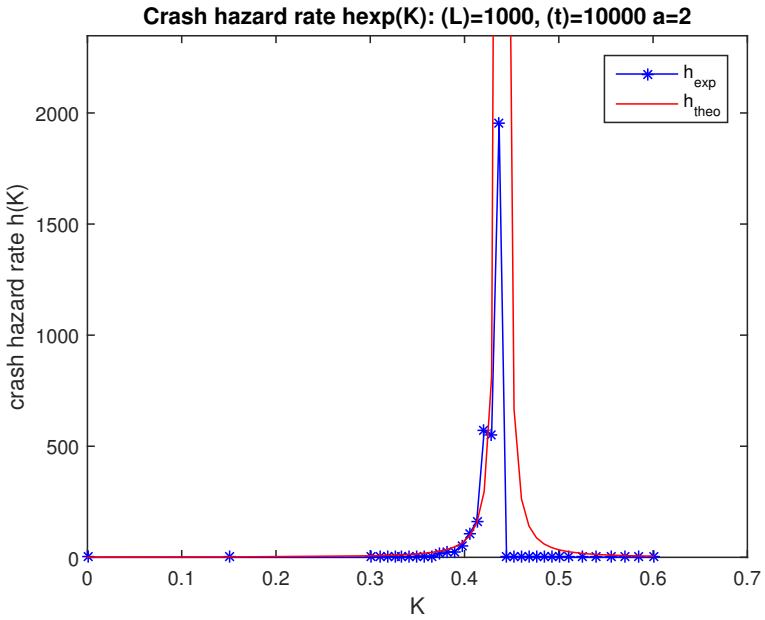

Figure 3.14: Plot of the explicitly calculated crash hazard rate $h_{\exp}(p)$ and the theoretical one $h_{\exp}(p)$ for $t = 10000$ rounds of Glauber dynamics on the square lattice of size $L = 1000$. The crash hazard rate shows a divergence in a very good agreement with the theoretical estimate if one approaches the percolation threshold p_c. No volatility is visible, finite size effects are negligible due to the self-averaging property of large lattice sizes in analogy to previous results.

parameter $K = 0.4413$ still close to p_c, the crash hazard is drastically decreased with respect to the peak. The increase in the volatility which we had in the precedent results, is disappeared due to the self-averaged property of large lattices. Finite size effects become negligible as we have a sharp enough transition for $L = 1000$.

3.5 Proposition: Ising droplets instead of the Ising clusters by using site-bond-percolation

Better results may be obtained by using site-bond-percolation as proposed in [19] to create Ising droplets. The advantage of using the Ising droplets is that we describe the crash hazard rate in analogy with an interacting physical process (magnetization in the Ising model) and not with a phase transition due to graphical processes. Recall that the probability of a bond between two occupied sites is a function of K.

$$p_B = 1 - e^{-2K} \tag{3.18}$$

This probability is a measure of the couplings between agents within a cluster as a function of the ratio K = coupling/temperature . K is again the coupling strength.

The algorithm:

1. Generate Ising clusters with Glauber dynamics as in the previous case for a given K. A cluster is the ensemble of neighbored spins up.
2. Generate a bond between neighbored ″spin up″s with bond probability $p_B = 1 - e^{-2K}$. The new clusters are the Ising droplets. They are the ensemble of ″spin-up″ traders that are neighbored and bonded.
3. Calculate the crash hazard rate by taking the sum over the droplets multiplied by the contribution rate.

Chapter 4

Results II: Bubbles in Price Simulations

In this chapter, we present a wide variety of price simulations containing bubbles and crashes.

If we know the crash hazard rate in the JLS model for all time t, we can describe the price at any time t before a crash up to a Random Walk according to the following recursive equation (see 2.5):

$$p_{\text{rice}}(t) = p_{\text{rice}}(t-1)\left[\kappa h(t) - \kappa dj(t) + \eta dw(t)\right] \qquad \text{for } t < t^* \tag{4.1}$$

We can simulate real stock prices if we know the underlying network evolution. Unfortunately, it is not so easy to rebuild the real-life networks, especially if we describe the networks using the stylized site percolation model on the square lattice. Yet, despite its simpleness, the random site percolation model on the square lattice is able to provide interesting price curves. We present price simulations for different network evolution on the site percolation model in the following. The probability p of a site being occupied is the control parameter in the simulation. Taking the clusters formed under the given value of p at each time step, we can calculate the crash hazard rate and consequently the price. We use a non-homogeneous Poisson process to simulate the exact time when the crash occurs. Note that the time of the crash is the random variable t^* described by the deterministic hazard crash rate h. The hazard crash rate plays the role of the intensity function of the Poisson process, i.e., $h(t)dt$ gives the probability for having a crash in the interval $[t, t+dt]$.

4.1 A First Simple Crash Scenario

To understand a potential bubble or crash process, we assume simple network dynamics. The number of traders participating in the market is linearly

increasing with t up to the time of crash t^*.

$$p(t) = C \cdot t + p_0 \qquad \text{for } t < t^*. \tag{4.2}$$

We set the initial value of the control parameter to $p_0 = 0.4$ and the constant to $C = 10^{-4}$. Each time-step, more and more traders get participating in the market leading to a increasing crash hazard rate. If the crash occurs, the price loose $\kappa = 0.2$ of its price. We can say in a way that the jump process resets the price. We do the same with the control parameter that is, right after the crash, we reset it to its initial value $p_0 = 0.4$.

We use random site percolation on the square lattice of size $L = 500$. The result for the price simulation of this first simple network evolution model is shown in figure 4.1. The first plot shows the price evolution, the second the crash hazard rate and the third the control parameter p. We implement 10000 time steps with length $\Delta t = 10^{-4}$. Although we have identical network dynamics and thus the same crash hazard rates raising from $p_0 = 0.4$ after a crash, the time between two crashes is not a fixed constant, but varying. The time of the crash is a random variable. We see again the diverging character of the crash hazard rate as we get close to the critical value of the control parameter p. The simple model is able to illustrate the key features of the JLS model:

1. A crash is preceded by a bubble.
2. The duration of the bubble is varying. The death of the bubble occurs spontaneously, being a random variable.
3. The crash hazard rate exhibits diverging character in time near the percolation threshold.

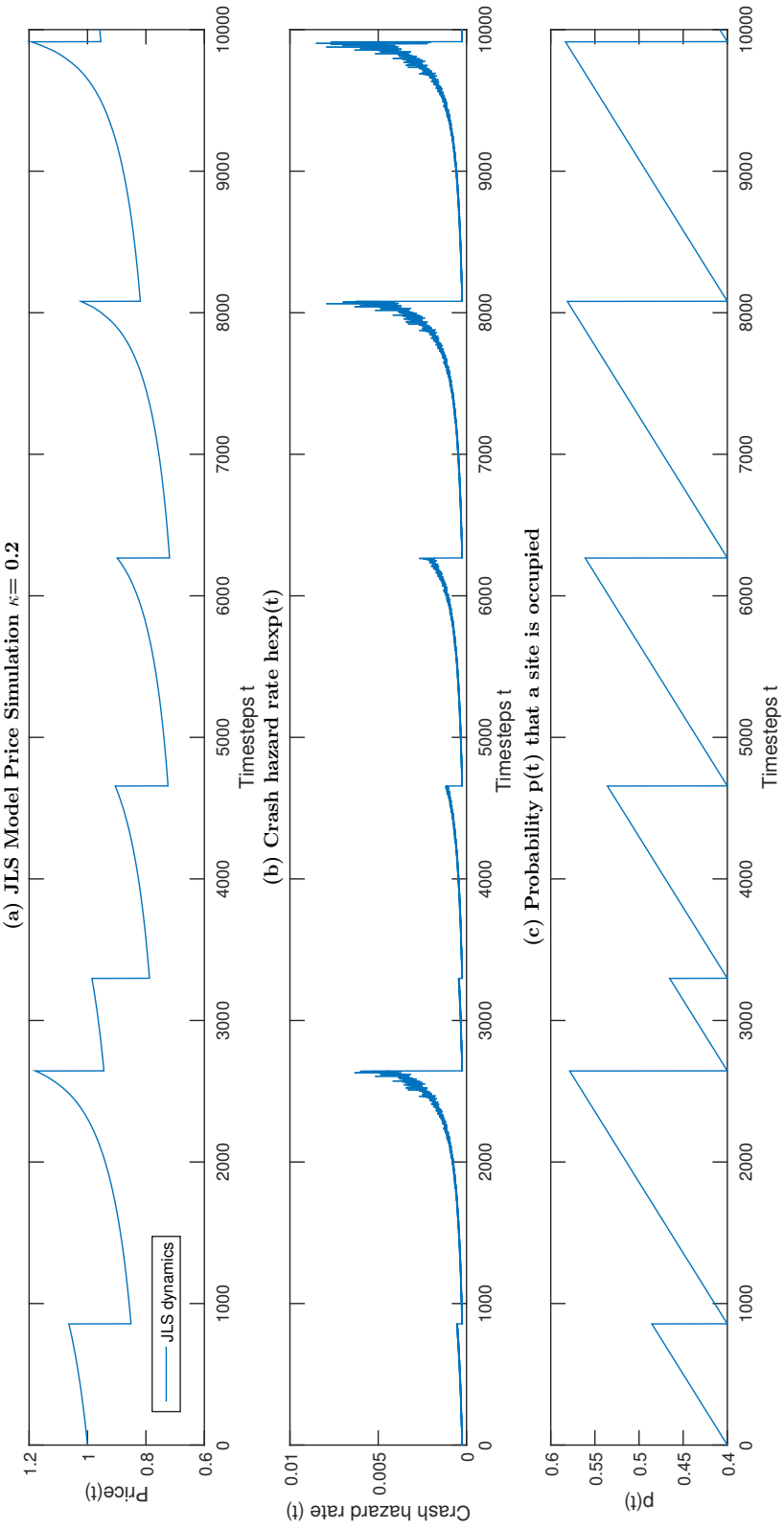

Figure 4.1: Plot of (a) the JLS model price simulation without random walk, (b) the associated crash hazard rate and (c) the linear increasing control parameter p determining the crash hazard rate on a random site percolation square lattice of size $L = 500$. The condition parameter is chosen to be $a = 2$. We see bubbles of different length and intensity. Each bubble ends with a crash as the crash hazard rate is diverging in time. The duration of a bubble varies being a random variable. We see again the diverging character of the crash hazard rate as the control parameter p comes close to the percolation threshold. The price returns to the region of its starting point $p_{\text{rice}}(0) = 1$. The JLS model is consistent in the sense of an isolated system.

4.2 Ornstein-Uhlenbeck Simulations

We use an Ornstein-Uhlenbeck (OU) process to describe the control parameter p (see section 2.6.2). The Ornstein-Uhlenbeck process is a mean-reverting Wiener process. It should simulate network dynamics more realistically than the simple linear growth of the control parameter p. As in the previous case, we calculate the crash hazard rate and the price via the cluster configuration given by the parameter parameter at each time-step. The time of the crash dj is again realized by a non-homogeneous Poisson process in analogy to the previous simulation. After a crash, we reset the control parameter to its initial value. Turbulent and complex changes can occur which we cannot describe in our stylized model. We are only interested in the time preceding the crash. As an approximation, we reset the control parameter to its initial value if a crash has occurred. We present many scenarios of bubbles and crashes for various lattice sizes L and conditions (exponent a) as well as OU memory values and volatility of the price process. First, we vary the lattice size L while all other parameters are held constant. We use $L = 10$ and $L = 1000$. We vary the condition to $a = 1.5$ and $a = 2.5$. We present results for varying memory of the underlying Ornstein-Uhlenbeck process. We distinguish three types of excursions, long memory excursions that last more than 1000 time-steps, normal memory excursions lasting around 1000 time-steps and short memory excursion lasting much less than 1000 time-steps. The according parameter is the mean-reverting parameter ϑ in combination with the volatility parameter σ. The significance of our bubbles with respect to the volatility of the price process is investigated by changing the ratio of the JLS parameter κ divided by parameter η which weighs the random walk. The former is held constant to $\kappa = 0.2$, we change only the latter by using $\eta = 0.01$, $\eta = 0.005$ and $\eta = 0.001$. We end this section by a simulation where we do not reset the price after a crash. Again, the first plot in each figure shows the price evolution, the second the crash hazard rate and the third the control parameter p. We implement 10000 time steps with artificial length of time-intervals $\Delta t = 10^{-4}$.

We summarize our observations in the following. We state the number of the figures where we made the observations in brackets.

1. The JLS model is consistent in the sense of an isolated system. The price returns to 1 in the $L \to \infty$-limit (see all figures).
2. We are able to generate reasonable bubbles. Bubbles occur basically if the control parameter takes a long-memory excursion in the direction of the critical value. By construction, these times are the most likely times for a crash to occur (see all figures)
3. Bubbles can end with a crash or survive without a crash leading to a new price plateau (see figures 4.3, 4.4, 4.6, 4.8, 4.12).

4. During bubbles, price is growing convexly if the control parameter is increasing. Bubbles exhibit a linearly increasing price if the control parameter is constant. (4.9)
5. large lattices are less susceptible to crashes than smaller ones (compare the figures 4.3 and 4.4 to figure 4.5). For higher values of the minimum cluster size s_m that is needed for a crash, this effect can even increase or occur for smaller lattice sizes (see figure 4.13). We investigate the issue immediately after this enumeration.
6. The higher the condition a, the sharper and larger the bubbles can get. Crashes occur more frequently (compare the figures 4.3, 4.6 and 4.7).
7. Long memory of the OU process leads to larger bubbles that end very likely with a crash. Short memory of the OU process leads to small bubbles that occur very often, but rarely end with a crash (compare the figures 4.3, 4.8 and 4.9).
8. For the parameter of the price volatility process equal to $\eta = 0.005$ and $\eta = 0.01$, volatility of the price process can amplify the bubble or cover it completely. For a lower value $\eta = 0.001$, no price volatility is visible and the price is only dominated by the crash hazard rate (Compare figures 4.10, 4.11 and 4.12).

We have seen that crashes become very unlikely for lattice sizes $L = 1000$ as we choose the minimal cluster size for a crash $s_m = 0.01 \cdot p \cdot L^2$. In figure 4.5, the crash hazard rate is still zero even for $p = 0.52$. We need clusters of sizes larger than $s_m(L = 1000) \simeq 5000$ as opposed to $s_m(L100) \simeq 50$ for a lattice size $L = 100$. We have excluded all the small clusters and their possibility to cause a crash. In a sense, larger systems exhibit less bubbles as the crash hazard rate is zero unless we are very close to the critical region. But if there is a bubble, then it will be a huge one. In figure 4.13, we have seen that this effect occurs also for $L = 100$ if we take a higher value for s_m. The reason for this dependence on L is the fractal structure of the clusters. The minimum cluster size goes quadratic in L:

$$s_m = 0.01 \cdot p \cdot L^2 \tag{4.3}$$

whereas the cluster number

$$n(s) = \text{const} \cdot \frac{s^\tau \cdot L^2}{/L^2}, \tag{4.4}$$

the probability of having a cluster of s sites *per site*, does not depend on L. This is explained by the fractal structure of the clusters or, in other words, self-similarity. If we increase the system size, s_m gets larger in contrast to the cluster number $n(s)$. That is why we cut more and more contributions from smaller clusters of the crash hazard rate as the system size gets larger. We

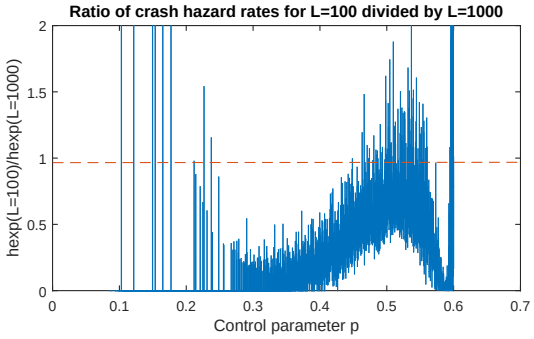

Figure 4.2: Ratio of the crash hazard rate for $L = 100$ divided by the one for $L = 1000$. The minimum cluster size was chosen to be $s_m = 0.01 \cdot p \cdot L^2$. The crash hazard rate is clearly larger for $L = 1000$ than it is for $L = 100$, around five times larger near $p = 0.4$. The outliers are explained by the high volatility for a single realization.

conclude that it is more difficult to get an imbalance in the market book if the system size L is large. Larger systems are rarely susceptible to large bubbles and pretty insusceptible for normal bubbles because of self-similarity. We can express this in a more general way. If the underlying networks of traders are self-similar, large systems exhibit less risk to bubbles due to herding of noise traders than smaller systems.

This effect occurs only when we set s_m as a function of L as above. If we set s_m to a fixed small value for all L,we do not see this effect. Indeed, we observe exactly the opposite effect in figure 4.2. The crash hazard rate is larger for $L = 1000$ than it is for $L = 100$, around five times larger near $p = 0.4$.

We can add a volatility process dW to our price simulation. Then, the process $dW(t)$ takes one of the two values ± 1 with equal property at each time-step. Its magnitude is described by η. Plugging this random walk into the price equation yields

$$p_{\text{rice}}(t) = p_{\text{rice}}(t-1) * (1 + \kappa h(t-1) - \kappa * dj(t-1) + \eta dW(t)). \tag{4.5}$$

We present results for varying parameter η. The price volatility can amplify the bubble (see 4.10) or even cover it completely (see figure 4.11).

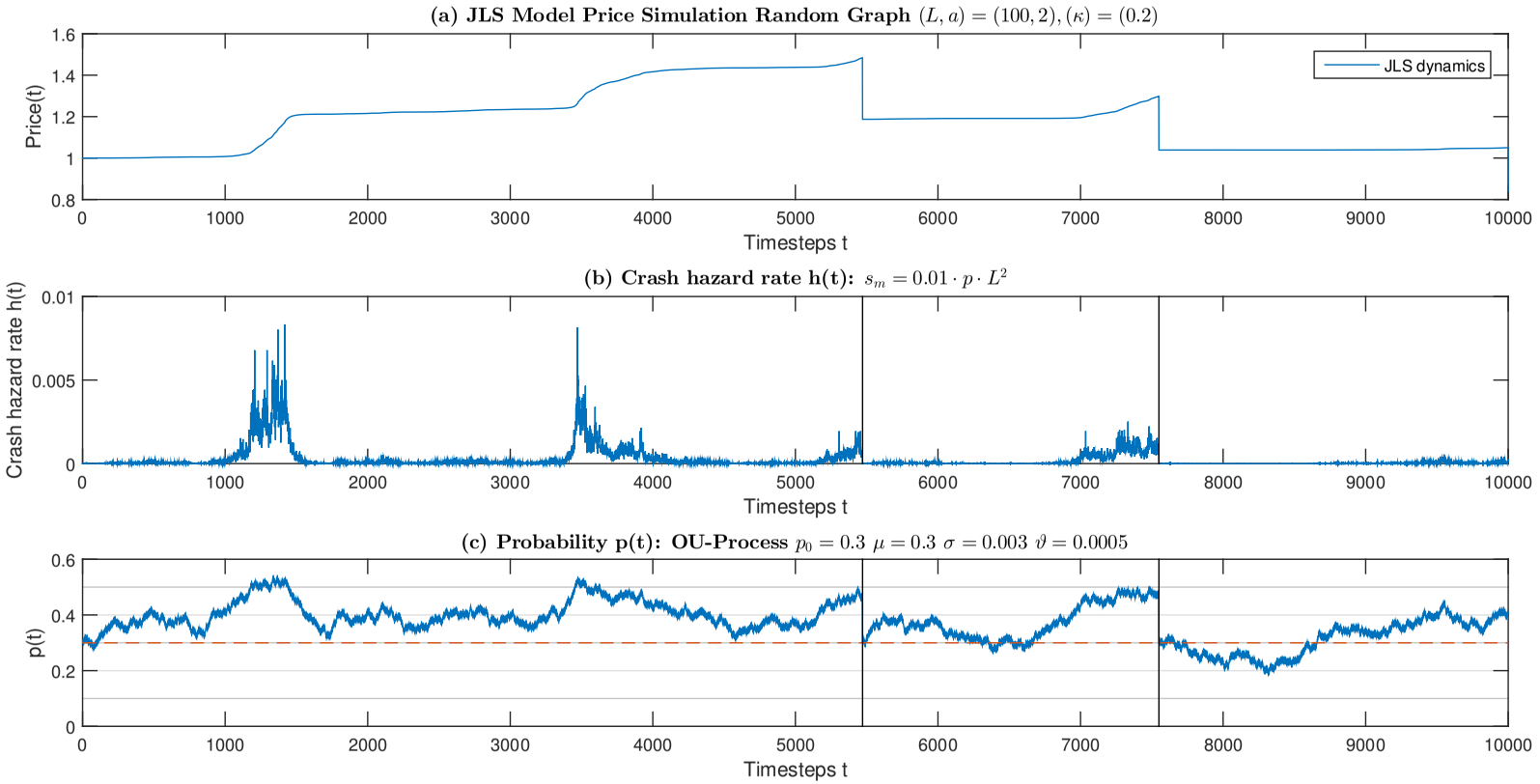

Figure 4.3: Plot of (a) the JLS model price simulation, (b) the associated crash hazard rate and (c) the linear increasing control parameter p determining the crash hazard rate on a random site percolation square lattice of size $L = 100$ with condition $a = 2$. The control parameter p follows an Ornstein-Uhlenbeck process. Bubbles of different magnitude are created. The first two bubbles around $t = 1200$ and $t = 3700$ end without a crash. Their surveillance lead to new price plateaus. The third and fourth one, although much smaller than the previous ones, end with crashes. The time series end near the starting price $p_{\text{rice}}(0) = 1$.

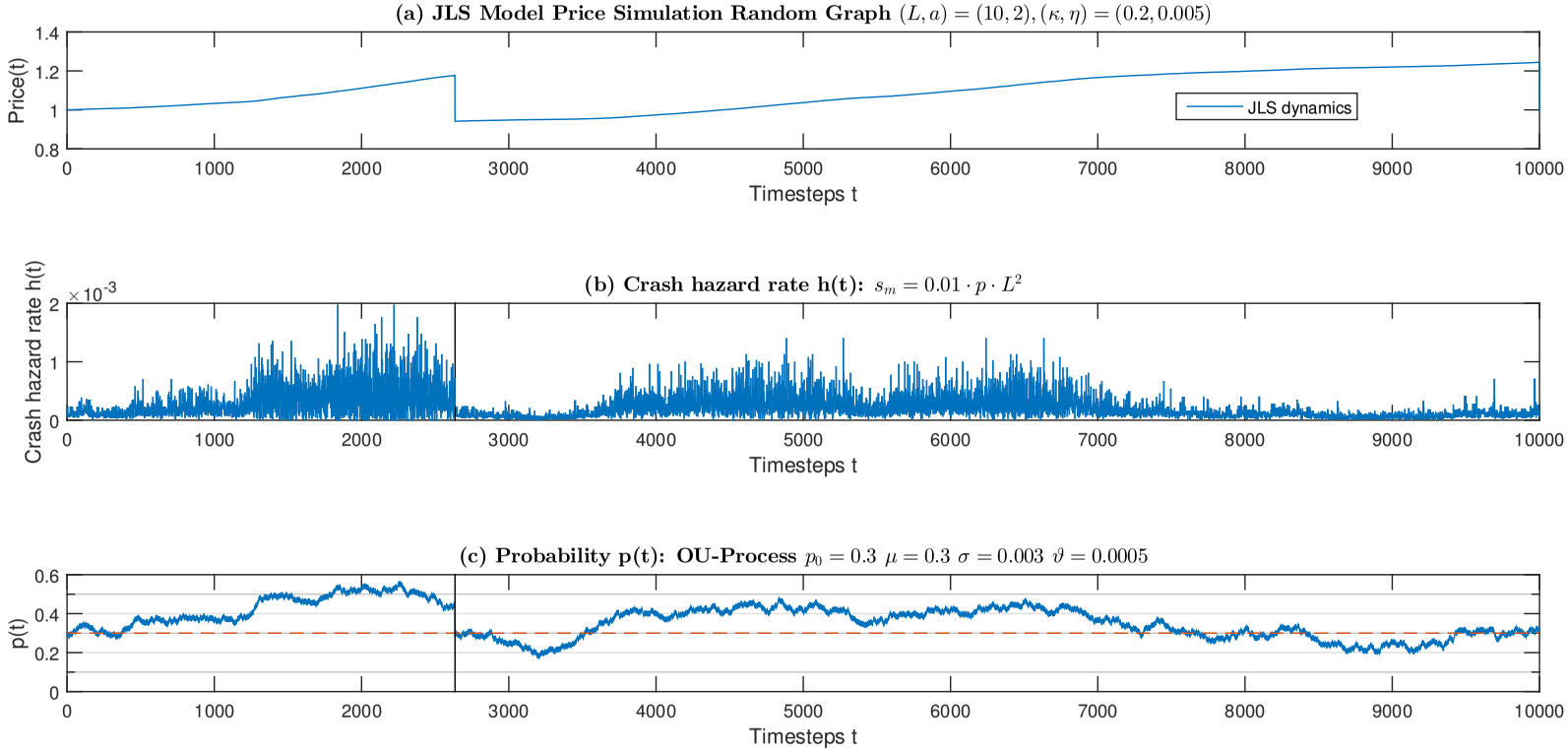

Figure 4.4: Plot of (a) the JLS model price simulation, (b) the associated crash hazard rate and (c) the linear increasing control parameter p determining the crash hazard rate on a random site percolation square lattice of size $L = 10$ with condition $a = 2$. The control parameter is controlled by an Ornstein-Uhlenbeck process. Bubbles of different magnitude are created. The Ornstein-Uhlenbeck possesses long memory allowing itself to take long excursions. We get a bubble that ends with a crash and a bubble that survives until the end. Generally, crashes occur less often for this lattice size $L = 10$ than for larger sizes $L = 100$. We need the control parameter to come close to the critical value that a crash will happen.

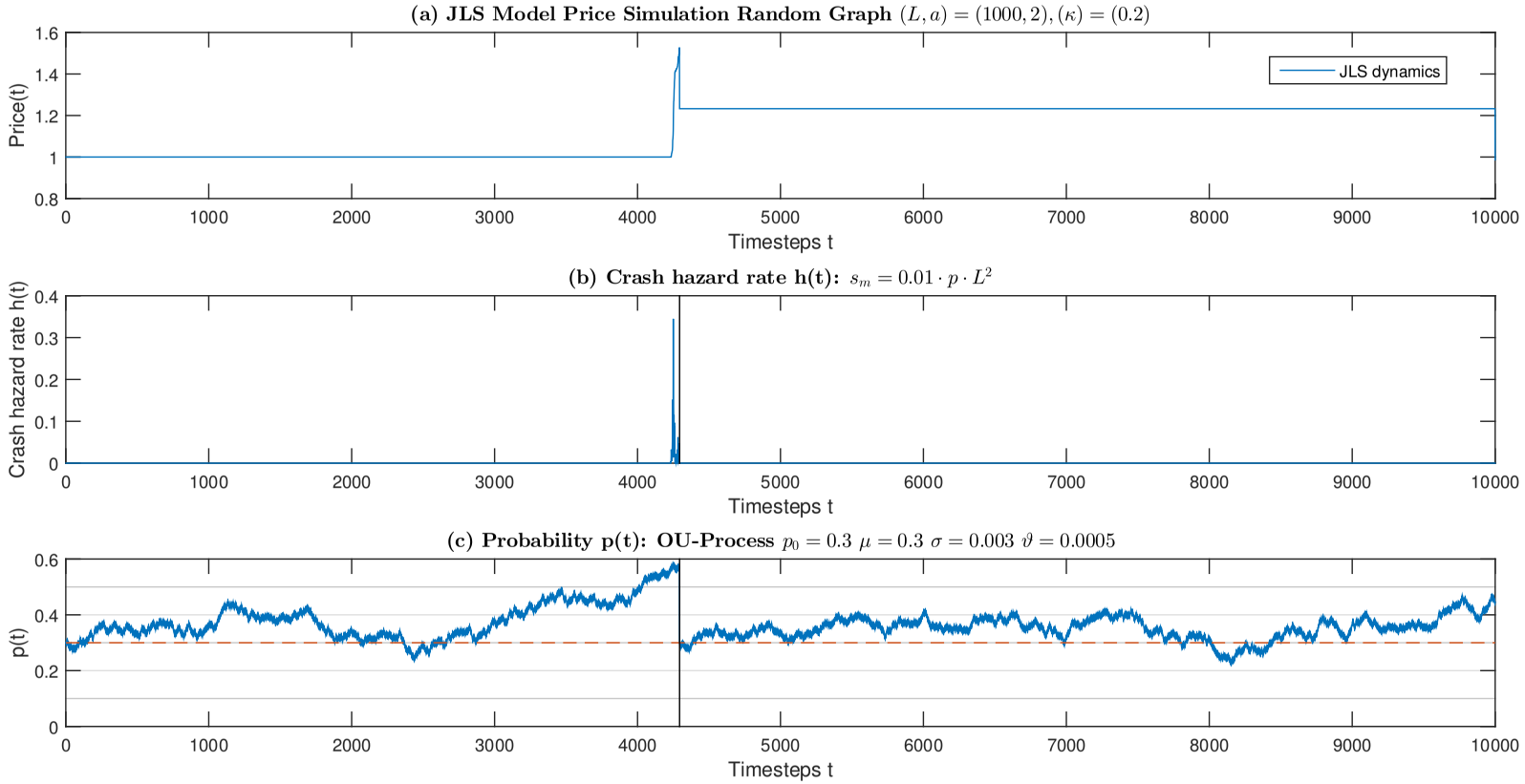

Figure 4.5: Plot of (a) the JLS model price simulation, (b) the associated crash hazard rate and (c) the linear increasing control parameter p determining the crash hazard rate on a random site percolation square lattice of size $L = 1000$ with condition $a = 2$. The control parameter is controlled by an Ornstein-Uhlenbeck process. The crash hazard rate is zero until we are very close to the critical region of the control parameter p. We do not see bubbles in the region $p = 0.5$ as opposed to before. We need extreme excursions of the OU process for bubbles. Then, the crash hazard rate gets very large leading to a sharp bubble. The bubble ends by a crash. larger systems seem to be much less susceptible to bubbles. We observe rarely, only extreme sharp bubbles.

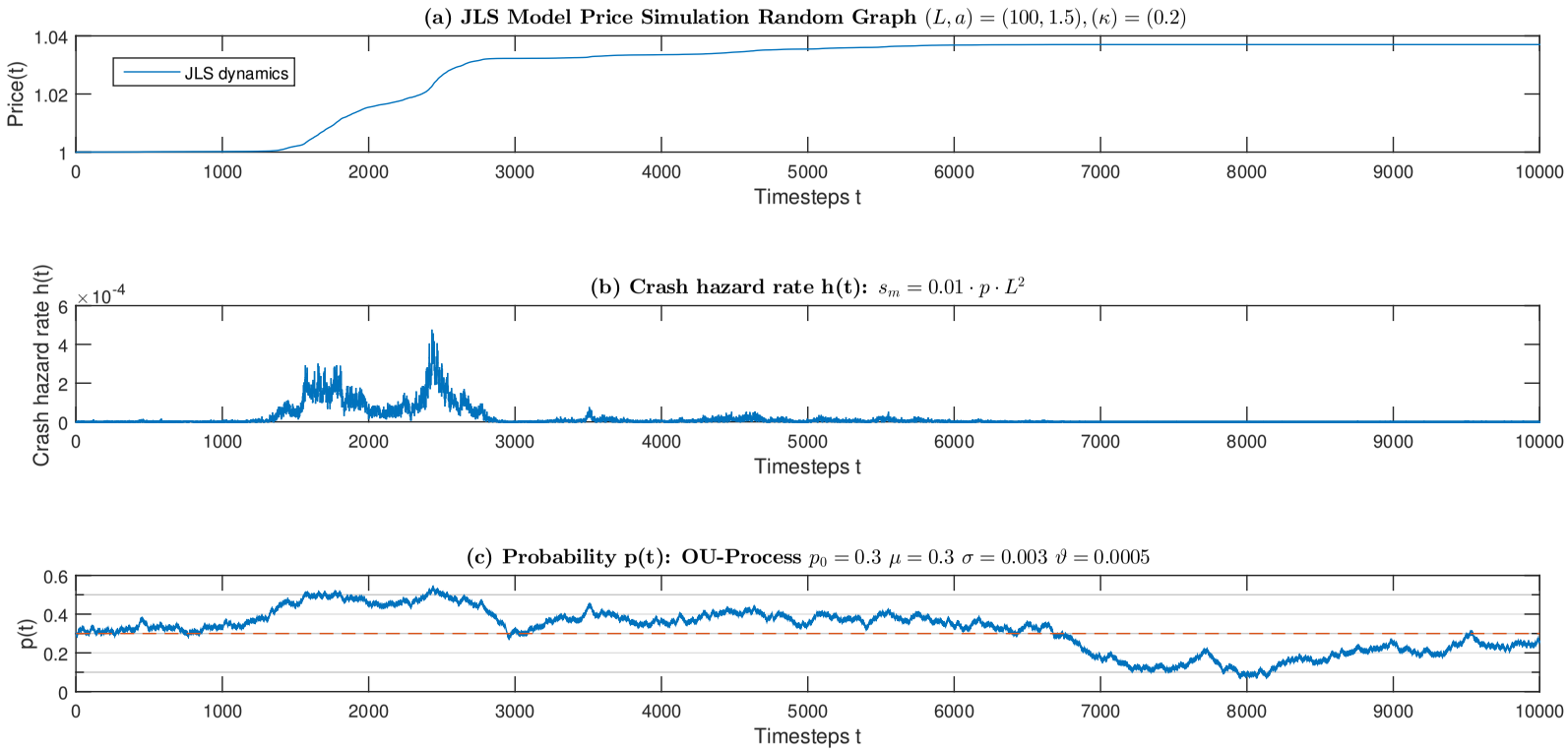

Figure 4.6: Plot of (a) the JLS model price simulation, (b) the associated crash hazard rate and (c) the linear increasing control parameter p determining the crash hazard rate on a random site percolation square lattice of size $L = 100$ with condition $a = 1.5$. The control parameter is controlled by an Ornstein-Uhlenbeck process. We see again a bubble, but it is a very small one for that we are in the critical region $p \simeq 0.5$. The magnitude of the crash hazard rate is small compared to simulations with $a = 2$ diverging with an smaller exponent. The bubble is of 4%. We see much less crashes in general and even no crash in this plot. A rule of thumb: We expect each κ percent price increase a crash where the price looses κ percent since our model is an isolated system.

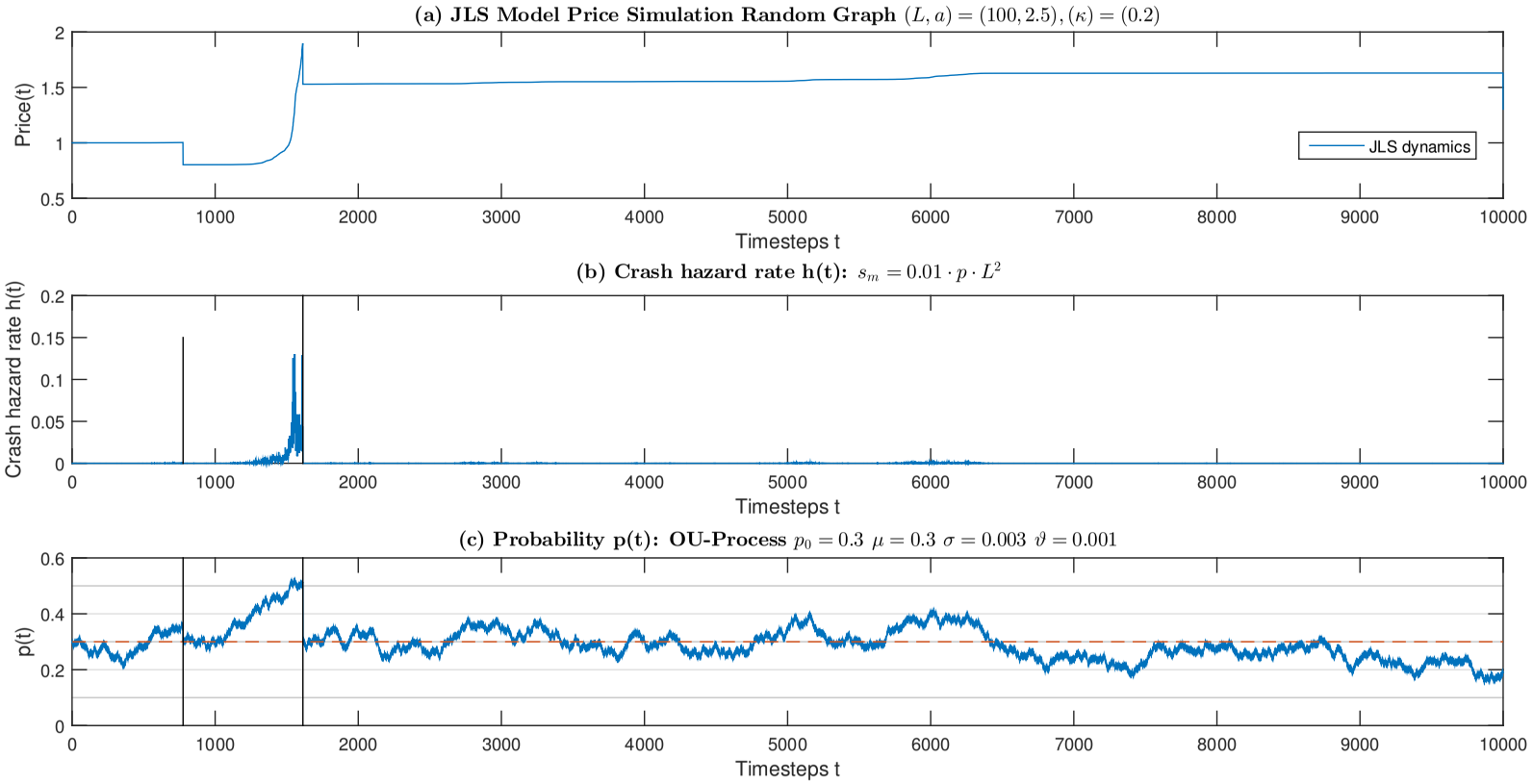

Figure 4.7: Plot of (a) the JLS model price simulation, (b) the associated crash hazard rate and (c) the linear increasing control parameter p determining the crash hazard rate on a random site percolation square lattice of size $L = 100$ with condition $a = 2.5$. The control parameter is controlled by an Ornstein-Uhlenbeck process. We observe a crash not preceded by a bubble for $p \simeq 0.35$ and an intensive bubble during a short excursion to $p = 0.5$ ended by a crash. Note the low values of the control parameter compared to the values in the first plot for $a = 2$. The OU memory parameter ϑ has been lowered as a preventive measure to avoid price simulation with too many crashes. For higher values of the condition, bubbles and crashes get generally more likely due to the raised value of the crash hazard rate and occur already for lower values of p.

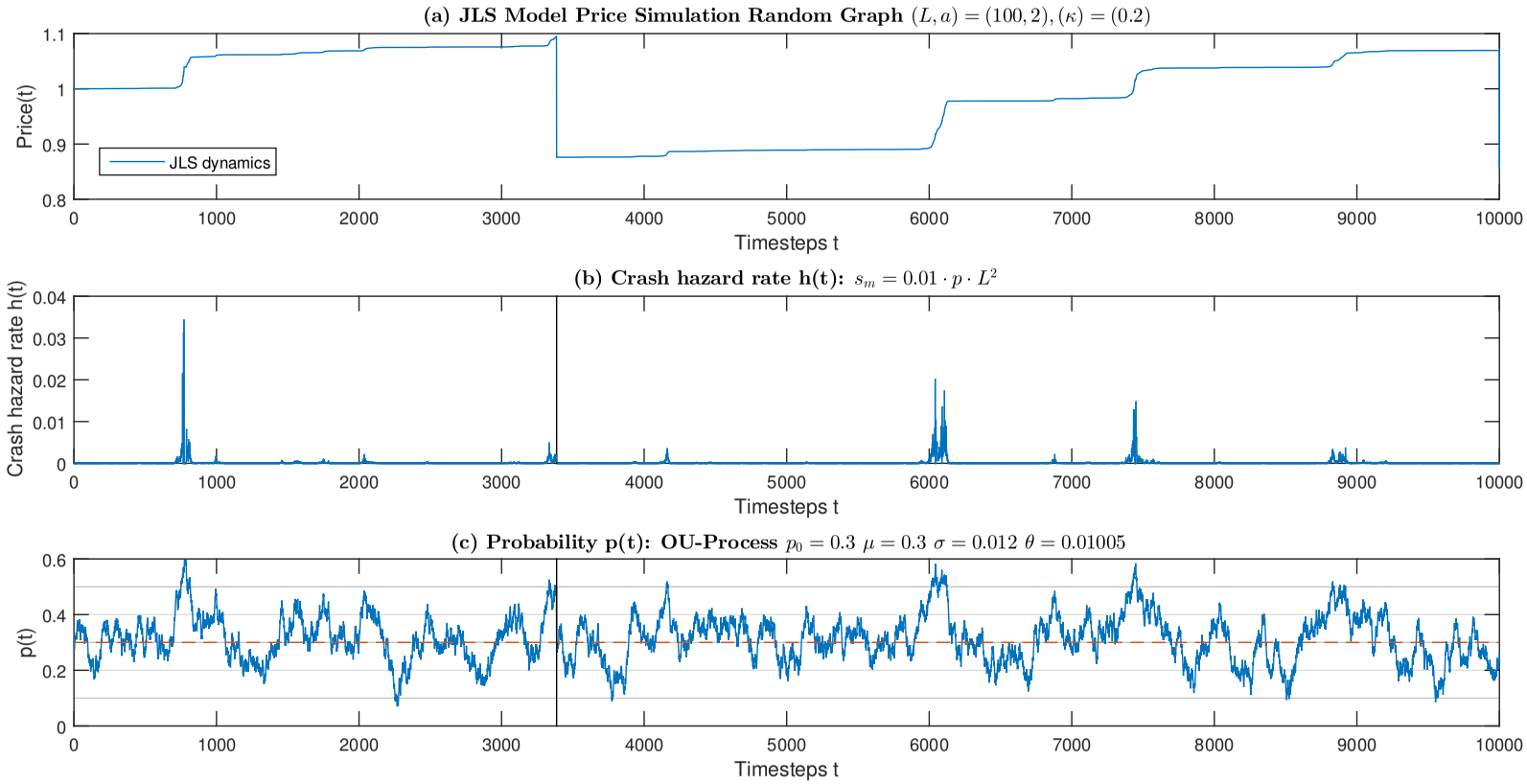

Figure 4.8: Plot of (a) the JLS model price simulation, (b) the associated crash hazard rate and (c) the linear increasing control parameter p determining the crash hazard rate on a random site percolation square lattice of size $L = 100$ with condition $a = 2.5$. The control parameter is controlled by an Ornstein-Uhlenbeck process and exhibits short memory. We observe a lot of small bubbles. However, they end rarely by a crash.

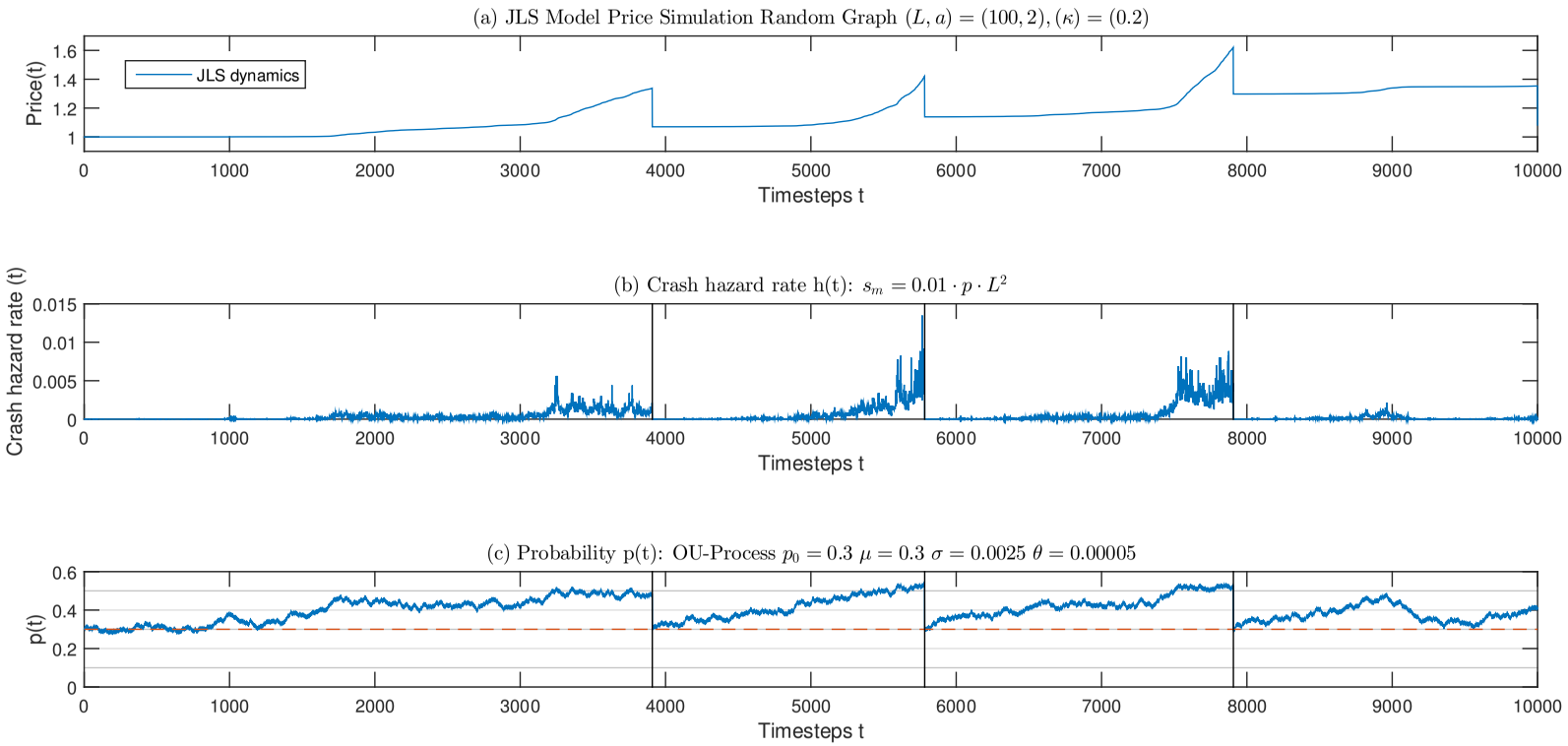

Figure 4.9: Plot of (a) the JLS model price simulation, (b) the associated crash hazard rate and (c) the linear increasing control parameter p determining the crash hazard rate on a random site percolation square lattice of size $L = 100$ with condition $a = 2$. The control parameter is controlled by an Ornstein-Uhlenbeck process and exhibits long memory. Each bubble ends with a crash. The last bubble ends with the end of our price simulation.

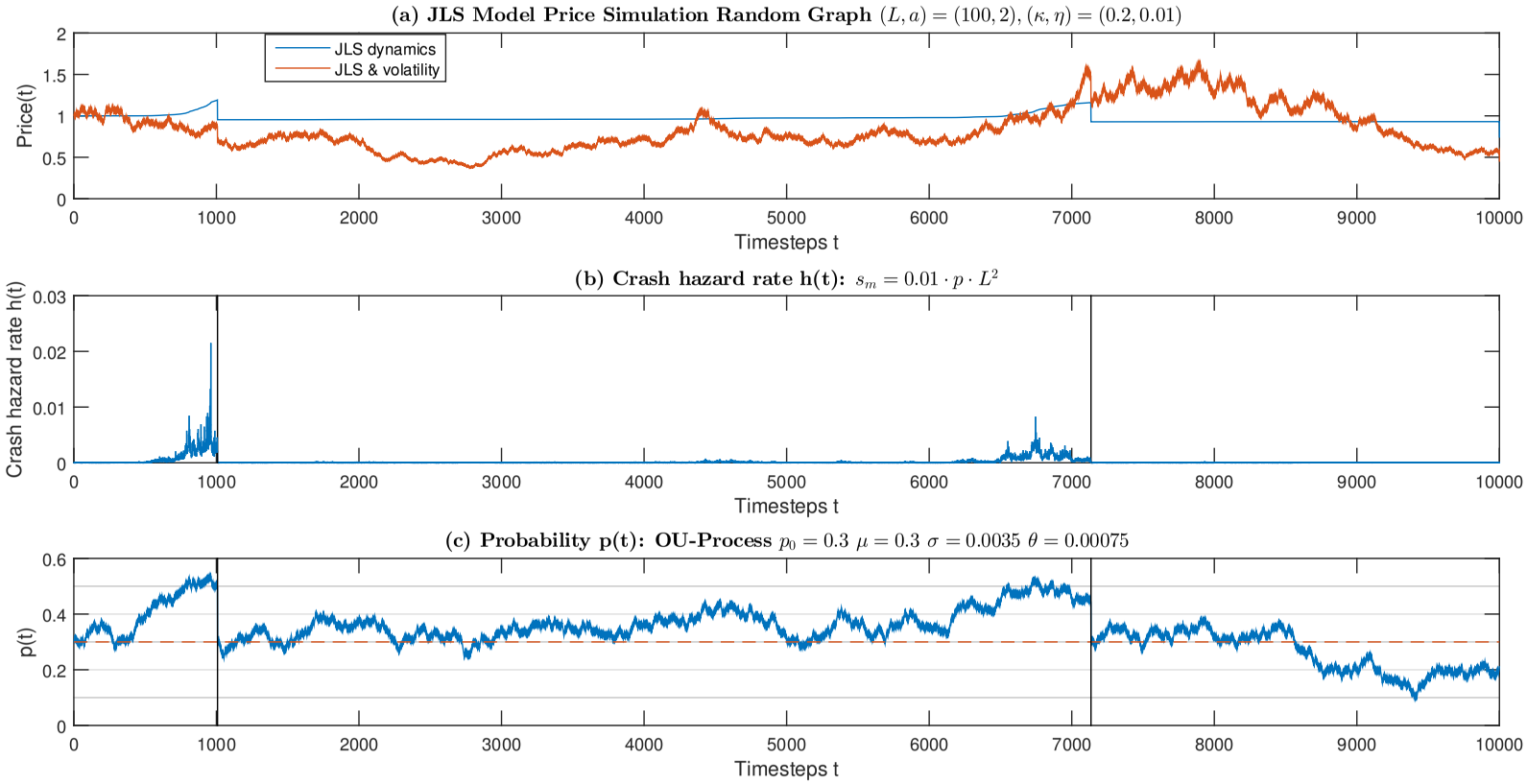

Figure 4.10: Plot of (a) the JLS model price simulation with (red) and without (blue) price volatility process, (b) the associated crash hazard rate and (c) the linear increasing control parameter p determining the crash hazard rate on a random site percolation square lattice of size $L = 100$ with condition $a = 2$. The price volatility parameter is $\eta = 0.01$. The control parameter p is controlled by an Ornstein-Uhlenbeck process. The first bubble is covered partially by the price volatility, while the second bubble is amplified by the price volatility process.

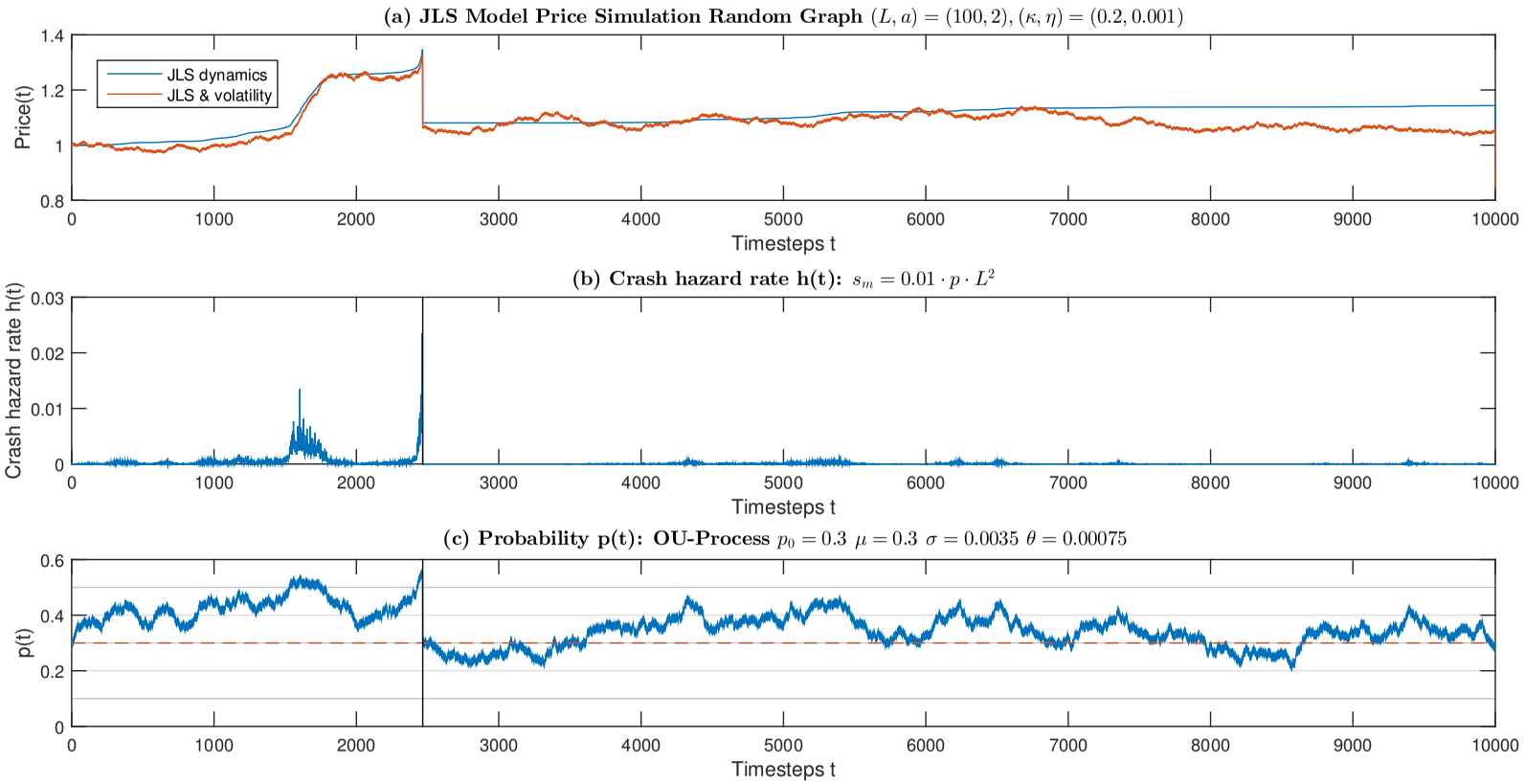

Figure 4.11: Plot of (a) the JLS model price simulation with (red) and without (blue) price volatility process, (b) the associated crash hazard rate and (c) the linear increasing control parameter p determining the crash hazard rate on a random site percolation square lattice of size $L = 100$ with condition $a = 2$. The control parameter p is controlled by an Ornstein-Uhlenbeck process. The price volatility parameter is $\eta = 0.001$. It is to small to have visible influences on the price process. Bubbles are neither covered nor amplified. The JLS dynamics dominate the price simulation.

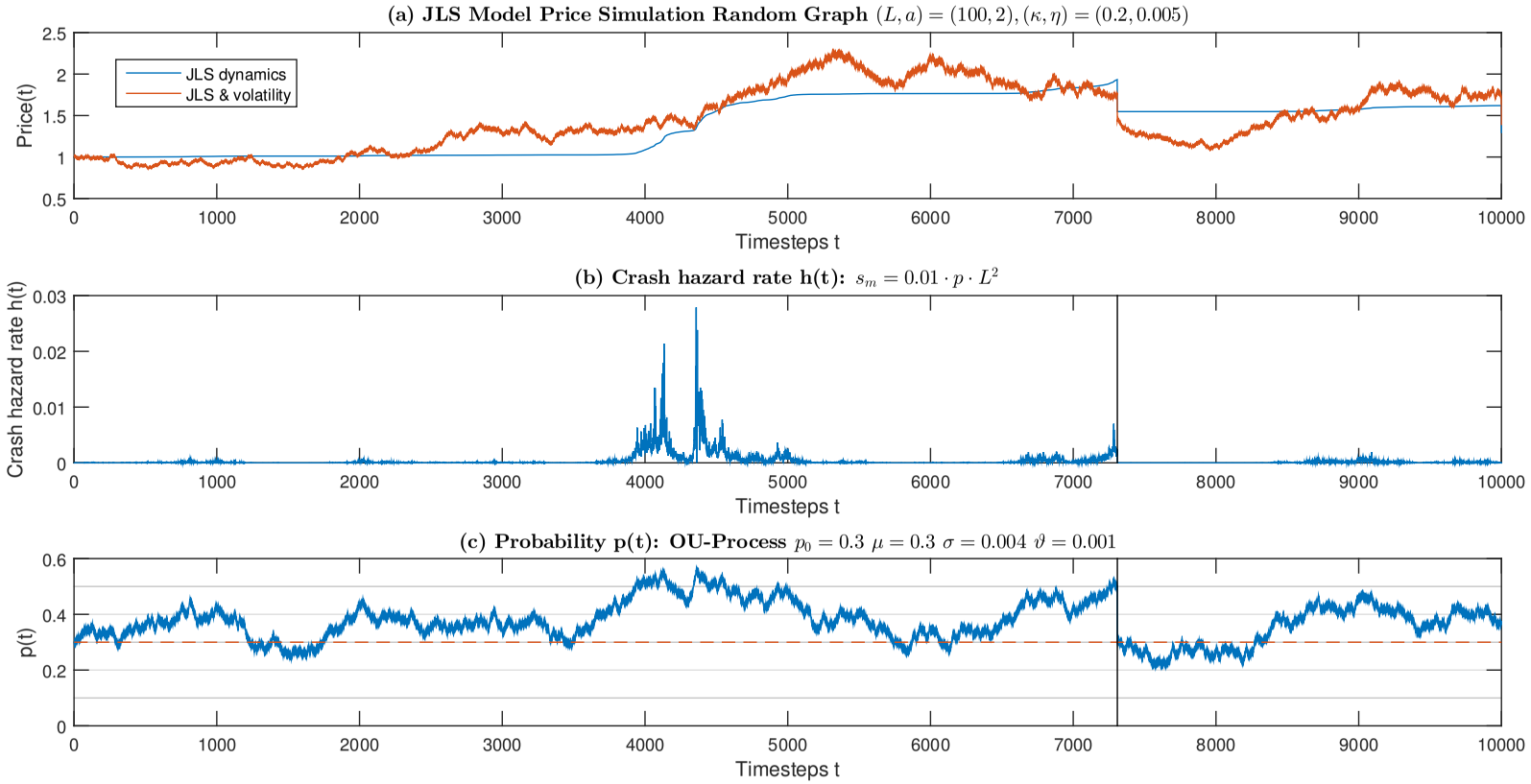

Figure 4.12: Plot of (a) the JLS model price simulation with (red) and without (blue) price volatility process (b) the associated crash hazard rate and (c) the linear increasing control parameter p determining the crash hazard rate on a random site percolation square lattice of size $L = 100$ with condition $a = 2$. The control parameter p is controlled by an Ornstein-Uhlenbeck process. The price volatility parameter is $\eta = 0.005$. The price volatility covers all the JLS dynamics. We would not be able to predict any of the crashes in this scenario.

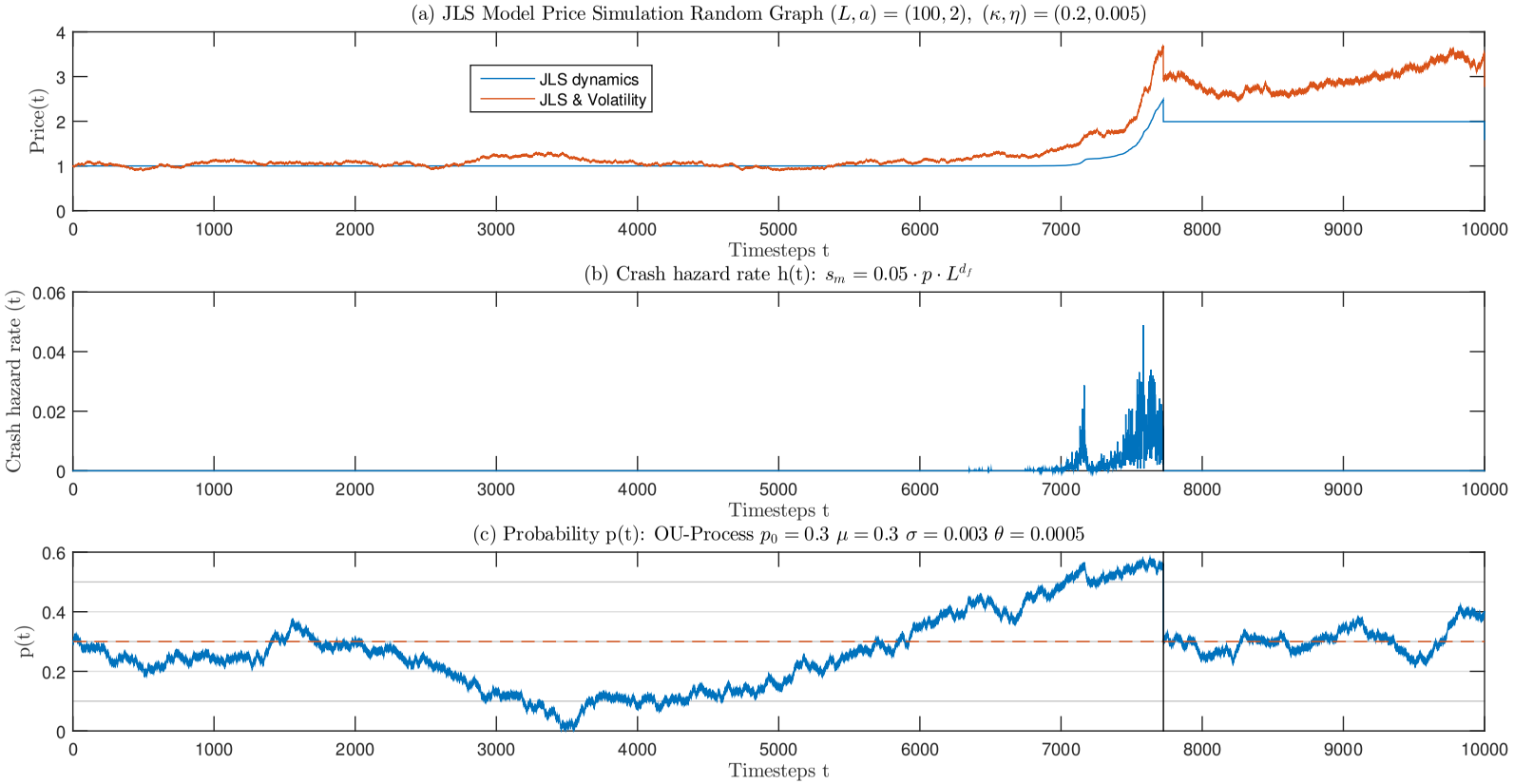

Figure 4.13: Plot of (a) the JLS model price simulation, (b) the associated crash hazard rate and (c) the linear increasing control parameter p realized for $s_m = 0.05 \cdot p \cdot L^{d_f}$ on a random site percolation square lattice of size $L = 100$ with condition $a = 2$. The control parameter p follows an Ornstein-Uhlenbeck process. The crash hazard rate is zero almost everywhere although we are in the region $p \in [0.4, 0.5]$ where we had crash hazard rates that leads even to crashes earlier. If we raise the minimum cluster size s_m for a crash, the system becomes less susceptible for bubbles as it was the case for larger lattice sizes. This is important to keep in mind as we have not fixed an exact value for s_m.

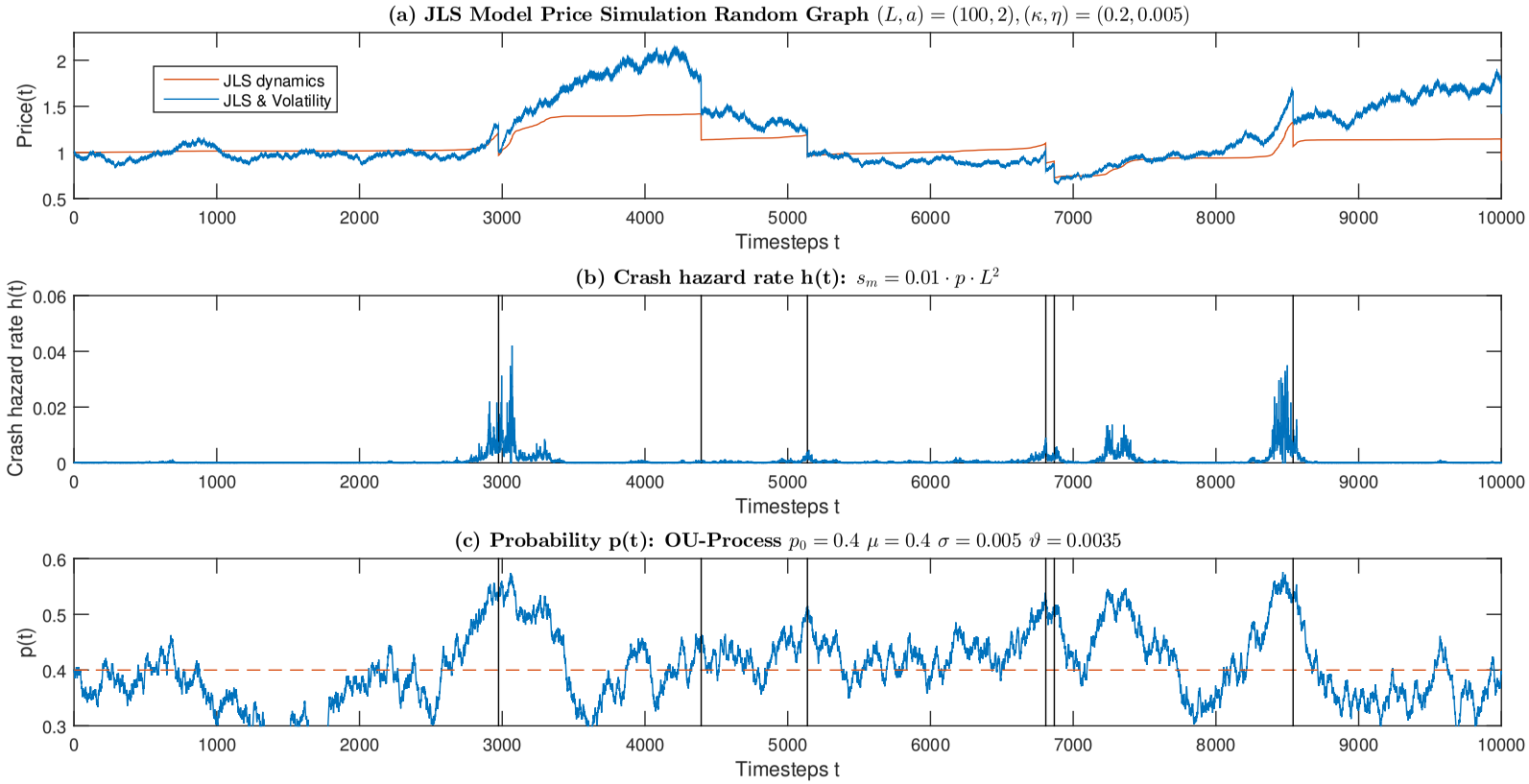

Figure 4.14: Plot of (a) the JLS model price simulation with (blue) and without (red) random walk, (b) the associated crash hazard rate and (c) the linear increasing control parameter p determining the crash hazard rate on a random site percolation square lattice of size $L = 100$ with condition $a = 2$. The control parameter is controlled by an Ornstein-Uhlenbeck process and it not reset after a crash. Bubbles of different magnitude are created. Except the one in the region $t = 7300$, all bubbles lead to a crash. The bubble around $t = 6900$ shows even two crashes. Bubbles occur quite often also after crashes.

4.3 Collection of Interesting Price Curves

Our framework is able to produce nice looking prices curves with bubbles. We present them in the following for varying price volatility parameter η, super-linear contribution exponent a and Ornstein-Uhlenbeck parameters on a square lattice of fixed size $L = 100$. We also fix the value of the minimum cluster size required for a crash to $s_m = 0.01 \cdot p \cdot L^{d_f} (\approx 30)$.

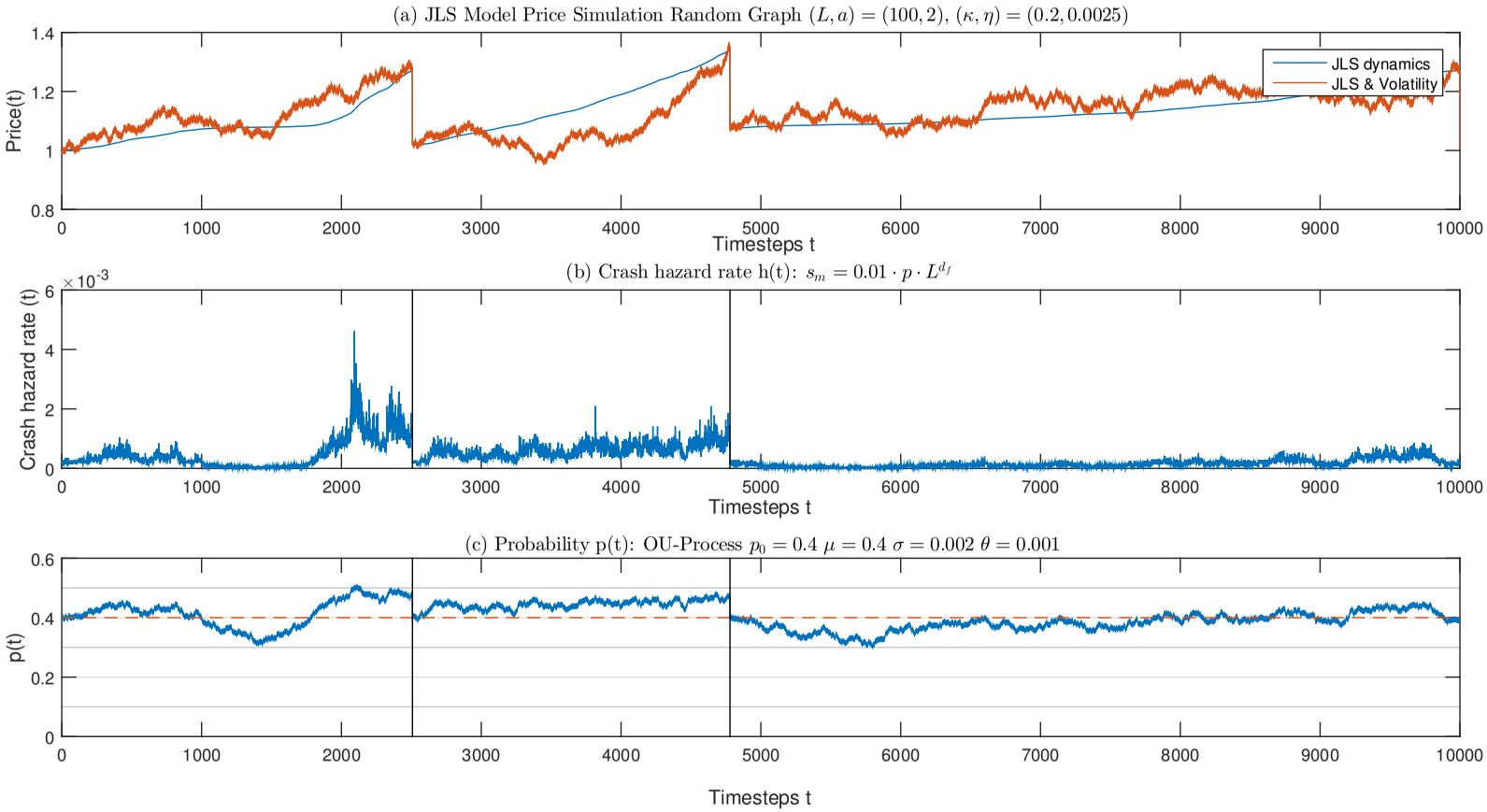

Figure 4.15: Plot of (a) the JLS model price simulation with (blue) and without (red) random walk, (b) the associated crash hazard rate and (c) the linear increasing control parameter p determining the crash hazard rate on a random site percolation square lattice of size $L = 100$ with condition $a = 2$. The price volatility parameter is $\eta = 0.0025$. The control parameter p is described by an Ornstein-Uhlenbeck process with drift respectively starting value $\mu = p_0 = 0.4$. We observe two clear bubbles that end with a crash.

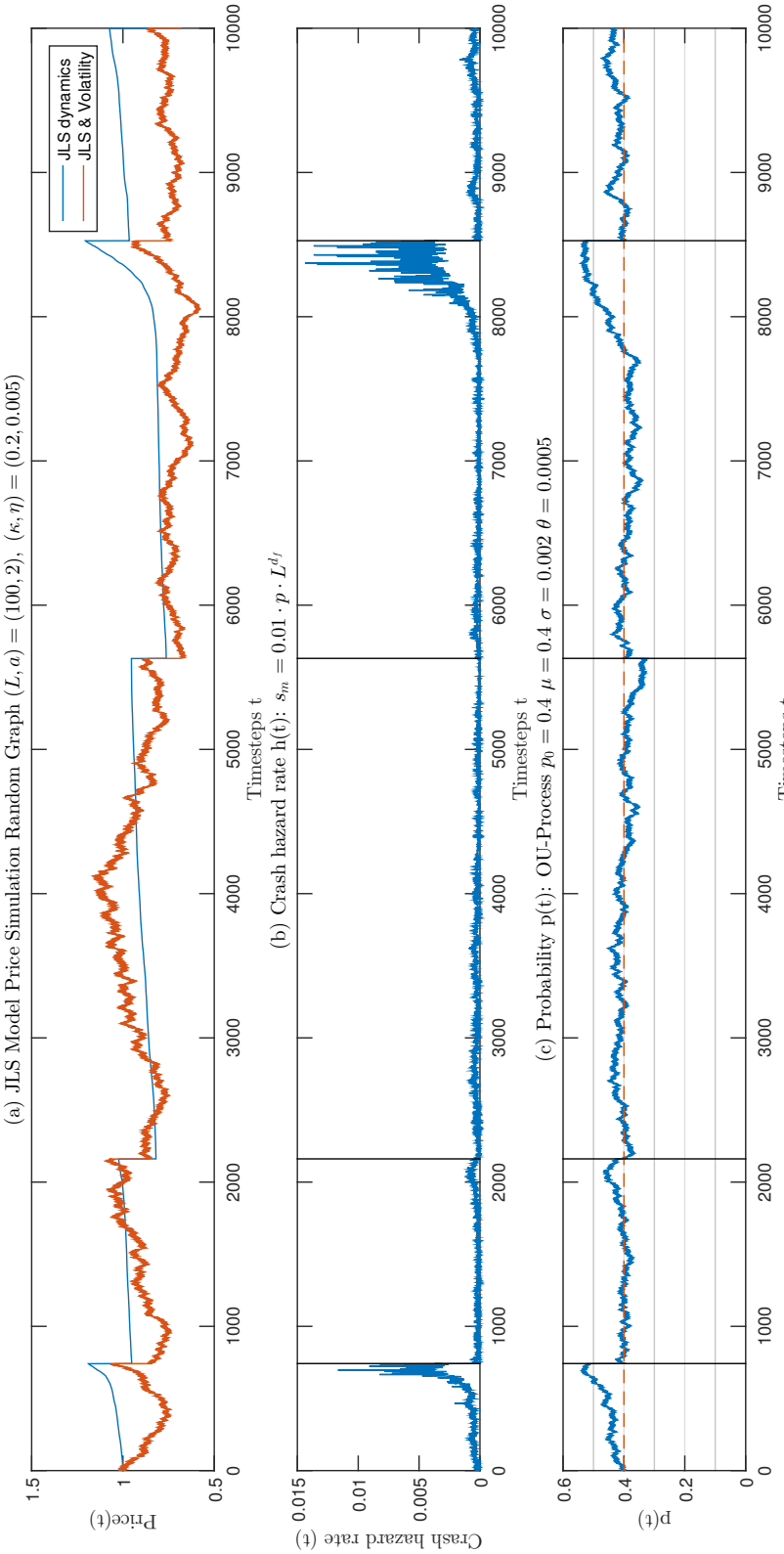

Figure 4.16: Plot of (a) the JLS model price simulation with (blue) and without (red) random walk, (b) the associated crash hazard rate and (c) the linear increasing control parameter p determining the crash hazard rate on a random site percolation square lattice of size $L = 100$ with condition $a = 2$. The price volatility parameter is $\eta = 0.005$. The control parameter p is described by an Ornstein-Uhlenbeck process with drift respectively starting value $\mu = p_0 = 0.4$.

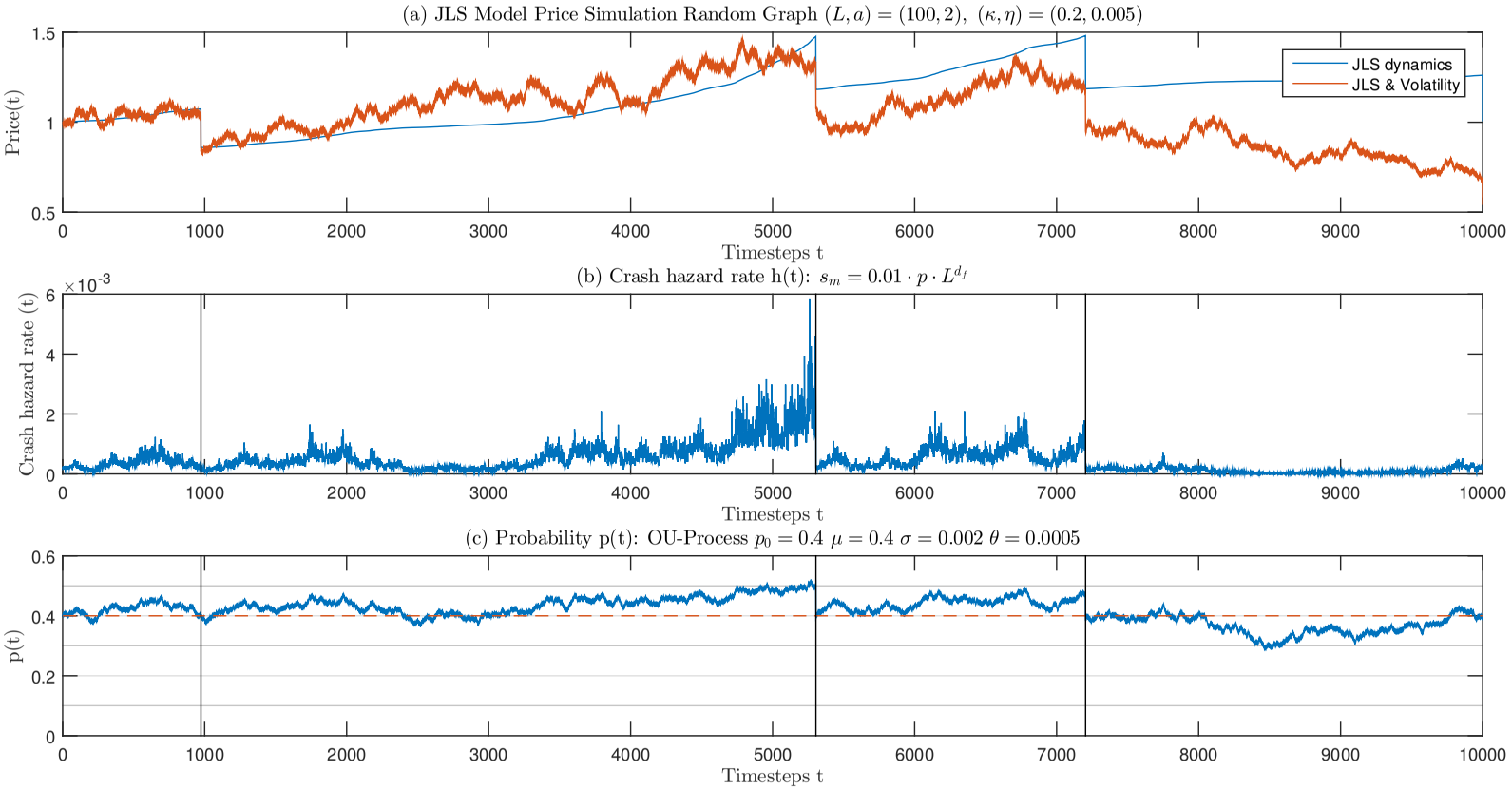

Figure 4.17: Plot of (a) the JLS model price simulation with (blue) and without (red) random walk, (b) the associated crash hazard rate and (c) the linear increasing control parameter p determining the crash hazard rate on a random site percolation square lattice of size $L = 100$ with condition $a = 2$. The price volatility parameter is $\eta = 0.04$. The price volatility parameter is $\eta = 0.005$. The control parameter p is described by an Ornstein-Uhlenbeck process with drift respectively starting value $\mu = p_0 = 0.4$.

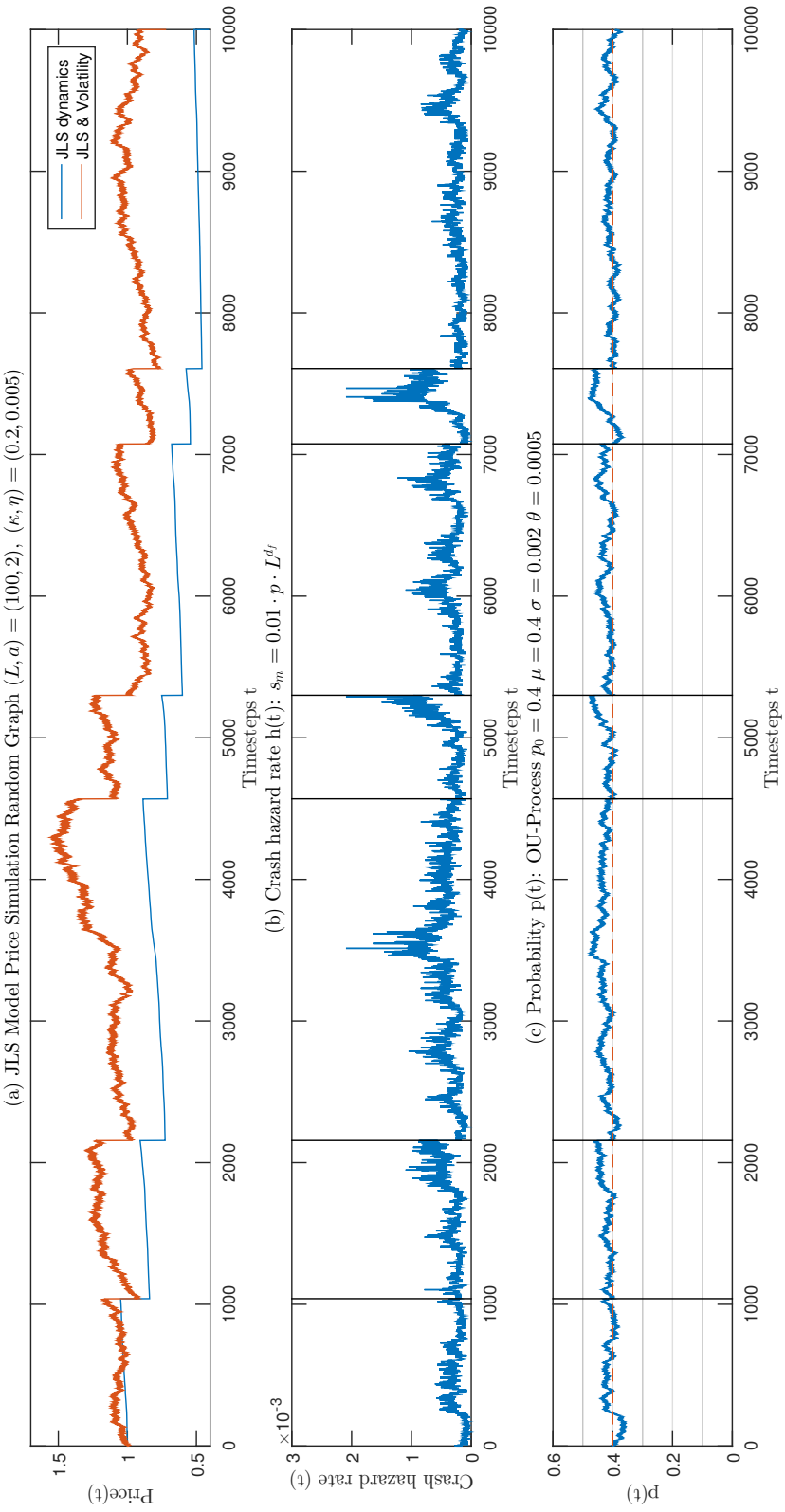

Figure 4.18: Plot of (a) the JLS model price simulation with (blue) and without (red) random walk, (b) the associated crash hazard rate and (c) the linear increasing control parameter p determining the crash hazard rate on a random site percolation square lattice of size $L = 100$ with condition $a = 2$. The price volatility parameter is $\eta = 0.005$. The control parameter p is described by an Ornstein-Uhlenbeck process with drift respectively starting value $\mu = p_0 = 0.4$.

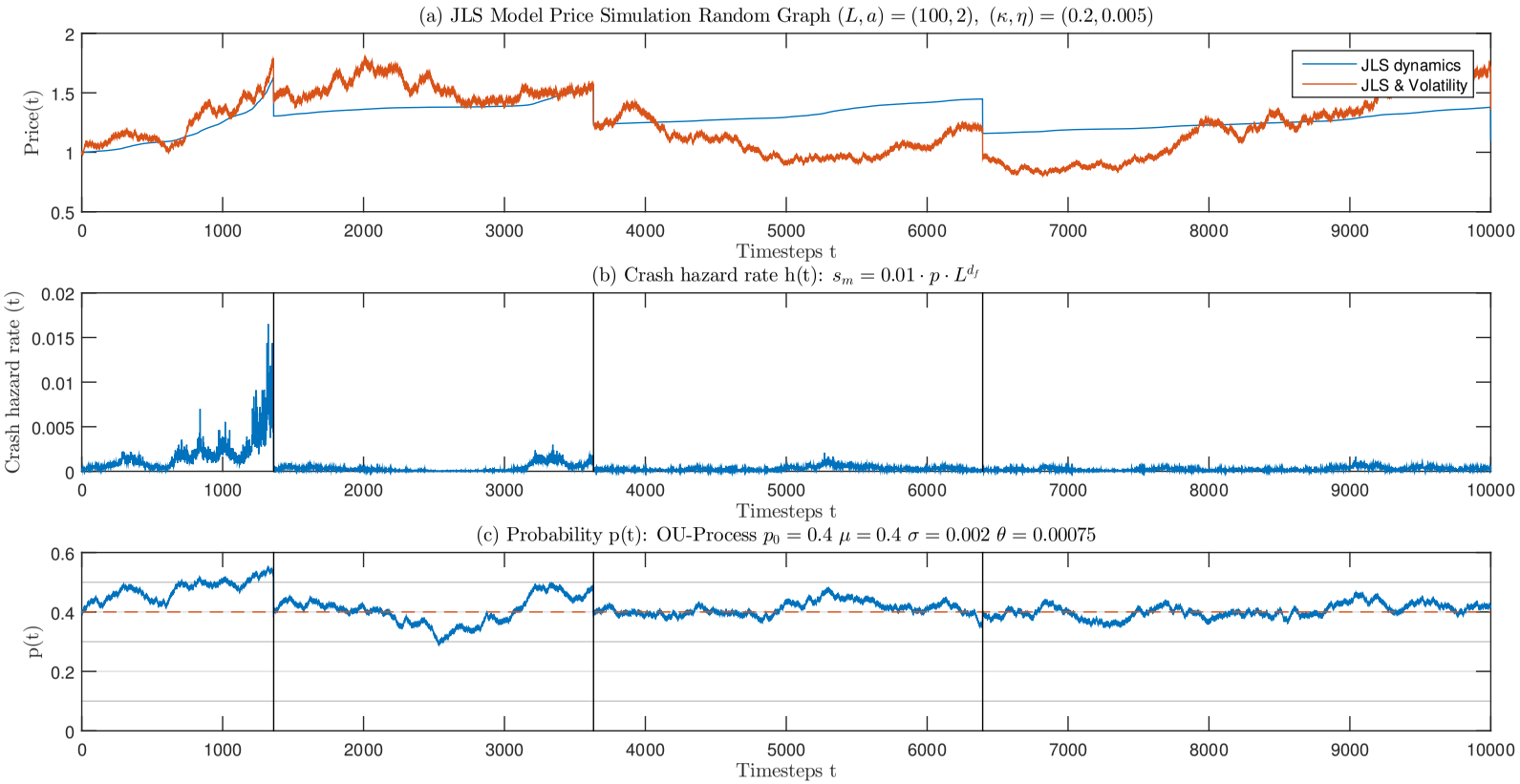

Figure 4.19: Plot of (a) the JLS model price simulation with (blue) and without (red) random walk, (b) the associated crash hazard rate and (c) the linear increasing control parameter p determining the crash hazard rate on a random site percolation square lattice of size $L = 100$ with condition $a = 2$. The price volatility parameter is $\eta = 0.005$. The control parameter p is described by an Ornstein-Uhlenbeck process with drift respectively starting value $\mu = p_0 = 0.4$.

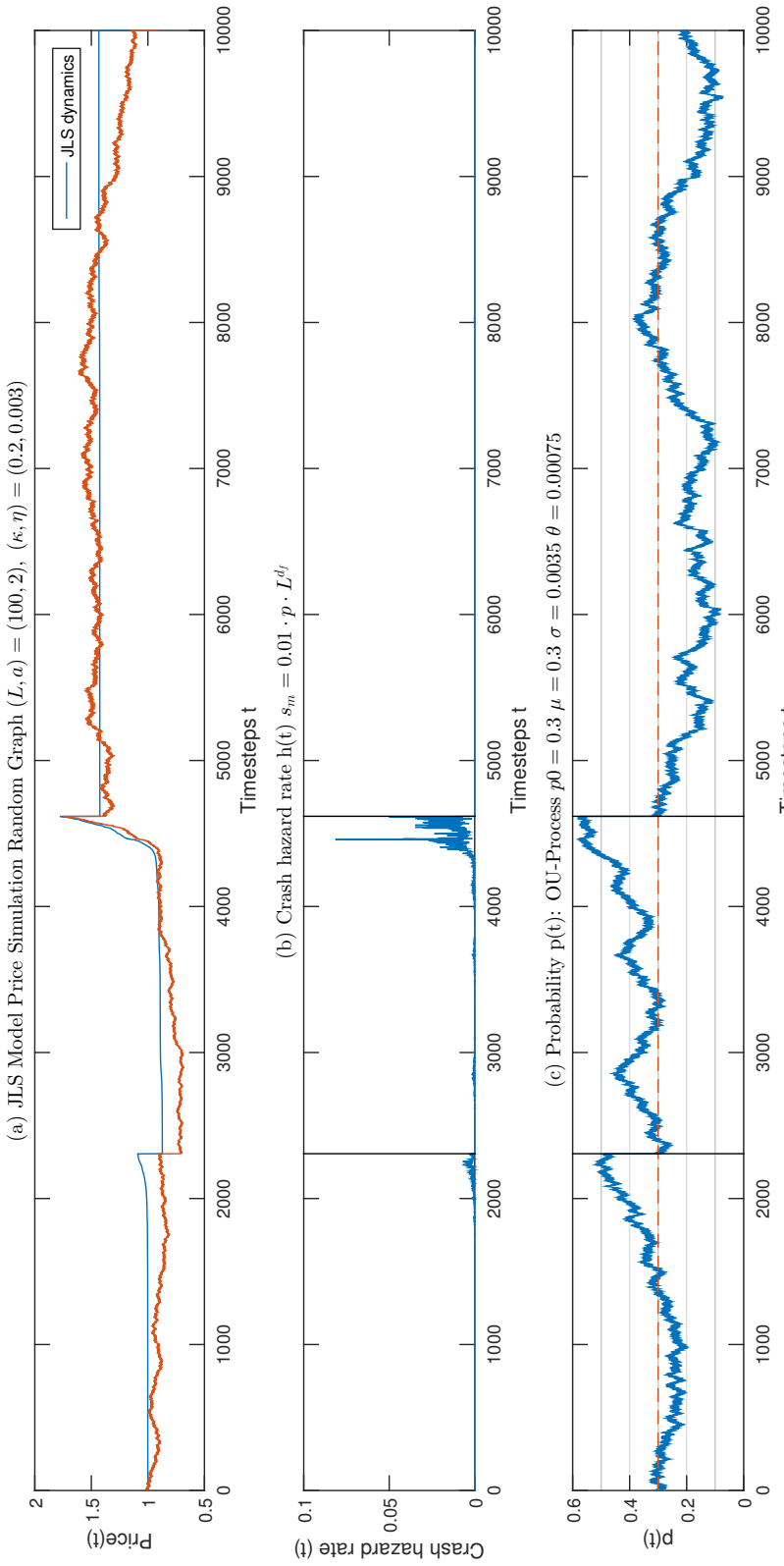

Figure 4.20: Plot of (a) the JLS model price simulation with (blue) and without (red) random walk, (b) the associated crash hazard rate and (c) the linear increasing control parameter p determining the crash hazard rate on a random site percolation square lattice of size $L = 100$ with condition $a = 2$. The price volatility parameter is $\eta = 0.003$. The control parameter p is described by an Ornstein-Uhlenbeck process with drift respectively starting value $\mu = p_0 = 0.3$.

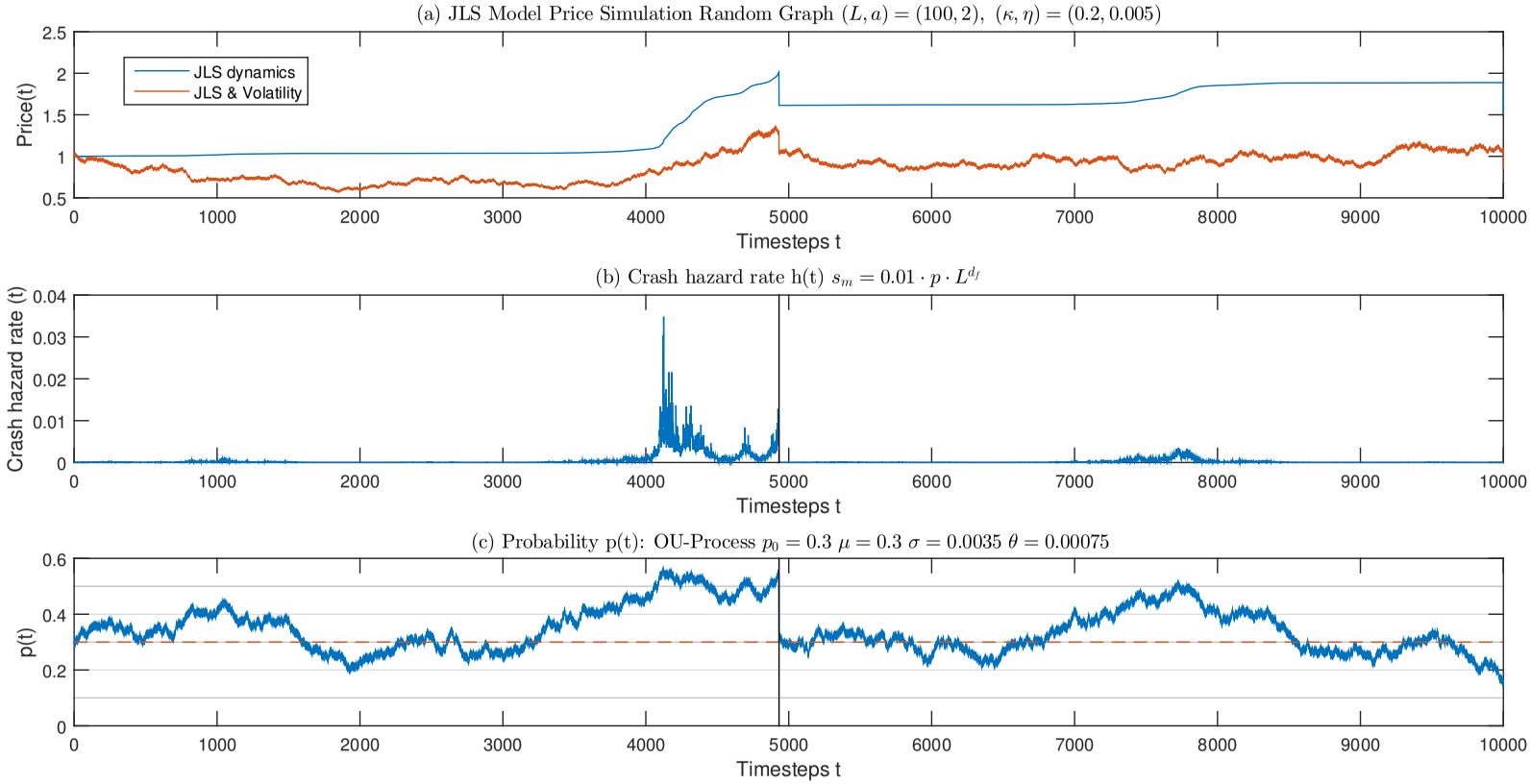

Figure 4.21: Plot of (a) the JLS model price simulation with (blue) and without (red) random walk, (b) the associated crash hazard rate and (c) the linear increasing control parameter p determining the crash hazard rate on a random site percolation square lattice of size $L = 100$ with condition $a = 2$. The price volatility parameter is $\eta = 0.005$. The control parameter p is described by an Ornstein-Uhlenbeck process with drift respectively starting value $\mu = p_0 = 0.3$.

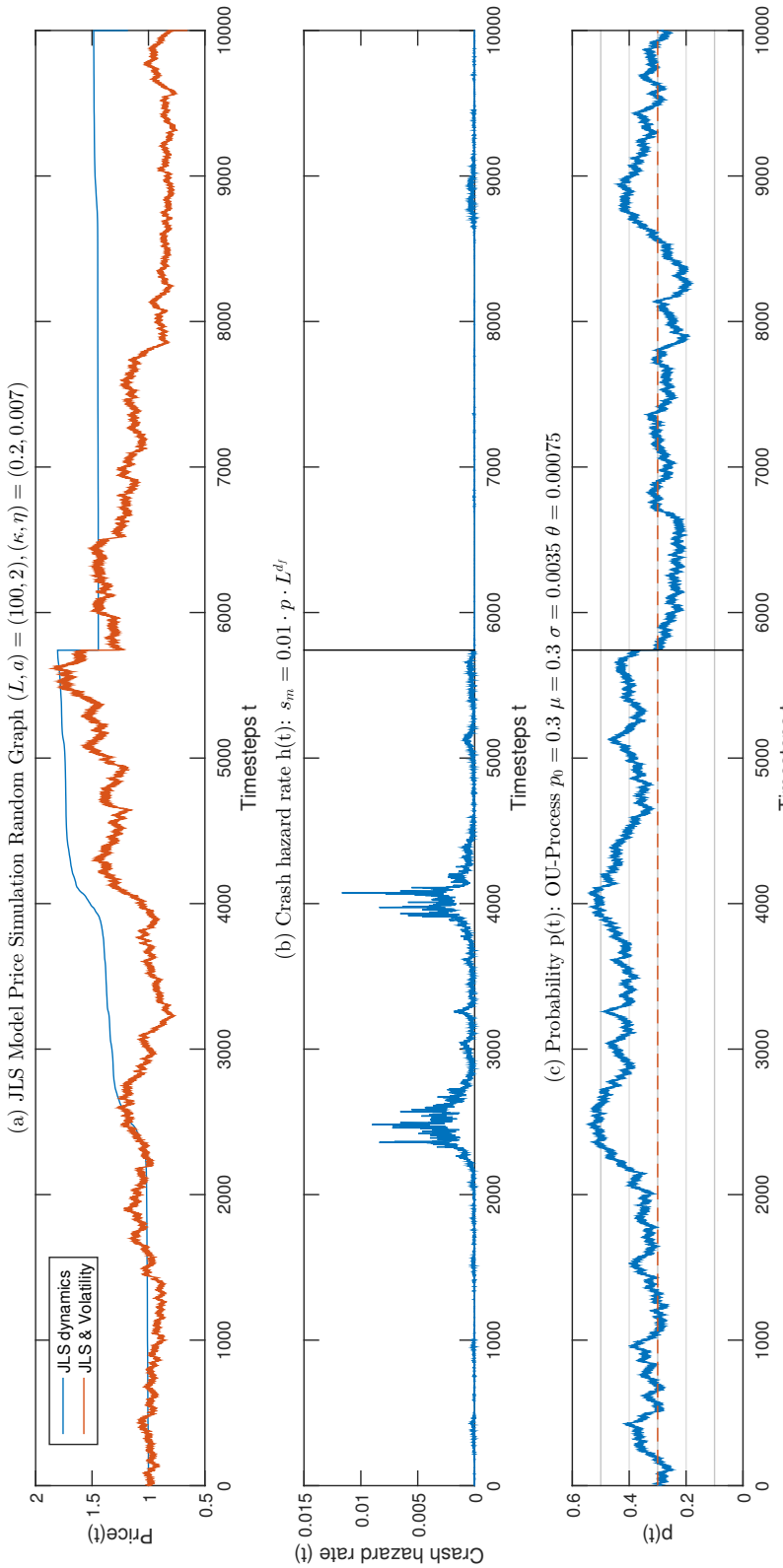

Figure 4.22: Plot of (a) the JLS model price simulation with (blue) and without (red) random walk, (b) the associated crash hazard rate and (c) the linear increasing control parameter p determining the crash hazard rate on a random site percolation square lattice of size $L = 100$ with condition $a = 2$. The price volatility parameter is $\eta = 0.007$. The control parameter p is described by an Ornstein-Uhlenbeck process with drift respectively starting value $\mu = p_0 = 0.3$.

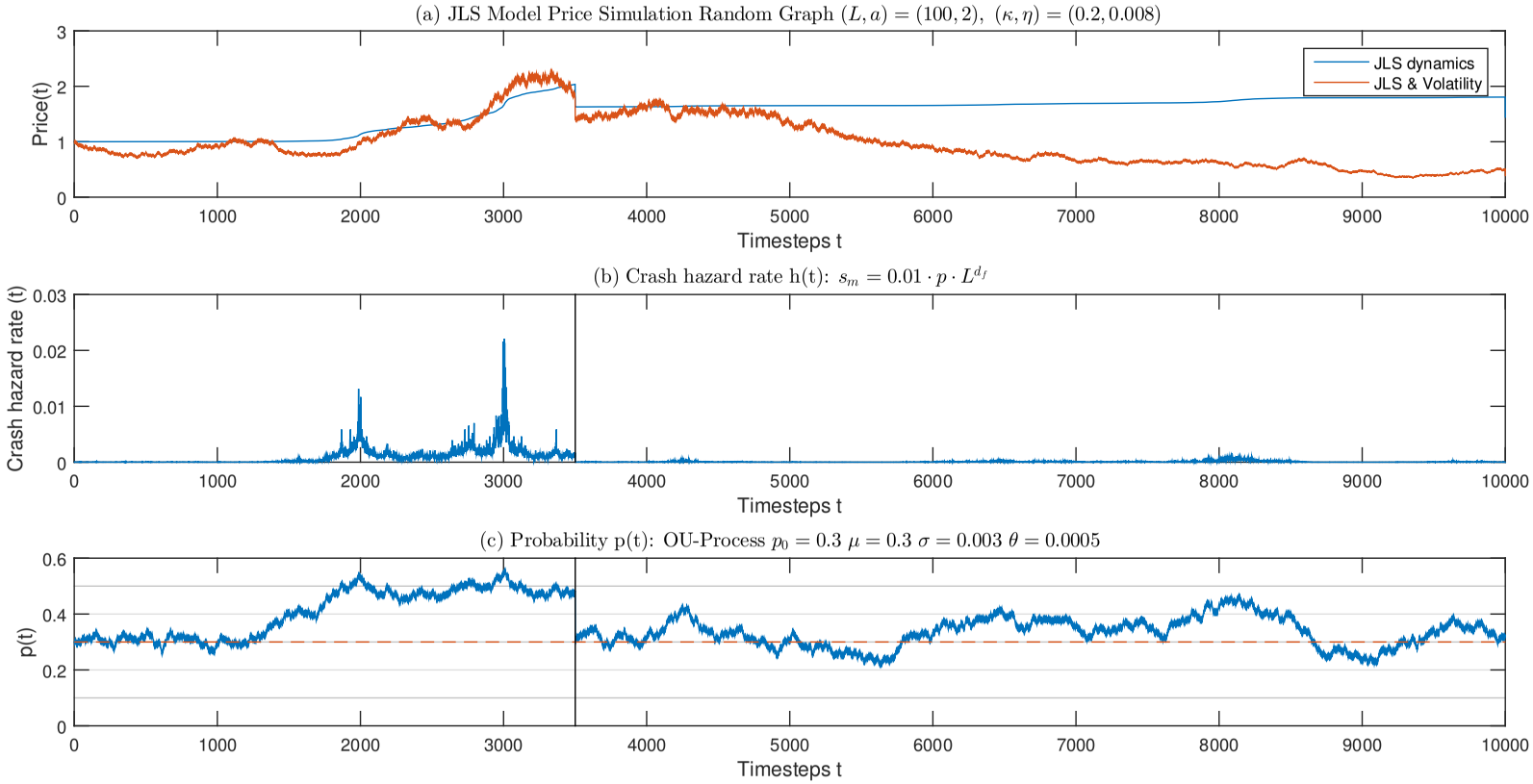

Figure 4.23: Plot of (a) the JLS model price simulation with (blue) and without (red) random walk, (b) the associated crash hazard rate and (c) the linear increasing control parameter p determining the crash hazard rate on a random site percolation square lattice of size $L = 100$ with condition $a = 2$. The price volatility parameter is $\eta = 0.008$. The control parameter p is described by an Ornstein-Uhlenbeck process with drift respectively starting value $\mu = p_0 = 0.3$.

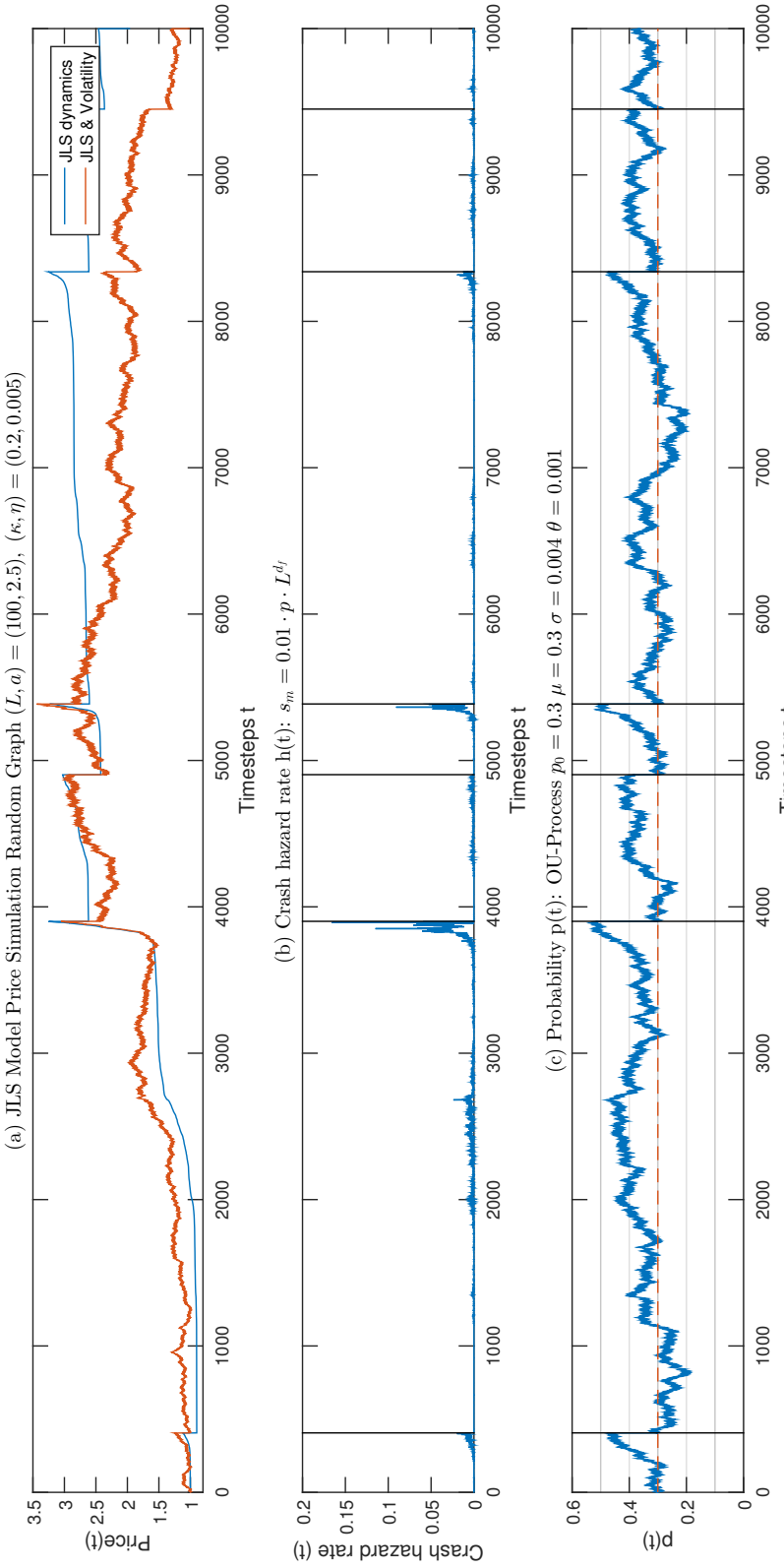

Figure 4.24: Plot of (a) the JLS model price simulation with (blue) and without (red) random walk, (b) the associated crash hazard rate and (c) the linear increasing control parameter p determining the crash hazard rate on a random site percolation square lattice of size $L = 100$ with condition $a = 2.5$. The price volatility parameter is $\eta = 0.005$. The control parameter p is described by an Ornstein-Uhlenbeck process with drift respectively starting value $\mu = p_0 = 0.3$.

4.4 Price Simulation Using the Ising Model

To understand a potential crash process using the Ising model, we assume a simple process of constant strengthening of imitation: Let the coupling strength be proportional to time, $K(t) \propto t$. In the beginning, K is small and there are only small clusters. The crash hazard rate is very low, a crash is very uncertain. As the coupling strength $K(t)$ grows, the typical size of clusters increases and one gets a broad distribution $n(s$ of cluster sizes. The coupling strength $K(t)$ approaches its critical value K_c when a macroscopic large cluster of synchronous agents is formed. If a large enough cluster gets active, certainly before K_c, a crash will occur.

We present a price simulation for a network whose evolution is realized by Glauber dynamics. We take the linearly increasing control parameter as simple network dynamics. We simulate the price on a market, where the imitation strength of traders is raising each time step. We do this by applying one round of Glauber dynamics each time-step giving the agents the possibility to change their cluster. Using the new configuration of states, we can calculate the crash hazard rate and consequently the price round for round. The occurrence of a crash is realized by a non-homogeneous Poisson process as above. After a crash, we reset our networks to a random and uncritical configuration. Figure 4.25 illustrate such a simulation for growing control parameter $K = 0.05 \cdot t + 0.1$.

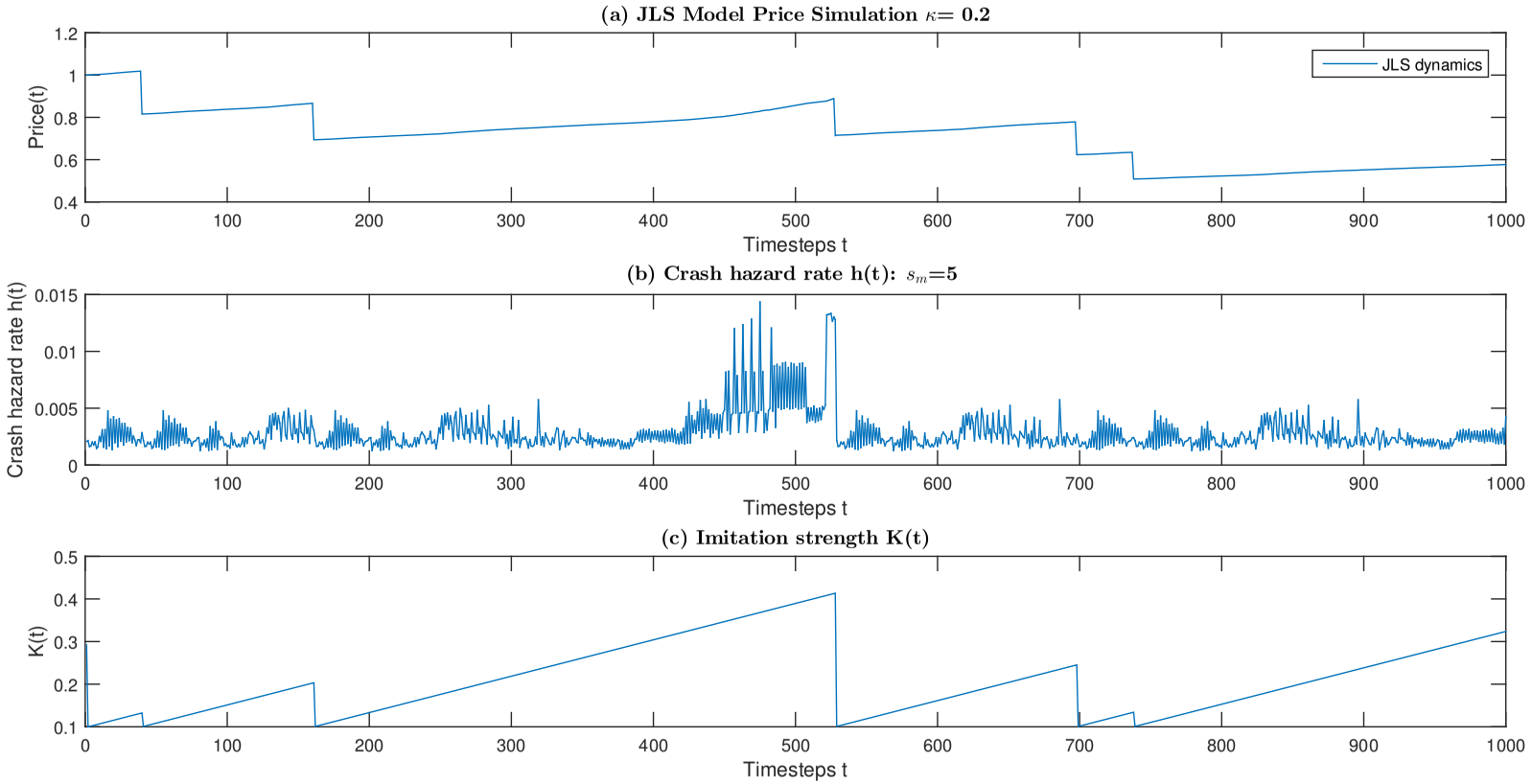

Figure 4.25: Plot of (a) the JLS model price simulation without random walk, (b) the associated crash hazard rate and (c) the linear increasing control parameter K determining the crash hazard rate on a random site percolation square lattice of size $L = 50$. The condition parameter is chosen to be $a = 2$. We see bubbles of different length and intensity. Each bubble ends with a crash as the crash hazard rate is diverging in time. The duration of a bubble varies being a random variable. We see again the diverging character of the crash hazard rate as the control parameter K comes close to the percolation threshold. The price returns to the region of its starting point $p_{\text{rice}}(0) = 1$. The JLS model is consistent in the sense of an isolated system.

Chapter 5

Conclusion and Outlook

In the present work, we clarified the herding effect due to cluster dynamics of traders. We provided a framework which is able to derive the crash hazard rate of the JLS Model as a power law diverging function of the scaling parameter. Using this framework, we are able to create reasonable bubbles and crashes in price time series. Our simulations show that bubbles occur basically if the scaling parameter takes long-memory excursions in the direction of the critical value. Most of the times, a crash is preceded by a bubble. The time of the crash, however, is a random variable. The bubble must not end with a crash, we also observe bubbles that survive without a crash leading to a new price plateau when the scaling parameters removes itself away from the critical region. Our simulations suggest that larger systems are less susceptible to bubbles and crashes, but if a bubble occurs, it is a very sharp one as opposed to smaller systems. We explained this by the self-similarity of the clusters. It is more difficult to get an imbalance in the market book if the system size L is large. We conclude that if the underlying networks of traders are self-similar, large systems exhibit less risk to bubbles due to herding of noise traders than smaller systems.

Furthermore, our simulations relate the occurrence of a bubble and a crash to the memory of the process (OU-process in our case) that describes the networks. We found out that the larger the memory, the heavier are the bubbles and the more likely are crashes. In order to access the crash hazard rate, we made the assumption that connected traders form a cluster that acts perfectly coherently. We use the critical phenomena of the diluted magnet from percolation theory to describe the imitation between traders. The clusters can cause a crash if clusters of imitating traders are large enough and get active, that is, they change their choice from buying to selling. Transferred to financial market, the scaling parameter becomes the fraction of traders that are actively participating in the market. We propose that the rate, which describes how often a cluster gets active, is depending on its size following

a super-linear relation between contributions of a group and group size. A single contribution, which is nothing else than one single trader who gets active, is enough to flip the choice of the whole cluster.

Combining the super-linear flipping rate and the cluster distribution we derive a theoretical estimate of the power law exponent of the crash hazard rate h as a function of the scaling parameter p:

$$h(p) \propto |p - p_c|^{-\frac{a-\mu}{\sigma}} \qquad \text{for } a > \mu. \tag{5.1}$$

It is a function of the condition a, which is the super-linear exponent that describes the flipping rate for clusters, and the universal critical exponents μ and σ of percolation theory. Being universal, the latter two ones are only depending on the dimension, the range, as well as the way of interaction of our system.

For the specific case of the site percolation model on the square lattice, we obtain $\alpha = 2.39$ as theoretical estimate for the super linear coefficient $a = 2$. Numerical calculations on this model of networks confirm the theoretical estimate as long as there is no infinite cluster. In the phase of no percolating cluster, we obtain $\alpha = 2.37$ for $a = 2$ and lattice size $L = 1000$. For the phase of percolation, we observe a faster decay due to rounding offs. The divergence of the crash hazard rate is not symmetrical. Note that equation 5.1 holds only for $a > \mu$. If we have $a < \mu$, we show that the crash hazard rate becomes a concave function which does not diverge.

The stylized framework of nearest neighbor connectedness can be substituted with a more general approach in further researches. Traders in the real world are organized into more complex networks than the simple nearest neighbor lattice. Although the square lattice is able to provide us with many insights, it could be interesting to investigate the crash hazard rate on well-behaving random graphs.

Furthermore, we are also able to confirm the power law diverging character of the crash hazard rate by using the Glauber dynamics on large lattices in the Ising model. The results for smaller lattice sizes like $L = 10$ are biased due to the overestimation of the Ising clusters. Further researches could improve the output for smaller lattice sizes L by using the Ising droplets instead. In this framework, we present price simulations only for $L = 50$, which is a value that compromises between a biased output and a numerically extensive calculation of the Glauber dynamics. The Ising clusters approach is also able to create bubbles and crashes. However, we need many rounds of the Glauber dynamics to see dynamics in the system. Further investigations could apply cluster flip dynamics like the Swendsen-Wang algorithm [33].

We constrained ourselves to negative price-shocks due to simplicity. However, our theoretical considerations also allow positive price-shocks. Indeed,

they are identical to the negative ones. They are just preceded by a negative bubble. A future work could simulate an asset that exhibits both negative and positive crashes. Further research could also apply a recently discovered triggering process of failing of interacting ponzi-firms (see [34]) to simulate the crash more dynamically.

Appendix A

Appendix

A.1 The crash hazard rate from a statistical point of view

The crash hazard rate $h(t)$ from the JLS model is the probability that a crash occurs in the interval $[t, t+dt]$ for $dt \to 0$ given that it has not occurred until time t. Let $F(t)$ be the cumulative distribution function (cdf) of the occurrence of a crash up to time t. The longer we wait the more likely a crash has happened. In other words, the cdf $F(t)$ is the cumulative incidence for incident events up to a proportion. The survival probability, which means that there is no crash up to time t, is directly linked to the cdf. It is the complementary event of that a crash has occurred up to time t whose probability is given by the cdf $F(t)$. We get

$$S(t) = 1 - F(t). \tag{A.1}$$

The probability that a crash occurs at time t is given by the derivative of the cumulative distribution function $dF(t)/\Delta t$. It is a probability density function (pdf).

With the help of the equation for conditional probability, the probability that a crash occurs at time t given that is has not occurred until time t is given just by:

$$h(t) = \frac{dF(t)/\Delta t}{1 - F(t)} \tag{A.2}$$

Note that the crash hazard rate itself is not a probability! Look at the units of the last equation: It is a probability divided by time divided by a probability leading to 1 over time. This explains the name hazard *rate*, since $h(t)$ is a rate and not a probability.], the product of crash hazard rate times time

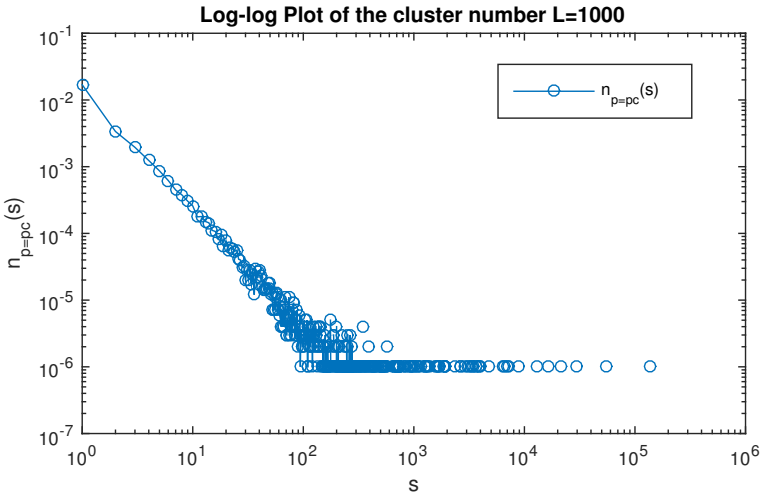

Figure A.1: Plot of the noisy tail of the cluster number.

is a probability. $h(t)dt$ denotes the unconditional probability that there is a crash in between $[t, dt]$.

A.2 Logarithmic Binning, Adaptive Kernel Estimation and the Hill estimator

As we can clearly see in figure A.1, the right hand side of the distribution is noisy. In contrast to the big values on the left side with its high frequency, fractional fluctuations are not suppressed in the tail. Data is small there, only a few clusters exist, if any. Indeed, fractional fluctuations are large for each cluster size counts in the tail. This is the reason for the statistical noise in the tail on the plot. We have three alternatives here to improve the results that we obtain with the help of simple linear regression in the log-log-plot.

1. Cumulative Distribution Function via Rank plot
2. Logarithmic binning
3. Data adaptive kernel estimation

A.2.1 Cumulative Distribution Function via Rank Plot

Sorting and ranking measurements is usually the quickest way to access the cumulative distribution function. If we rank the cluster sizes in order, then by definition there are s words with frequency greater than or equal to that of the s-th biggest cluster. Thus the cumulative distribution of the cluster number is simply proportional to the rank n of a word. If we want to

access the exponent of our cluster number, we start by sorting the clusters in decreasing order of frequency, then number them beginning with 1, plot their ranks as a function of their frequency in a log-log-plot and determine the gradient of the straight line. Finally, the exponent for the cluster number is exponent-1.

A.2.2 Data adaptive kernel estimation: Logarithmic binning

We divide the different values for s into bins B of varying length l_B. Logarithmic binning means that each bin is a multiple k wider one than the one before it. In numbers: $l_B = l_1 * k^B$. $\{y_B1, y_B2, \ldots, y_BN\}$ are the data points that fall in the B-th bin. The frequency histogram must be normalized by the width of the bins, i.e. the number of integers that fall in the bin. We get the following equation:

$$y_B = \frac{y_B1 + \ldots + y_BN}{n} \tag{A.3}$$

The normalized sample count gets independent of the bin width on average. Using bins with increasing width one has the advantage that the bins in the tail of the distribution get more samples and therefor suppress the fractional fluctuations compared to them with fixed bin sizes.

A.2.3 Hill estimator $\hat{\mu}$

The Hill estimator has a wide variety of applications. Its advantages and disadvantages are well known (Drees et al,2000). E.g., modeling the tails of the distribution of returns is important in the evaluation of risk (Embrechts et al.,1997) Suppose that $X_1, ..., X_N$ are independent and identically distributed (i.i.d) random variables with cumulative density function (cdf) $P(X_i < x) = x^{-\mu}L(x)$. Let $X_{(1)} \geq X_{(2)} \geq ... \geq X_{(k_N+1)}$ be the $k_N + 1$ largest order statistics. We take the exponential approximation of the normalized log-spacings $Y_j = j\log(X_{(j)}/X_{(j+1)})$ for $j = 1, ..., k$ and estimate a pseudo-maximum likelihood. This estimator of the tail index μ is called Hill estimator [35]. More precisely, the Hill estimator is defined for some k_N by

$$\hat{\mu}_N = \left\{ \frac{1}{k_N} \sum_{i=1}^{k_N} \log(X_{(i)}/X_{(k_N+1)}) \right\}^{-1} \tag{A.4}$$

We apply the Hill estimator to get an estimation for our cluster distribution. Note that the random variables are the cluster sizes s. Having the site percolation model initialized, we have to take all the formed clusters into account. Each cluster is a realization of our random number. Consequently, the total number of clusters denotes the number of different random numbers N. The

pdf is the probability to pick a cluster of size s if I pick a cluster out of the set of all the clusters that are realized. The according cdf is the theoretical cluster number $n(s) = \frac{1}{s^{\mu}}$. $n(s)$ is also called cluster distribution. Being a constant we set $L(x) \equiv 1$.

We take the order statistics of our cluster sizes, i.e. we sort descendant all the realized cluster according to the size. The function $L(x)$ is a constant, thus, we do not need a threshold k_n for cutting our sample to have L(x) slowly varying.

But we do have set a limit for the sample. As we have seen in figure A.1, the right hand of the distribution in the loglog-plot is noisy. Therefor we skip the noisy part and set an according limit to the cluster sizes s.

Error calculation: The variance is proportional to $\frac{\alpha^2}{k}$

$$\frac{\Delta\mu}{\mu} \approx \frac{1}{\sqrt{k_n}} \tag{A.5}$$

Bibliography

[1] A. Johansen and D. Sornette. Shocks, crashes and bubbles in financial markets. *Brussels Economic Review (Cahier economiques de Bruxelles) 53 (2) 201-253*, 2010.

[2] Anders Johansen, Olivier Ledoit, and Didier Sornette. Crashes as critical points. *International Journal of Theoretical and Applied Finance*, 3(1):219–255, Jan 2000.

[3] Anders Johansen, Didier Sornette, and Olivier Ledoit. Predicting financial crashes using discrete scale invariance. *Journal of Risk*, 1(4):5–32, 1999.

[4] Anders Johansen and Didier Sornette. Critical crashes. *Risk*, 5(1):91–94, 1999.

[5] V. Filimonov and D. Sornette. A stable and robust calibration scheme of the log-periodic power law model. *Swiss Finance Institute*, 2013.

[6] Didier Sornette. Critical market crashes. *Physics Reports 378*, 2003.

[7] E. Ising. *Beitrag zur Theorie des Ferromagnetismus*. PhD thesis, University of Hamburg, 1924.

[8] A. Kyle. Continuous auctions and insider trading. *Econometrica, vol.53(6), pages 1315-35*, 1985.

[9] R. Cont J-P Bouchaud. Herd behaviour and aggregate fluctuations in financial markets. *Macroeconomic Cynamics, 4, 2000, 170-196*, 2000.

[10] Dietrich Stauffer and Amnon Aharony. *Introduction to Percolation Theory*. Taylor and Francis, 1991.

[11] M.D. Donsker. An invariant principle for certain probability limit theorems. *Memoirs, 6, Amer. Math. Soc.*, 1951.

[12] C. Vanneste, A. Gilabert, and D. Sornette. Finite-size effects in line-percolating systems. *Physics Letters A*, 1991.

[13] C.N. Yang. The spontaneous magnetization of a two-dimensional ising model. *Physical Review, vol.85, Issue 5, pp. 808-816*, 1952.

[14] Lars Onsager. Crystal statistics. i. a two-dimensional model with an order-disorder transition. *Physical Review, vol. 65, Issue 3-4, pp. 117-149*, 1944.

[15] R.J. Glauber. *J. Math Phys 4, 294*, 1963.

[16] Ronen Segev Elad Schneidman, Michael J. Berry and William Bialek. Weak pairwise correlations imply strongly correlated network states in a neural population. *Nature 440*, 2006.

[17] S. F. Edwards and P. W. Anderson. Theory of spin glasses. *J. Phys. F: Met. Phys. 5 965*, 1975.

[18] D Sornette. *Why Stock Markets Crash (Critical Events in Complex Financial Systems)*. Princeton University Press, 2003.

[19] A. Coniglio and W. Klein. Clusters and ising critical droplets: a renormalisation group approach. *J. Phys. A 13, 2775-2780*, 1980.

[20] M.E. Fisher. The theory of condensation and the critical point. *Physics 3 5, 255-283*, 1967.

[21] F. Canizarro and et al. Results of the measurements carried out in order to verify the validity of the poisson-exponential distribution in radioactive decay events. *The International Journal of Applied Radiation and Isotopes 29 (11): 649*, 1978.

[22] Ming-Xia Li, Wei-Xing Zhou, Zhi-Qiang Jiang, Wen-Jie Xie, and Didier Sornette. Two-state markov-chain poisson nature of individual cellphone call statistics. *ETH preprint*, 2015.

[23] D. Vere-Jones and Y. Ogata. Statistical principles for seismologists. *An international handbook of earhquake and engineering seismology.*, 2003.

[24] D. Vere-Jones and D.J. Daley. *Introduction to the theory of point processes. Vol 1: Elementary Theory and MMethod (2nd edition)*. Springer, 2003.

[25] P.A.W Lewis and G.S. Shedler. Simulation of non-homogeneous poisson processes by thinning. *Naval Research Logistics Quarterly*, 1979.

[26] Karl Sigman. Poisson processes, and compound (batch) poisson processes. 2007.

[27] Y. Ogata. On lewis' simulation method for point processes. *IEEE transactions on information theory, Vol. IT-27, No.1*, 1981.

[28] G. E. Uhlenbeck and L. S. Ornstein. On the theory of brownian motion. *Physical Review*, 1930.

[29] R.B. Potts. Some genegeneral order-disorder transformations. *Mathematical Proceedings*, 1952.

[30] Luis M. A. Bettencourt. The origins of scaling in cities. *Science 340, 1438*, 2013.

[31] Didier Sornette, Thomas Maillart, and Giacomo Ghezzi. How much is the whole really more than the sum of its parts? 1 + 1= 2.5: Superlinear productivity in collective group actions. *PLoS ONE 9(8): e103023.*, 2014.

[32] J.S.S. Martins and P.M.C. de Oliveira. Computer simulations of statistical mmodel and dynamic complex systems. *Braz. J. Phys.*, 2004.

[33] R.H. Swendsen and J.-S. Wang. Nonuniversal critical dynamics in monte carlo simulations. *Phys. Rev. Lett., 58(2): 86-88*, 1987.

[34] Sorin Solomon and Natasa Golo. *Minsky Financial Instability, Interscale Feedback, Percolation and Marshall-Walras Disequilibrium*. De Gruyter, 2013.

[35] B. Hill. A simple general approach to inference about the tail of a distribution. *The Annals of Statistics, 3, 1163-1173*, 1975.

Eidgenössische Technische Hochschule Zürich
Swiss Federal Institute of Technology Zurich

Declaration of originality

The signed declaration of originality is a component of every semester paper, Bachelor's thesis, Master's thesis and any other degree paper undertaken during the course of studies, including the respective electronic versions.

Lecturers may also require a declaration of originality for other written papers compiled for their courses.

I hereby confirm that I am the sole author of the written work here enclosed and that I have compiled it in my own words. Parts excepted are corrections of form and content by the supervisor.

Title of work (in block letters):

Percolation theory on financial markets: A cluster description of herding behavior leading to bubbles and crashes

Authored by (in block letters):

For papers written by groups the names of all authors are required.

Name(s):	**First name(s):**
Seyrich	Maximilian Gustav Albert

With my signature I confirm that

- I have committed none of the forms of plagiarism described in the 'Citation etiquette' information sheet.
- I have documented all methods, data and processes truthfully.
- I have not manipulated any data.
- I have mentioned all persons who were significant facilitators of the work.

I am aware that the work may be screened electronically for plagiarism.

Place, date	**Signature(s)**
Zurich, 20th February 2015	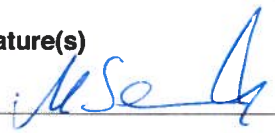

For papers written by groups the names of all authors are required. Their signatures collectively guarantee the entire content of the written paper.